universität wien

DISSERTATION

Titel der Dissertation

Characterization of Thrombospondin-1 as novel ligand for the Reelin pathway receptors ApoER2 and VLDLR in the postnatal mouse brain

angestrebter akademischer Grad

Doktor/in der Naturwissenschaften (Dr. rer.nat.)

Verfasserin / Verfasser:	Sophia Maria Blake
Matrikel-Nummer:	0021434
Dissertationsgebiet (lt. Studienblatt):	A 091490 Molekulare Biologie
Betreuerin / Betreuer:	Univ.-Prof. Dr. Johannes Nimpf

Wien, am 06. Dezember 2008

Contents

1 Abstract

The LDLR family members ApoER2 and VLDLR are receptors for the extracellular glycoprotein Reelin, triggering a signal transduction cascade that has been shown to be involved in the correct lamination of the cerebral cortex during embryonic brain development. More recently, Reelin signaling was linked to postnatal neuronal precursor migration in the murine forebrain in the formation of the rostral migratory stream (RMS). The RMS is a stream of tangentially migrating neuronal precursors originating in the postnatal neural stem cell niche, the subventricular zone (SVZ), and extending into the most rostral region of the mouse brain, the olfactory bulb (OB). Mouse mutants for the Reelin pathway modules, *apoER2*$^{-/-}$/*vldlr*$^{-/-}$, *dab1*$^{-/-}$ and *reelin*$^{-/-}$ all display a severe failure of RMS formation, with precursors remaining in the SVZ unable to initiate migration along the RMS. Quite intriguingly though, the only known functional ligand for the pathway, Reelin, is not expressed either in the SVZ or along the RMS while ApoER2 and Dab1 have been located to these regions, thus providing the necessary components for an active Reelin pathway. This suggests that other ligands besides Reelin commence the signal transduction cascade, to initiate postnatal neuronal precursor migration.

The aim of this thesis was to identify and functionally characterize Thrombospondin-1 (THBS-1) as a newly recognized ApoER2 and VLDLR ligand in the postnatal mouse brain and its function in neuronal precursor migration in the RMS.

Thrombospondin-1 was shown to be expressed in the SVZ and RMS of the postnatal mouse brain thereby representing a good candidate ligand for the Reelin pathway. Subsequent ELISA studies confirmed specific binding of THBS-1 to ApoER2 and VLDLR with nanomolar affinity. Like Reelin, THBS-1 induced tyrosine phosphorylation of Dab1 in primary neurons but failed to induce phosphorylation of AKT and to initiate Dab1 degradation. More striking differences between the two ligands were revealed in SVZ migration assays

where THBS-1 displayed a neuro-adhesive effect in initiating and maintaining neuronal precursor chain formation while Reelin dissolved existing chains. Using SVZ explants from *THBS-1*$^{-/-}$ mice, it was shown that THBS-1 is not only sufficient but also necessary for postnatal chain formation as lack of THBS-1 in SVZ explants drastically increased the number of single cells not organized into chains. This adhesive effect on chain formation was shown to be mediated by ApoER2 and VLDLR as blocking of these receptors by RAP completely abolished the THBS-1 effect to background level. Analyses of *THBS-1*$^{-/-}$ brain structures revealed a significant widening of the RMS in the region of entry into the OB with migratory chains failing to remain in their compact chain structure, and subsequently less neuronal precursors migrating into outer OB layers.

Summarizing, this PhD thesis presents *in vitro* and *in vivo* data of a previously unknown function of THBS-1 in the plasticity of neuronal precursor chains in the postnatal brain within the RMS. This function is mediated by ApoER2 and might also depend on the presence of Dab1, but stands in clear contrast to the Reelin signal that promotes disintegration of neuronal precursor chains.

2 Zusammenfassung

Zwei Mitglieder der LDLR Familie, ApoER2 und VLDLR, sind Rezeptoren des extrazellulären Glycoproteins Reelin, welches während der embryonalen Hirnentwicklung eine Signaltransduktionskasde zur korrekten Etablierung des zerebralen Kortex initiiert. Kürzlich wurde der Reelin Signalweg auch als entscheidender Faktor während der postnatalen Migration neuronaler Vorläuferzellen im Vorderhirn von Mäusen identifiziert wo es an der Etablierung des „rostral migratory streams“ (RMS) beteiligt ist.
Der RMS ist eine aus tangential migrierenden neuronalen Vorläuferzellen gebildete Struktur, welche in der postnatalen neuronalen Stammzellnische, der Subventrikulärzone (SVZ), entstehen und in die rostralste Region des Mäusehirns, den olfaktorischen Bulbus (OB), wandern. Mausmodelle in denen Komponenten der Reelin Signaltransduktionskaskade deletiert wurden, wie *apoER2*$^{-/-}$/*vldlr*$^{-/-}$, *dab1*$^{-/-}$ und *reelin*$^{-/-}$ Mäuse, weisen einen schwerwiegenden Defekt in der Bildung des RMS auf, da neuronale Vorläuferzellen in der SVZ verharren und keine Migration entlang des RMS starten können. Interessanterweise wird Reelin, der bisher einzige bekannte Ligand für den Signalweg, weder in der SVZ noch im RMS exprimiert, während ApoER2 und Dab1 sehr wohl in diesen Regionen lokalisiert sind. Die Präsenz dieser essentiellen Komponenten impliziert, dass es andere Liganden als Reelin geben muss, die die Signaltransduktionskaskade aktivieren können um die Migration der postnatalen neuronalen Vorläuferzellen zu initiieren.

Zielsetzung dieser Dissertation war es, Thrombospondin-1 (THBS-1) als neuen Liganden für ApoER2 und VLDLR im postnatalen Mäusehirn zu identifizieren und seine Rolle in der Migration neuronaler Vorläuferzellen im RMS zu charakterisieren.

Es konnte gezeigt werden, dass Thrombospondin-1 sowohl in der SVZ als auch im RMS des postnatalen Mäusehirns exprimiert wird und daher eine interessanter Kandidaten für einen neuen Liganden des Reelin Signalwegs

darstellt. In ELISA Studien konnten spezifische Bindungen von THBS-1 an ApoER2 und VLDLR mit sub-nanomolarer Affinität gezeigt werden. Weiters kann THBS-1, wie Reelin, die Phosphorylierung von Dab1 in primären neuronalen Kulturen induzieren jedoch nicht die Phosphorylierung von AKT oder die Degradation von Dab1.

Weitere Gegensätze der beiden Liganden wurden in SVZ Migrations Assays sichtbar, in denen THBS-1 die Adhäsion neuronaler Vorläuferzellen bei der Bildung und Stabilisierung von Ketten induzierte, wogegen Reelin bereits existierende Ketten auflöste. Anhand von SVZ Explanten von *THBS-1*$^{-/-}$ Mäusen konnte weiters gezeigt werden, dass THBS-1 nicht nur hinreichend sondern auch notwendig für die Entstehung der postnatalen Kettenformation ist, da ein Fehlen von THBS-1 in den Explanten die Anzahl individueller Zellen deutlich erhöhte. Dieser adhäsive Effekt wird über ApoER2 und VLDLR vermittelt, da eine Blockierung dieser Rezeptoren mittels RAP den Einfluss von THBS-1 komplett aufhebt.

Untersuchungen zur Hirnanatomie von *THBS-1*$^{-/-}$ Mäusen zeigten eine signifikante Erweiterung des RMS beim Eintritt in den OB und einen Verlust der kompakten Struktur der migrierenden Ketten. Außerdem konnten weniger neuronale Vorläuferzellen in den äußeren OB-Schichten dieser Mäuse gefunden werden.

Zusammenfassend präsentiert diese Doktorarbeit neue *in vitro* und *in vivo* Daten über eine bisher unbekannte Funktion von THBS-1 in der Plastizität neuronaler Vorläuferzellketten im RMS des postnatalen Mäusegehirns. Diese Funktion wird von ApoER2 und VLDLR vermittelt und ist womöglich von der Anwesenheit von Dab1 abhängig, steht aber in klarem Gegensatz zum Reelin Signal welches die Auflösung neuronaler Vorläuferzellketten begünstigt.

3 Introduction

3.1 Neocortical development

3.1.1 The Neocortex

The Neocortex is defined as the outermost region of the cerebral cortex and is involved in higher order processes like memory formation, sensual perception and learning. It is the newest part of the cortex to evolve and in mammals is vertically organized into six distinct neuronal layers with distinct morphological and functional identities and horizontally splits into different areas, with each anatomically distinctive area specialized in a particular sensory, motor, or associative function.

Within the cortex, one can distinguish two classes of neurons: interneurons that make local connections and do not leave the cortex itself, and projection neurons which can extend axons to very distant targets like the brain stem or spinal cord. Interneurons, producing the inhibitory gamma-aminobutyric acid (GABA), and Cajal Retzius cells are generated in the lateral and medial ganglionic eminences and migrate tangentially long distances before reaching their final destination in the neocortex.

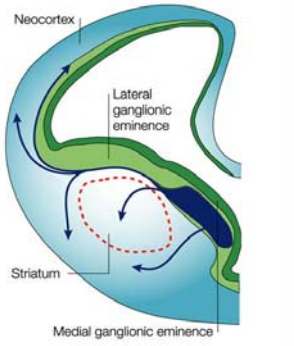

Fig 1: Migration routes of interneurons from the medial and lateral ganglionic eminence to the cortex. Schematic illustration of an embryonic day 13.5 (E13.5) mouse brain showing pathways of migrating interneurons emanating from the medial ganglionic eminence. Adapted from [10].

Projection neurons or pyramidal neurons, referring to their typical pyramidal morphology release glutamate as neurotransmitter and are the main excitatory component of the cortex, representing around 80% of the neurons in the cortex. They transmit information between different regions of the cortex and to other regions of the brain.

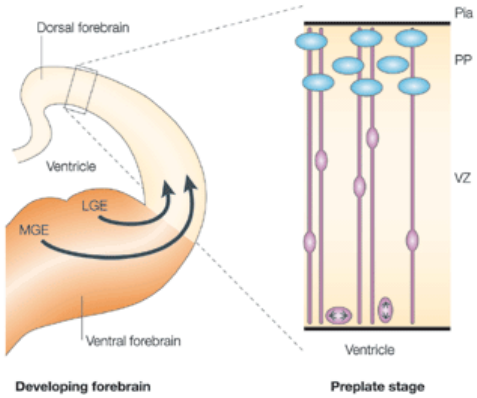

Fig 2: Radially migrating projection neurons in the neocortex Schematic section through the developing telencephalon. Postmitotic Projection neurons arise from the ventricular zone (VZ) and form the preplate (PP). Taken from [6].

Unlike interneurons, they are generated from progenitors residing in the ventricular zone (VZ), located in the dorso-lateral wall of the telencephalon. It is from this region that around embryonic day 10.5 (E10.5) the first neurons emanate to form a cortical structure referred to as the preplate. As neurogenesis proceeds, an additional proliferative layer referred to as the subventricular zone (SVZ) forms above the VZ.

3.1.2 Neuronal migration in the developing neocortex

Radial migration

Two distinct modes of cell movement, *nuclear translocation* and glia-guided *locomotion*, are responsible for the radial migration of neurons generated in the cortical ventricular zone during embryonic development [14].

During *nuclear translocation* the cell first extends a leading process in the

direction of migration and then moves the nucleus through the elongated process to its destination, thereby inducing a shortening of the leading edge over time. As the leading edge is attached to the pial surface this enables a radial glia independent migration.

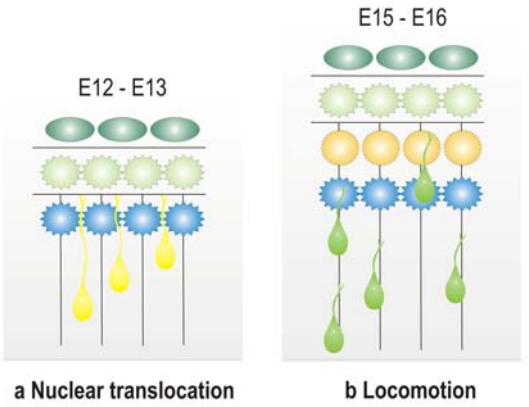

Figure 3: Two types of radial migration in the developing brain. (a) Nuclear translocation between E12-E13 is glia independent, while **(b)**, migration by locomotion between E15-E16 requires the presence of radial glia as scaffold. Modified from [8].

Locomotion involves movement of the entire cell, including its leading and trailing processes and maintenance of the leading edge length. While nuclear translocation is a very smooth movement, locomotion is interspersed by pauses and is dependent on the presence of radial glia [8].

Nuclear translocation is the prevalent form of radial movement of the early-born cortical neurons during E12-E13 when the preplate is split, while locomotion is adopted by neurons between E15-E16 after the preplate has already split and the cortical plate is expanding rapidly [15].

Tangential migration

Although radial migration is the prevalent mechanism by which neuronal precursors reach their final position in the developing brain, studies conducted over 40 years ago [16] first postulated the existence of tangentially orientated cells in the intermediate zone of the cortex. Retroviral cell lineage studies [17] and X-inactivation mosaics [18] performed 30 years later confirmed the existence of non-radial migration and a tangential movement of several cortical

neurons. Chimera analysis also showed that the final function of lineage related cells correlated with the mode of migration they used. Therefore, non-pyramidal GABAergic neurons were found to migrate tangentially while pyramidal glutamatergic neurons were radially orientated [19].

3.1.3 Cortical layering

In the mouse, neuronal layer formation is initiated at E10.5, when a wave of neuronal precursor cells exits the ventricular zone and migrates outwards along radial glial fibers to the pial surface of the brain. This first wave of postmitotic neurons leaving the VZ establishes a neuronal layer known as the preplate. Some of these neurons are destined to become Cajal Retzius (CR) cells and subplate neurons. At E13 a second wave of postmitotic neurons emanates from the VZ and splits the existing preplate into the superficial marginal zone and the deeper subplate. The subplate is located proximal to the ventricular zone, while the marginal zone which harbors Reelin secreting CR cells [20] is positioned just underneath the pial surface of the brain. The new layer between the subplate and the marginal zone is referred to as the cortical plate. Following waves of postmitotic neurons traverse the cortical plate and align above the existing layers of neurons thereby generating a layering of the cortex.

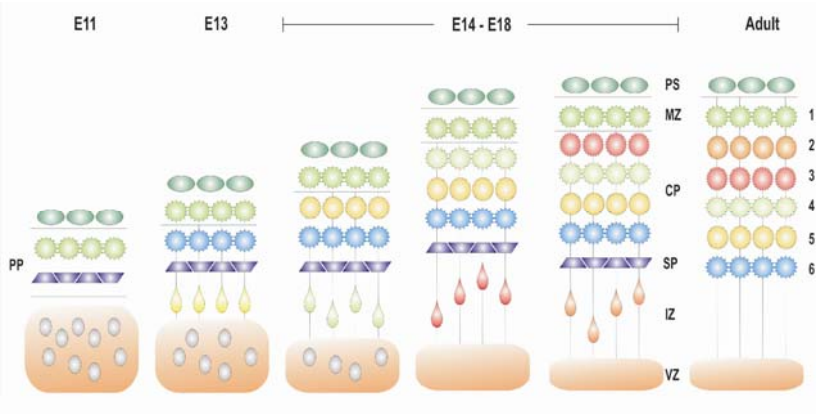

Figure 4: Neocortical layer formation. At E10.5, the preplate (PP) is established by a wave of postmitotic neurons that has migrated from the ventricularzone (VZ) to the pial surface (PS). By E13, a second postmitotic neuronal wave has migrated through the intermediate zone (IZ) and has split the PP into the marginal zone (MZ) and subplate (SP) creating the cortical plate (CP). During E14-18, subsequent waves of neurons expand the CP in an inside-out fashion, as each wave of neurons passes its predecessors to settle underneath the MZ. The SP degenerates, leaving behind a six-layered neocortex. Modified from [8].

This layering occurs “inside out” and is characterized by early-born neurons residing in deeper layers of the cortical plate while later-born neurons, occupy more superficial layers. The remaining subplate degenerates once the cortical plate has been fully established and leaves behind a six-layered neocortex [8].

3.1.4 Mouse strains with defects in cortical architecture

The description of mutant mouse strains all of which share identical anatomical defects in the formation of correct cortical architecture, prompted scientists to believe that the genes affected in these mutants might be part of a signaling cascade governing the correct layering of the developing mouse brain.

3.1.4.1 reeler

In the early 1950’s, Falconer DS first described a mouse line with severe ataxic features, impaired motor coordination and tremors [21]. Nearly 50 years later the gene responsible for this phenotype was cloned and termed reelin [22]. The phenotype in rodents is most prominent in the cerebral cortex, where instead of the six neuronal layers forming in the characteristic “inside out” manner, neurons in the *reeler* brain fail to reach their correct locations in the developing brain. Malformations can also be seen in the cerebellum and other laminated brain regions [22]. In humans, loss of reelin results in a disease referred to as Norman-Roberts type of Lissencephaly [23] which has a similar phenotype when compared to the mouse model.

3.1.4.2 dab1$^{-/-}$ (scrambler, yotari)

A few years after successful cloning of the reelin gene, two other mouse strains were identified that were phenotypically indistinguishable from *reeler* mice, but were caused by a mutation in the dab1 gene. These mouse strains were termed *scrambler* and *yotari* [24]. Independently, an additional mouse strain was generated by targeted deletion of dab1 [25]. As *reeler* and *dab1*$^{-/-}$ animals had an indistinguishable phenotype it was suggested that Reelin and Dab1 function

in a linear signaling pathway. Reelin present in the extracellular space and Dab1 as cytoplasmic protein however, were dependent on specific cell surface receptors that bind Reelin and transmit incoming signals to Dab1.

3.1.4.3 vldlr$^{-/-}$/apoER2$^{-/-}$

When in the 1990s knockout mouse strains for the lipoprotein receptor VLDLR were generated, researchers were expecting a dramatic alteration in the lipoprotein profile of these mice as this receptor was known to bind apolipoproteins in the blood circulation. However, lipoprotein profiles of *vldlr* knockout mice **(*vldlr*$^{-/-}$)** showed no difference to wild-type littermates and extensive studies failed to reveal any significant phenotype in homozygous knockout mice, with the sole exception that the animals were somewhat smaller and leaner than their wild-type littermates. Male and female mice homozygous for a disrupted vldlr allele were viable and fertile and produced litters of normal size. When looking at specific brain regions, differences between wildtype littermates and homozygous knockouts became more obvious. Neurons in the hippocampus and dentate gyrus were more loosely associated, the cerebellum was smaller and less foliated and the granule cell layer appeared less compact with fewer cells. Cortical lamination showed only a mild phenotype with neurons arranged in a radial pattern [12].

Generation of homozygous knockout lines for apoER2 ***(apoER2*$^{-/-}$)** also revealed grossly normal phenotypes apart from a reduced fertility of the males. As in *vldlr*$^{-/-}$ mice, subtle defects were only noticed when examining certain brain regions. Neurons of the dentate gyrus were not only less compact organized but clearly split into two layers. The phenotype in the cerebellum was less severe but clearly showed a marked reduction in size. The lamination defect of the neocortex was more pronounced than in *vldlr*$^{-/-}$ mice. The distinct neuronal layers were indistinguishable but nevertheless horizontally orientated [12]. Specifically, there was no ataxia in either of the single receptor knockout strains, a hallmark of *reeler* mice.

Although first analysis of the corresponding single knock out mouse strains, of

apoER2 and *vldlr,* were rather deflating, the function of these receptors became most evident when both were knocked out simultaneously and strikingly displayed a *reeler* phenotype including inverted cortical layering, hypoplasia of the cerebellum, ataxia, wide gait and tremor [12]. This was the first direct evidence linking both lipoprotein receptors to a function in neuronal migration in embryonic brain development. Moreover these findings established a hitherto unidentified linear signaling cascade controlling cell positioning during mammalian brain development in which VLDLR and ApoER2 bind extracellular Reelin and transmit the signal to the cytoplasmic protein Dab1.

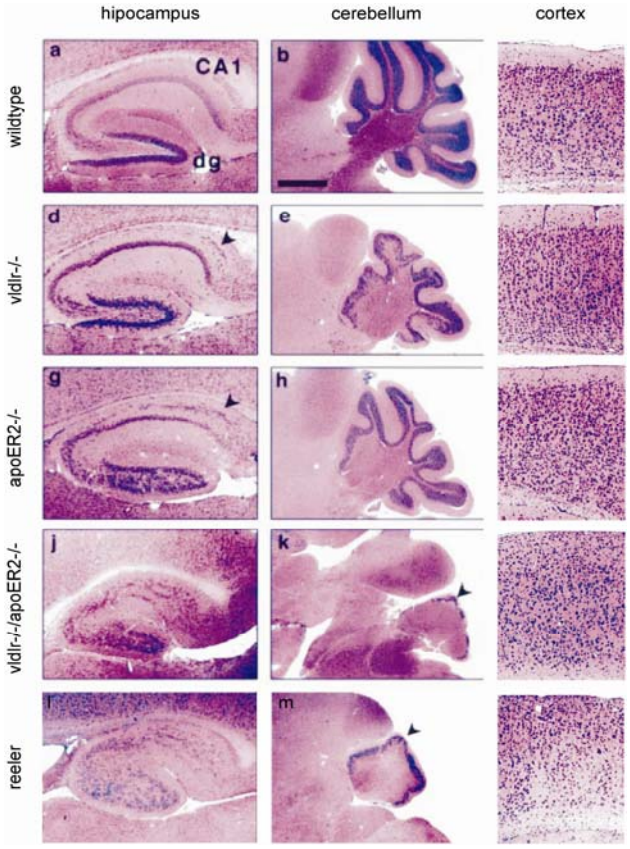

Figure 5: Anatomy of hippocampus, cerebellum and cortex in wildtype, *vldlr*$^{-/-}$, *apoER2*$^{-/-}$, *vldlr*$^{-/-}$*/apoER2*$^{-/-}$ double knockout and *reeler* mice. Hematoxylin/eosin sagittal sections of hippocampus (**a, d, g, j and l**), cerebellum (**b, e, h, k and m**), and cortex of P20 wild type, *vldlr*$^{-/-}$, *apoER2*$^{-/-}$, *vldlr*$^{-/-}$*/apoER2*$^{-/-}$ and *reeler* mice. Arrows in **(d)** and **(g)** point at the split in the CA1 region, which is also a characteristic feature in *reeler* ***(l)*** mice. The arrow in **(k)** points to the small rim of dysplastic granule cells in the double knockout. Adapted from [12].

3.2 The Reelin signaling cascade

Detailed analysis of mutant mouse lines has established that the ECM protein Reelin, members of the LDL receptor family, ApoER2 and VLDLR, and the intracellular protein Dab1 are main mediators of an intricate signaling cascade involved in correct brain development.

Signal transduction is induced by Reelin via the plasma membrane and requires at least VLDLR or ApoER2. Binding of Reelin-dimers to the ligand binding domains of VLDLR and/or ApoER2 leads to dimerization or oligomerization of the corresponding receptors [26], which are then able to induce phosphorylation of Dab1. Interaction with the receptors is mediated by binding of Dab1 via its PTB domain to the unphosphorylated NPxY motif in the cytoplasmic tail of VLDLR and/or ApoER2 [27], after which it becomes phosphorylated on two distinct tyrosine-residues, Y198 and Y220 [28] by members of the Src family of kinases (SFK). To be a substrate for tyrosine phosphorylation, Dab1 has to be primed by phosphorylation of serine/threonine residues by cyclin-dependent kinase 5 (Cdk5). This phosphorylation event however, occurs independently of the presence of Reelin [29].
Fyn seems to be the main kinase mediating Dab1 phosphorylation *in vivo* but can be compensated for by Src and to a lesser extent by Yes [30, 31]. Although Src can phosphorylate all five tyrosines of Dab1 *in vitro*, Y198 and Y220 represent the major sites of Reelin-induced Dab1 phosphorylation in embryonic neurons [32]. Abl is not involved in Dab1 phosphorylation [30].
Dab1 phosphorylation stimulates phosphatidylinositol 3-kinase (PI3-K) regulatory subunit p85 alpha, resulting in activation of AKT/protein kinase B (PKB) and inhibition of glycogen synthase kinase 3 beta (GSK3β), a major kinase for the microtubule-associated protein tau [13, 33]. In addition to PI3-K, other proteins have been shown to interact with Dab1 in a Reelin-dependent and phosphorylation state-dependent manner. These include lissencephaly 1 (Lis1) [34], Tau Nck (noncatalytic region of tyrosine kinase) adapter protein β (Nckβ) [35], Crk family members [36-38] and neuronal Wiskott-Aldrich

syndrome protein (N-WASP) [39], all of which are involved in microfilament organization and hence in cell migration.

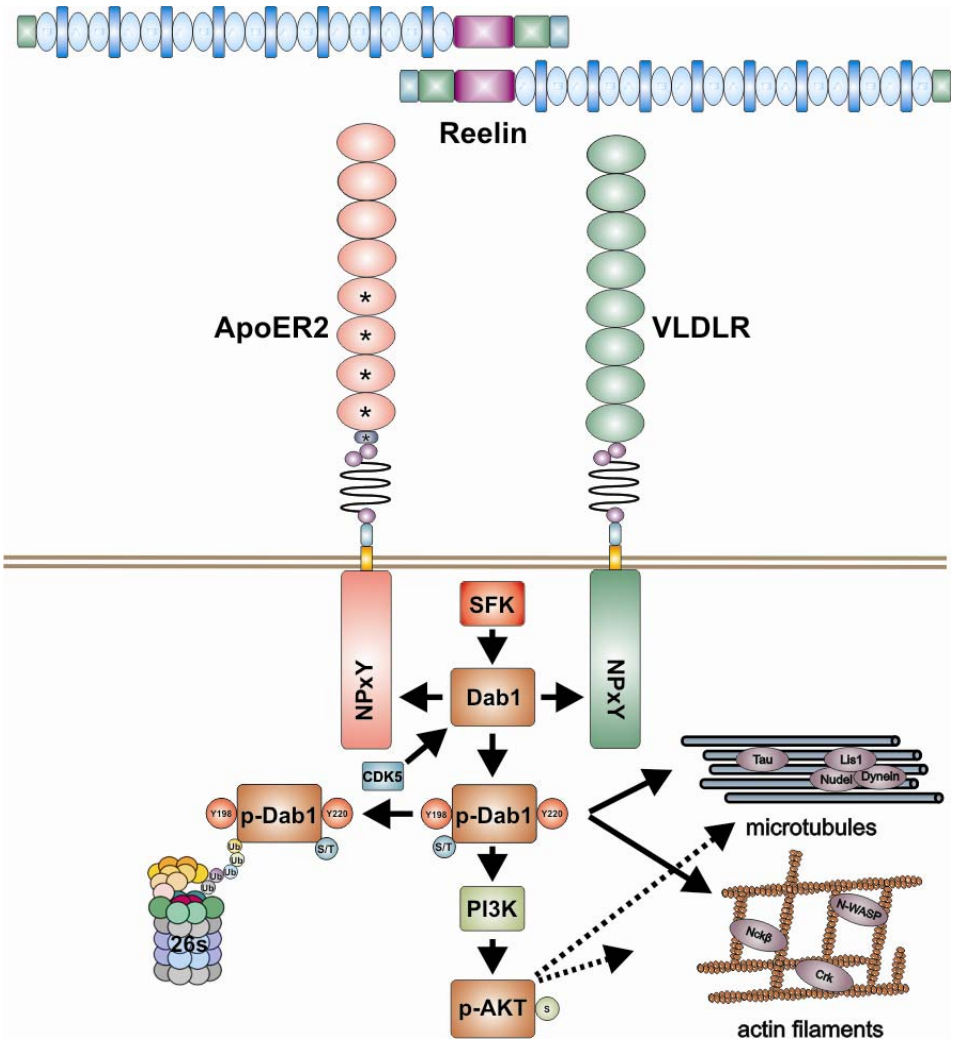

Figure 6: The Reelin signaling cascade. Reelin dimers bind to ApoER2 and VLDLR which results in dimerization or oligomerization of the receptors. Dab1 is serine/threonine phosphorylated by (Cdk5) which makes it a substrate for tyrosine phosphorylation by SFK. While Cdk5 acts independently from the Reelin signal, tyrosine phosphorylation is induced by Reelin dependent clustering of ApoER2 and VLDLR. [13]. Phosphorylated Dab1 induces cytosceletal rearrangement by interacting with microtubule binding proteins like Lis1, Nudel and Dynein, and regulates actin filaments by interaction with N-WASP, Nckß and Crk. Tyrosine phosphorylated Dab1 can then either interact with phosphoinositide-3-kinase (PI3-K) which leads to activation and serine phosphorylation of AKT or becomes polyubiquitinated and degraded via the 26s proteasome pathway. Hatched arrow lines indicate that it is not known whether phosphorylation of AKT is directly involved in cytosceleton rearrangement.

In an *in vitro* model, it was shown that Dab1, in response to Reelin, becomes polyubiquitinated and degraded via the proteasome pathway, which depends on

the phosphorylation of Dab1 at tyrosine residue Y198 and on the E3 ubiquitin ligase component Cullin 5 (Cul5). Cul5 forms complexes with SOCS (suppressors of cytokine signalling) proteins, that bind to phosphorylated Dab1 and target it for degradation [40]. As tyrosine phosphorylation of Dab1 is required for its degradation, this ensures a transient response to the Reelin signal. Non-tyrosine phosphorylated Dab1 is stable with a half-life time of 12 h, but shows a decreased half-life time of about 3 h when tyrosine phosphorylated.

3.2.1 Reelin co-receptors

As neither VLDLR nor ApoER2 contain a kinase domain in their cytoplasmic tails it was quite puzzling that the key event in activating the Reelin signaling cascade was tyrosine phoyphorylation of Dab1. It was therefore proposed that Reelin binds other cell surface receptors which in turn bind at least one kinase on their intracellular tails which could then cluster with VLDLR and ApoER2. Interesting candidates where identified to be members of the integrin family of proteins.

Integrins are the major cell surface receptors for the extracellular matrix (ECM) comprising a large family of receptor molecules forming hetero-dimers which are involved in ECM as well as cell-cell interaction. In the developing mouse cortex, neurons have been shown to specifically express a subgroup of integrins, the α3β1 integrin. They are primarily found in the proliferating cells of the ventricular zone and the intermediate zone. Blocking α3β1 integrin in *in vitro* cortical migration assays inhibited neuronal migration by 40%. Further, in mice mutant for the α3 subunit, cortical neurons preferentially adhered to other neurons than to the radial glia scaffold leading to abnormal cortical layer formation similar to the *reeler* phenotype. These results indicate that α3β1 integrins seem to be involved in the maintenance of optimal neuron-to radial glia scaffold adhesion to enable organized layering of the cortex [41].
Reelin has previously been shown to induce reduction of cortical neuronal migration speed and detachment of neurons from glia scaffold *in vitro* and *in*

vivo. This Reelin-mediated detachment of neurons from radial glia was found to depend on a Reelin-α3β1 integrin specific interaction, as Reelin failed to measurably affect neuronal migration after depletion of this specific integrin. α3β1 integrin expression was further co-localized to Dab1 expressing cells in the developing cortex leading the authors to speculate that Reelin may form a complex with α3β1 integrin, ApoER2 and VLDLR, coupled with an endocytosis driven removal of α3β1 integrin from the cell surface which in turn leads to a dissociation of neurons from their glial scaffold and initiating a migration stop [42]. However, as the integrin family comprises a vast amount of family members it is very likely that one can compensate for the other. Furthermore, it was shown that α5 integrin can also bind Reelin and thus is likely to compensate, at least partially, for the α3 defect or might even work in collaboration with α3β1 to facilitate the observed phenotype [41].

Another model has implicated protocadherins of the CNR family in recruiting kinases to the Reelin-receptor-Dab1 complex [43]. As yet confirmation of this observation has failed und remains to be clarified.

3.2.2 Dab1 phosphorylation

3.2.2.1 5F-Dab1

To determine whether the presence of Dab1 or tyrosine phosphorylation of Dab1 is essential for the transmission of the incoming Reelin signal, Howell *et al.* generated a mouse line in which the Dab1 protein had all the potential tyrosine phosphorylation sites mutated. This mutant protein was not tyrosine phosphorylated during brain development and was not upregulated to the extent observed in the *reeler* or the *apoER2* and *vldlr* receptor mutants. Animals expressing the non-phosphorylated Dab1 protein displayed a phenotype similar to the dab1-null mutant and *reeler* mice , which eventually led to the conclusion that Dab1 tyrosine phosphorylation and not downregulation of Dab1 protein is required for Reelin signaling [28]. In reciprocal experiments, most but not all features of *dab1*$^{-/-}$mutants were rescued by replacing the gene with a partial

cDNA coding for the PTB domain and the region corresponding to the tyrosine residues of Dab1. This indicated that tyrosine phosphorylation of Dab1 is necessary but not sufficient for the function of Dab1 [44].

3.2.2.2 SFK

As a consequence of Reelin binding to ApoER2 and VLDLR, Dab1 becomes phosphorylated on five distinct tyrosine-residues by members of the Src family of kinases (SFK) [28]. Although Fyn has been proposed as the main kinase in mediating this process, an objection is raised by the observation, that neither $Fyn^{-/-}$, $Src^{-/-}$ nor $Fyn^{-/-}/Src^{-/+}$ mutants posses a *reeler*-like phenotype, possibly due to functional redundancy [30]. However, treatment of brain slices with PP2a, a specific inhibitor for SFK, induces the characteristic *reeler* like phenotype. (Yossin and Goffinet, unpublished observation)

3.2.3 Downstream of Dab1

At present it is not known which pathways downstream from Dab1 are involved in Reelin signaling. C-jun N-terminal kinase interacting protein's (JIP's) might be candidates that mediate the incoming Reelin signal to the cytoskeleton and promote structural reorganization and migration of the cell. JIP can bind to the intracellular tails of ApoER2 and VLDLR and thereby activate further kinase pathways like MAPKK and JNK, which assemble on JIP [45]. Further, it has been proposed that JIP facilitates the presence of ApoER2 in the tip of neuritic processes by coupling it to kinesin, thereby allowing the process to bind extracellular Reelin and possibly activate the signaling cascade leading to coordinated cytoskeleton rearrangement and movement of the cell body [46].
Recently, it was also proposed that Reelin protects PC19 cells from retinoic acid induced cell death in an *in vitro* cell culture model by phosphorylation of the Bcl-2/Bcl-XL associated death promoter (BAD) at serine-136 [47]. This possible role of Reelin as anti-apoptotic agent remains to be further investigated.

3.3 Reelin signaling in neocortical development

The finding that mice mutant for components of the Reelin signal transduction cascade all share the same anatomical defect in cortical layering, indicated the involvement of a linear signal transduction cascade in the correct formation of cortical architecture.

In mice which are mutant for components of the Reelin pathway, migrating neurons are unable to bypass pre-existing layers which results in an unsplit preplate and inverted, disorganized cortical layers. More specifically, the second wave of neurons, emerging from the ventricular zone which in the wildtype situation splits the preplate into subplate and marginal zone, fails to do so and accumulates beneath the preplate forming a structure referred to as superplate. All the following waves of neurons arrange beneath this superplate and hence lead to an inverted “outside in” layering of the cortex, where oldest-born neurons are found in the outer layers and younger neurons in the deep layers of the cortex.

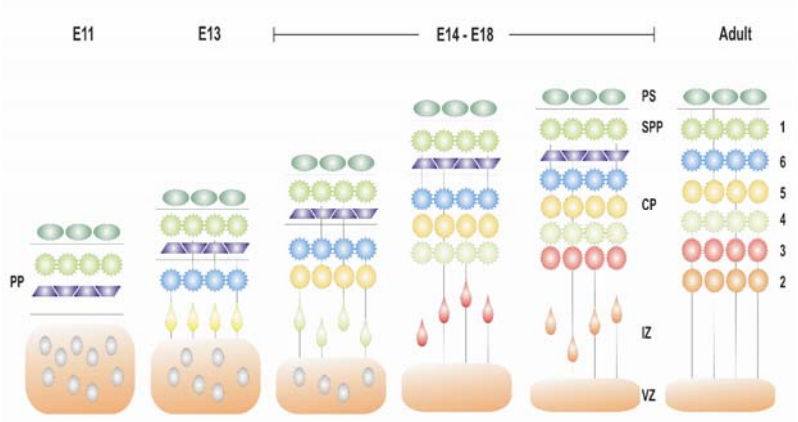

Figure 7: Defective neocortical layer formation in Reelin pathway mouse mutants. In mice with mutations in the Reelin pathway, the preplate (PP) does not split and forms a structure called the superplate (SPP). The cortical plate (CP) forms under the SPP and is inverted, indicating that late-migrating neurons are unable to migrate past their predecessors. Early-migrating and late-migrating neurons are positioned in the superficial and deep layers of the CP, respectively, and layering is disorganized. Modified from [8].

Several hypotheses have been proposed to explain the function of Reelin in neuronal layer formation: In the most recent hypothesis on the function of

Reelin in generating distinct neuronal layers, a “Detach and Stop” model was put forward [9]. In this model, early-born neurons are only able to migrate a short distance before they encounter Reelin producing MZ cells and thereby arrest their migration earlier than later-born neurons which, with increasing thickness of the cortical plate, migrate a longer distance and overtake their predecessors before encountering the Reelin source which again produces a stop-signal [48].

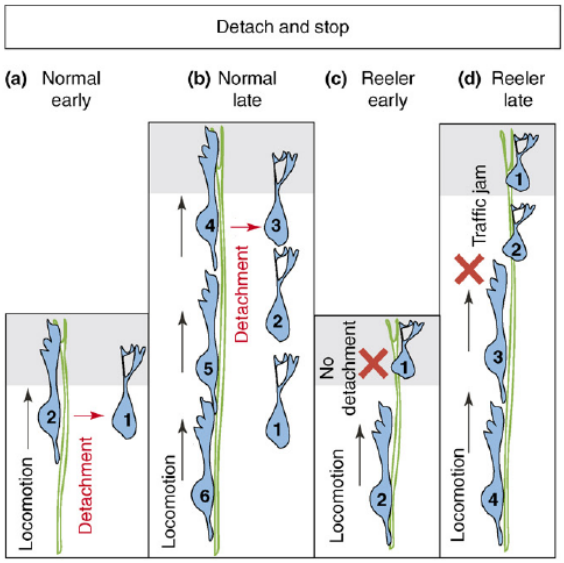

Figure 8: “Detach and Stop” model for Reelin mediated cortical layering. **(a)** During early development future layer VI neurons migrate along radial glia until they reach the Reelin secreting marginal zone (MZ) instructing them to detach, settle and differentiate. **(b)** Subsequent waves of neurons follow the same principle and rest above preexisting layers. **(c)** In the reeler mouse, layer VI neurons fail to detach from the radial glia scaffold and migrate into the MZ, hence **(d)** preventing later born neurons to pass preexisting layers, causing a “traffic jam”. (MZ in grey, neurons in blue are numbered in order of birth, radial glia in green, Reelin dependent events in red). Taken from [9].

Alternatively, it has been proposed that Reelin acts as a repellent for early neuronal populations [49] or by interrupting the association between migrating neurons and their radial glia scaffold [42]. However, all of these hypotheses are not consistent with the finding that ectopically expressed Reelin in the VZ fails to induce a premature termination of neuronal precursor migration or the formation of cortical plate heterotropia in the VZ [50]. Further, it was shown that ablation of CR cells did not impair correct inside-out lamination of the cortex [51] indicating that other sources of Reelin secretion might be sufficient for normal

cortical development.

Another model is based upon the finding that the initial, radial glia independent, movement of cortical neurons past the subplate is Reelin dependent while later, glia dependent migration relies on other factors [52]. In this “Detach and Go” model [9], future layer VI neurons extend a leading edge towards the marginal zone where they encounter the Reelin source that instructs them to translocate through the subplate and settle in their corresponding layer. Later in development, when younger neurons that migrate along radial glia scaffolds, encounter Reelin, they are instructed by Reelin to detach from the glial fiber and initiate nuclear translocation to pas preexisting layers and settle above them.

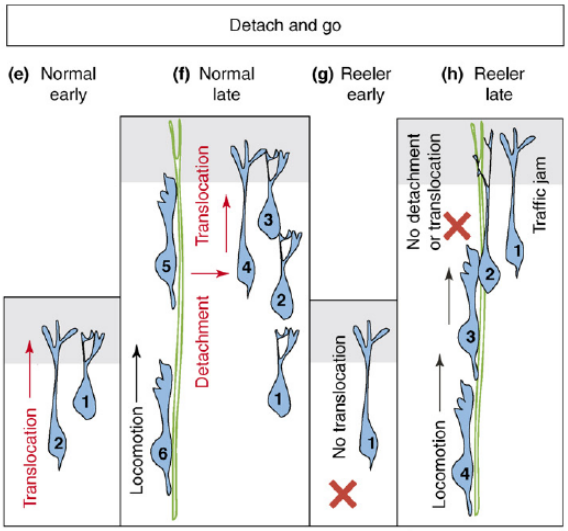

Figure 9: “Detach and Go” model for Reelin mediated cortical layering. **(e)** During early development, future layer VI neurons encounter Reelin in the marginal zone (MZ) instructing them to initiate nuclear translocation just beneath the MZ. **(f)** Later born neurons migrate along radial glia until they reach the Reelin secreting MZ where they are instructed to detach and initiate nuclear translocation above preexisting neuronal layers. **(g)** In the reeler mouse, layer VI neurons fail to undergo nuclear translocation and **(h)** pile beneath the later born neurons which migrate along radial glia Reelin independently but fail to initiate the final Reelin dependent nuclear translocation past preexisting layers into the cortical plate, causing a “traffic jam”. (MZ in grey, neurons in blue are numbered in order of birth, radial glia in green, Reelin dependent events in red). Taken from [9].

In the *reeler* mouse initial translocation of layer VI neurons is already prevented. Subsequent arriving waves of younger neurons, which initially migrate Reelin-independently along radial glia, are unable to pass layer VI neurons and remain

below them because the final Reelin-dependent nuclear translocation to the top of the cortical plate is prevented. Hence, neurons align in the classical inverted layering phenotype of *reeler* mutants.

3.3.1 Taking a closer look at Reelin pathway components

3.3.1.1 Reelin

The reelin gene was cloned in 1995 and was found to encode a very large mRNA of approximately 12 kb with an open reading frame of 10,383 bp [22]. It is composed of 65 exons, spreads over a genomic region of 450 kb [53], and encodes a large glycoprotein of 3461 amino acids with a relative molecular mass of approximately 430.

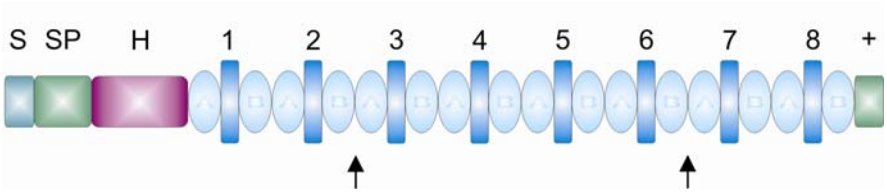

Figure 10: Structure of the Reelin protein. The sequence begins with a signal peptide of 27 residues (S), followed by a region with similarity to F-Spondin (SP), a unique region (H) followed by eight repeats of about 360 amino acids. Each repeat contains an epidermal growth factor (EGF) motif at the centre, flanked by two sub-repeats, A and B. The protein terminates with a stretch of 33 amino acids that is rich in basic residues (+).The two arrows point to the cleavage sites responsible for Reelin processing *in vivo*.

The protein harbors an N-terminal signal peptide, followed by a region with homology to F-Spondin, a consensus cleavage site which leads on to eight consecutive repeats, each containing two subdomains separated by EGF-like motifs [22], and a highly charged C-terminal region that was shown to be essential for secretion [54]. Reelin also contains two protease cleavage sites located between subdomains A and B after repeats two and six. *In vivo,* these sites are cleaved by an as yet unknown metalloproteinase [55], generating a total of six predicted proteins. In body fluids like cerebrospinal fluid or plasma, Reelin is mainly present in its cleaved form and can hardly be detected as full-length protein [56, 57]. Although the functions of most of the fragments remain largely unknown, the central fragment containing repeats 3–6, was shown to be

necessary and sufficient to induce Dab1 phosphorylation *in vitro* and to rescue preplate splitting in a slice culture assay with brains derived from *reeler* mice [58].

The highest level of transcript expression during embryonic development was found in Cajal-Retzius (CR) neurons in the marginal zone (MZ) of the telencephalon [59]. Cajal-Retzius cells are early generated transient neurons located in the MZ of the neocortex and hippocampus and were initially described by Ramon Cayal and Gustaf Retzius [20]. Reelin is not exclusively expressed in the MZ, as high levels were also seen in the olfactory bulb, the external granular layer of the cerebellum and, particularly at early developmental stages, tectum and spinal cord. Beside neuronal tissues, Reelin is also expressed at lower levels in peripheral organs such as liver and kidney [59]. In addition to its signaling properties, Reelin also acts as a serine protease on adhesion molecules of the extracellular matrix, thereby possibly facilitating cellular migration [60]

Early work on Reelin binding provided evidence that the N-terminal region of Reelin is actually not required for binding VLDLR and ApoER2 [61]. In the same year however, contradicting evidence was provided, claiming that the CR50 antibody, directed against an epitope in the N-terminal region of the protein, interfered with binding of full-length Reelin possibly through a steric mechanism [56]. Together, these data indicate that the N-terminus may contribute to, but is not sufficient for, Reelin signaling.

3.3.1.2 Disabled 1 (Dab1)

Dab1 is an intracellular adaptor protein that is expressed by Reelin-responding cells, predominantly in the brain. In its N-terminal region it harbors a PTB domain which interacts with high affinity with phospholipid-bilayers rich in phosphoinositides and membrane anchored proteins containing NPxY sequences. Interestingly, the Dab1 PTB domain does not bind to tyrosine-phosphorylated peptide ligands [27]. Following the PTB domain is a region that contains five tyrosine (Y) residues, two of which (Y198 and Y220) are

phosphorylated in response to Reelin, leading on to a C-terminal region of unknown function.

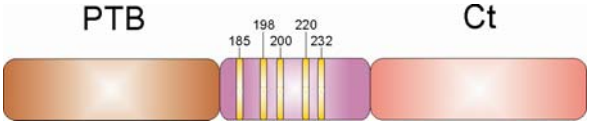

Figure 11: Structure of the Dab1 protein. The sequence begins "N-terminal" with a PTB domain of 180 residues (PTB), followed by a region with tyrosine residues. Five tyrsosine sequence begins with a PTB domain of 180 residues (PTB), followed by a region with tyrosine residues. Five tyrsosine residues are present within this region at positions 185, 198, 200, 220 and 232. Residues 198 and 220 are phosphorylated upon Reelin binding to ApoER2 and

Due to a number of alternative splicing events, several Dab1 isoforms have been identified. The 5`UTR spreads over 900Kb and contains at least four different 5`UTR's and four associated promoters. One of these UTR's is exclusively found in neuronal tissue and is developmentally regulated [62].

3.3.1.3 Very low density lipoprotein receptor (VLDLR)

The multifunctional VLDL receptor is part of the large LDL receptor family and shares many structural similarities with its most closely related family member, the LDLR. VLDLR was originally isolated from a rabbit heart cDNA library by cross-hybridization to cDNA corresponding to the ligand binding domain of the LDLR.

The original mRNA identified was as a 3.9 kb transcript, that was shown to be most abundantly expressed in heart, skeletal muscle and adipose tissue and barely in liver [63], while a larger variant of 5.2 kb was predominantly expressed in skeletal muscle [64]. VLDLR transcripts were also identified in the brain in resting and activated microglia, and cortical neurons. It was shown that two exons of the VLDLR mRNA are differentially spliced in the mature receptor mRNA. One set of splice forms gives rise to receptors containing an extracellular O-linked sugar domain near the transmembrane region of the molecule. The other set of splice forms lacking this domain appear to be brain-specific, and is responsible for the presence or absence of one of the cysteine-

rich repeat regions in the binding region of the molecule [65]. Due to its expression pattern and its high affinity for apolipoprotein E (apoE), the VLDLR was initially thought to function in the delivery of triglyceride rich lipoproteins to peripheral tissues. However, studies in homozygous knock out mice for the VLDLR revealed that these animals had a normal lipoprotein profile and merely a slight decrease in body weight and adipose tissue mass [66], indicating that it is most likely not a major receptor involved in lipoprotein catabolism. Despite the similarity between the LDL and VLDL receptor, the VLDL receptor also binds ligands other than those involved in lipid metabolism, like the urokinase plasminogen activator (uPA)/plasminogen activator inhibitor-1 complex [67], Reelin [56, 61] and Thrombospondin [68].

3.3.1.4 Apolipoprotein E receptor 2 (ApoER2)

Like the VLDL receptor, ApoER2 was identified during a genome-wide search for proteins bearing homology to the LDL receptor. While in chick, ApoER2 (LR8B) occurs as variant with either seven or eight ligand binding repeats, which are both predominately expressed in the brain [69], in mouse the receptor exists with only five LDL receptor ligand-binding repeats, comprising repeats 1-3, 7, and 8. Further analysis of mRNA derived from murine brain revealed the existence of two additional transcripts, one lacking repeat eight while in the other, repeat eight is substituted by a 13-amino acid insertion with a consensus site for furin cleavage arising from an additional small exon present in the murine gene. None of the transcripts in the mouse, however, contain repeats 4-6 [70]. Cleavage by furin leads to secretion of a soluble receptor fragment consisting of the entire ligand-binding domain. This receptor fragment inhibits Reelin signaling in primary neurons, indicating that it can act as a dominant-negative receptor in the regulation of Reelin signaling during embryonic brain development [71]. Further complexity arises from an alternatively spliced intracellular domain which encodes a 59 aminoacid proline rich insert that is capable of binding JIP-1 and JIP-2, two scaffold proteins originally described to be part of the MAP kinase pathway [69, 72, 73]. ApoER2 can further undergo

proteolytic processing of its extracellular domain which depends on the glycosylation state of the receptor, which in turn is regulated by the alternative splicing of an exon encoding several O-linked sugar attachment sites, reminiscent of the VLDL receptor [13]. Homozygous knockout mice are superficially normal but male animals are sterile, implying ApoER2 to be involved in male sperm production [12].

3.3.1.5 The LDL receptor family

Both ApoER2 and VLDLR are members of the LDL receptor gene family which arose early during metazoan evolution and is exclusively found in the genomes of multicellular eukaryotic organisms. In mammals, a total of seven core members of the gene family have been identified so far. These members include the LDL receptor (LDLR) itself, the very low density lipoprotein receptor (VLDLR), the apolipoprotein E receptor 2 (ApoER2 or LRP8), the LDLR-related protein (LRP), LRP1b, MEGF7 and Megalin (gp330 or LRP2) [74].

For a long time the function of lipoprotein receptors was believed to be confined to the endocytosis of macromolecules and subsequent transport to the lysosome for degradation. However, it is now well established that lipoprotein receptors are also directly involved in the transmission of extracellular signals across the plasma membrane including modulation of cytoskeletal organization by coupling of cytoplasmic adaptor proteins to the intracellular domains of the lipoprotein receptors [75] and regulation of neuronal migration in the embryonic [74] and postnatal mouse brain [11].

Structural organization of the LDLR family members

The core members of the LDL receptor gene family are characterized by five distinct functional domains present in characteristic numbers. These domains are (i) an amino-terminal ligand binding domain composed of multiple cysteine-rich repeats (ligand binding repeats of complement type A, also termed LA repeats) of about 40 aa, (ii) an epidermal growth factor (EGF) precursor

homology domain with modules of about 50 aa, termed YWTD repeats, which mediate the acid-dependent dissociation of the ligands from the receptors [76], (iii) a serine-and-threonine rich O-linked sugar domain which is partly responsible for the stability of the protein [77], (iv) a trans-membrane domain of 20 aa and (v) a cytoplasmic domain containing one or more consensus NPXY copies which are potential endocytosis signals [78-80].

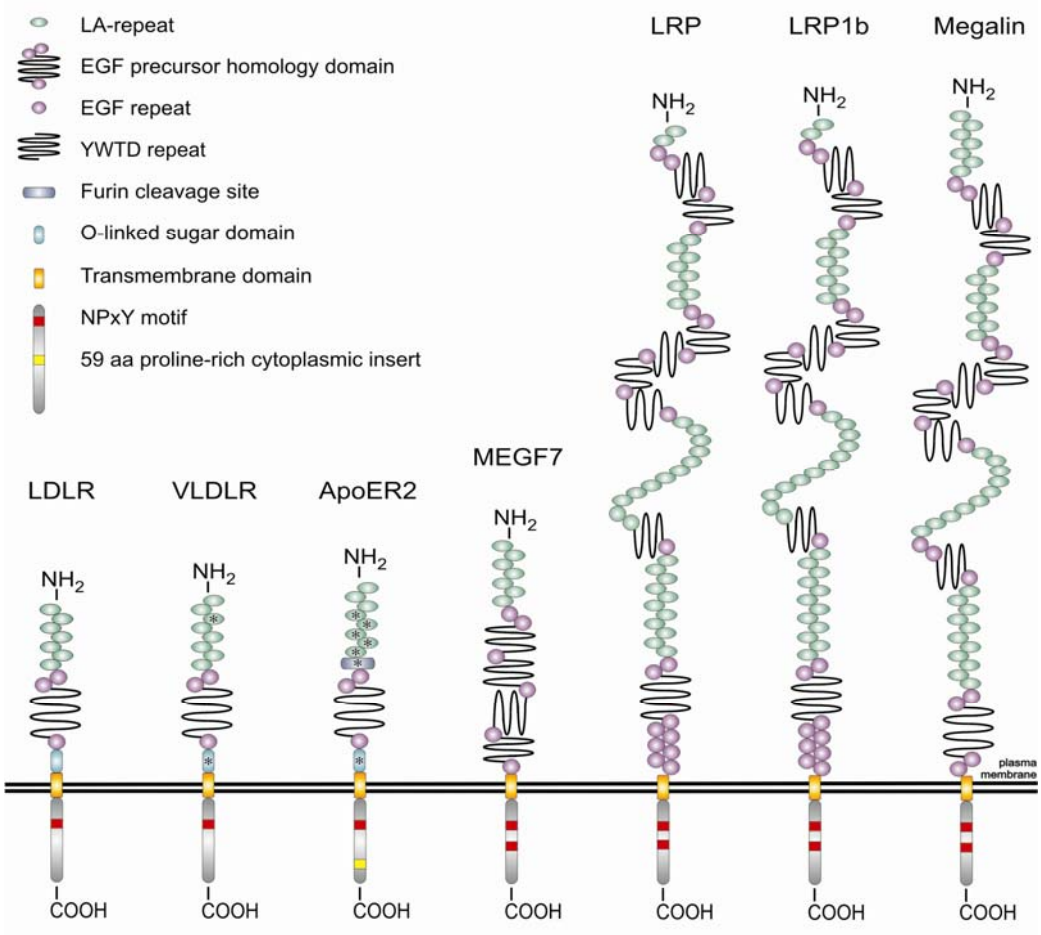

Figure 12: Structural organization of the LDLR family members. The LDLR family members contain different numbers of ligand binding repeats at the N-terminus, followed by the EGF precursor homology domain, the O-linked sugar domain and the transmembrane domain. For all members of this family the cytoplasmic tail at the C-terminus contains at least one NPxY motif. Marked domains in ApoER2 and VLDLR (*) as well as the furin cleavage site of ApoER2 are expressed in some isoforms of the respective receptors due to differential splicing. Another special feature of ApoER2 is the proline-rich insert exclusively present within the cytoplasmic tail of a receptor sub-population. LRP, LRP1b and Megalin are much larger than the other core members of the LDLR family and contain multiple clusters of LA-repeats and EGF precursor homology domains. Modified from Sarah Duit

A common property of LDL receptor family members is their ability to bind the receptor-associated protein (RAP). This protein functions physiologically as a chaperone for the receptors in the endoplasmic reticulum (ER) where it prevents the premature interaction of a broad spectrum of ligands with the receptors [81] and may also assist in their folding [82]. Three other proteins that do not fully comply with the strict structural requirements to be classified as core members of the LDL receptor family are LRP5, LRP6 and LR11 (SORLA).

The low density lipoprotein receptor (LDLR)

The best studied member of the LDL receptor family is the LDL receptor itself [83]. It is the most important component of a tightly controlled machinery regulating cholesterol homeostasis. This lipoprotein receptor is frequently mutated in an inherited human genetic disease termed familial hypercholesterolemia (FH), characterized by highly elevated plasma cholesterol, premature artherosclerosis and the appearance of heart attacks within the first two decades of life. All of these clinical symptoms arise through the inability of hepatocytes to remove LDL from the circulation.

Membrane bound transcription factors that are sensitive to membrane cholesterol levels have been shown to be responsible for the expression of the LDLR, and other components necessary for cholesterol homeostasis [84]. LDL-derived cholesterol and its intracellularly generated oxidated derivatives mediate a complex series of feedback control mechanisms that protect the cell from over-accumulation of cholesterol. Until now, no functions other than cholesterol regulation and LDL removal have been shown for this receptor [85].

The LDL receptor related protein (LRP1)

LRP1 is one of the largest cell surface molecules abundantly expressed in liver, where it mediates the hepatic uptake of circulating chylomicron remnants [86], serpin-enzyme complexes [87] and proteinases of the fibrinolytic pathway [88]. Besides its well established role in the liver, it is also highly expressed in the brain where it has been genetically linked to late onset Alzheimers disease. LRP1 directly interacts with the amyloid precursor protein (APP), a trans-

membrane protein, cleavage of which generates the amyloid β (Aβ) peptide which is the main component of the cerebral amyloid plaques that occur in Alzheimer's disease. Cells lacking LRP1 have increased APP plasma levels and an impaired Aβ reduction. Hence LRP1 plays an important role in the balance between synthesis and clearance of the Aβ peptide. Furthermore, LRP1 has an influence on synaptic plasticity due to PSD-95 mediated interaction with NMDA receptors induced by binding of activated α_2-macroglobulin to LRP [89]. Targeted deletion of the LRP1 gene in mice leads to embryonic lethality at day E13.5 [90] demonstrating that LRP1 plays a critical role during development.

LRP1b

LRP1b is highly related to LRP1, sharing 60% amino acid identity. The corresponding gene was originally found to be inactivated in 40% of non-small cell lung cancer cell lines [91], suggesting that LRP1b might play a role in growth regulation or migration of cells. While mouse LRP1b expression is mostly restricted to the brain, human LRP1b expression is more widespread with highest expression levels detected in the brain, adrenal gland, salivary gland, and testis [92]. As LRP1b is widely expressed in human tissue and has a potential function as tumor suppressor, this might implicate LRP1b to play a role in several types of human cancer.

Megalin (LRP2)

Megalin is mainly expressed from epithelial cells on the luminal surface of the renal proximal tubules. Several studies have shown that megalin functions in the trans-epithelial transport of various macromolecules, including the transcobalamin-vitamin B12 complex [93], thyroglobulin [94] and retinol-binding protein (RBP) in complex with retinol (vitamin A) [95]. Besides its known function as endocytotic receptor for apolipoprotein E and B, megalin also plays an important role in the formation of the central nervous system. Homozygous disruption of the corresponding gene leads to a malformation of the forebrain and cephalic midline structure, known as holoprosencephaly [96].

MEGF7 (LRP4)

One of the most recent additions to the LDL receptor family is MEGF7, that was first identified in the late 90's, in a screen for large transcripts containing EGF repeats in the mammalian brain [97]. Recently, it was revealed that MEGF7 deficient mice exhibit a severe malfunction of digit differentiation. Since signaling molecules like wingless/int proteins (Wnts), bone morphogenic proteins (Bmps), fibroblast growth factors (Fgfs) and sonic hedgehog (Shh) are known to be involved in proper limb patterning, these findings are consistent with a role of MEGF7 as a modulator of cellular signaling pathways.

Receptor	Ligands	Functions
LDLR	apoB,apoE, LDL	lipoprotein/cholesterol uptake
VLDLR	apoE, Reelin, lipoprotein lipase	regulation of neuronal migration during embryonic development (cerebellum)
ApoER2	apoE, Reelin	regulation of neuronal migration during embryonic development (hippocampus, neocortex)
LRP1	apoE, chylomicron remnants, APP, α2 macroglobulin,lipoprotein lipase, thrombospondin 1and 2, ...	lipoprotein and protease uptake, modulation of APP processing and intracellular signaling
LRP1b	unknown	unknown
Megalin	apoB, apoE,apoJ,apoH, albumin, cubilin,plasminogen activator, vitamin D binding protein	vitamin homeostasis, renotubular re-absorption of proteins, regulation of thyroid and parathyroid functions
MEGF7	unknown	unknown

Table 1: Core LDL receptor family members, their ligands and known functions. Adapted from [1]

3.4 Neurogenesis and neuronal migration in the adult brain

3.4.1 "Death of a Dogma"

It was long believed that neurogenesis, the continous generation of cells of a neuronal lineage from a multipotent neural stem cell, is restricted to the embryonic period of development. First contradicting evidence came from a study performed in song birds [98] which showed that specific neurons in the adult brain incorporated 3H-labeled thymidine, a marker of DNA synthesis. Nevertheless these studies were viewed as irrelevant to the mammalian brain, as lack of available cell-type specific markers for the immunohistochemical identification of the newly generated cells prevented further confirmation of the data. Only in the 1990's could the central dogma of neuroscience, the dogma that no new neurons are added to the adult brain, be overthrown. Evidence for the functional plasticity of the adult CNS was growing, and studies performed in crustaceans [99], reptiles [100] and mammals [101] were able to refute the dogma of adult neurogenesis being restricted to birds. In the late 90's, adult neurogenesis could also be shown in the primate dentate gyrus [102] and human hippocampus [103].

3.4.2 Adult neurogenesis

Neurogenesis in the adult brain occurs in four discrete regions, (I) the subventricular zone (SVZ) of the lateral ventricle [104], (II) the subgranular zone in the dentate gyrus of the hippocampus [105] and more recently it was also shown (III) in the subcallosal zone between hippocampus and corpus callosum [106] and (IV) in the cerebellum at the boundary between internal granular layer and white matter [107]. In this thesis we will further concentrate only on the SVZ.

The SVZ is the largest germinal area of the postnatal mammalian brain. It is located next to a thin layer of cells that line the lateral ventricles of the brain called ependyma. This region contains at least four different cell types: type E, B, C and A cells. Type E cells are ependymal cells separating the SVZ from the

ventricular cavity. They are in contact with type B cells, which are positive for the astrocytic marker GFAP, and have now been identified to be the self-renewing primary neural stem cells in the SVZ [104]. Type B cells divide to give rise to rapidly dividing transient amplifying, type C, cells which in turn generate the migrating neuronal precursor, type A, cells.

Originally, type E cells were thought to be neural stem cells (NSC), responsible for neurogenesis in the adult brain [108], but it is now well established [104] that these cells are quiescent and therefore not capable of expanding the neural stem cell niche. The observation that both B and C cells were constantly undergoing cell division prompted the guess that one of them might be the long sought after NSC giving rise to A cells. This was indeed verified in *in vitro* experiments when fractions enriched for B and C cells gave rise to large colonies of A cells. At the time quite unexpectedly however, follow up work indicated that B cells, the SVZ GFAP positive astrocytes, were the primary precursors of new neurons [104], as ablation of C and A cells with antimitotic drugs, did not compromise B cells to divide and generate new C and in turn more A cells.

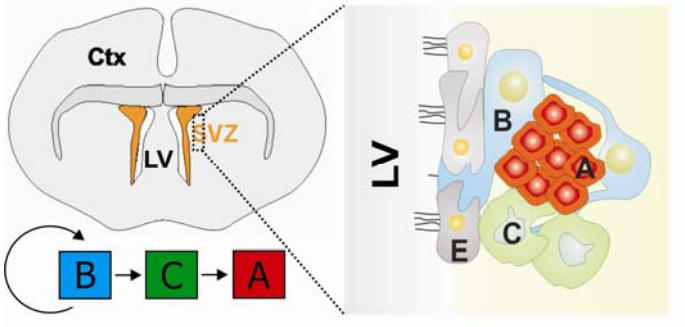

Figure 13: Neurogenesis in the postnatal sub ventricular zone (SVZ). Coronal section through an adult mouse brain. White shows the lateral ventricle (LV) space filled with cerebrospinal fluid. Orange corresponds to the SVZ. Boxed area is shown enlarged. Ependymal E cells line the ventricle and separate the SVZ from the ventricular cavity. B cells are the GFAP positive neural stem cells that give rise to type C, transient amplifying, cells. A cells are committed neuronal precursors that are derived from C cells.

In contrast to other regions of the adult mammalian brain, the olfactory bulb (OB) is continuously supplied with neuronal precursors (A cells) originating from SVZ neural stem cells (B cells) throughout life [109-112]. The OB is a laminated

structure in the vertebrate forebrain involved in olfaction and odour perception. Neuronal precursors coming from the SVZ migrate rostral as cellular chains to the olfactory bulb (OB). Unlike glia-guided migration these neuronal precursors glide along each other using neighboring cells as migration scaffold. These migrating neuronal precursors form the rostral migratory stream (RMS) [109]. A more detailed description of the RMS will follow in later sections.

Following the general concept of stem cells, one might assume that neuronal progenitors born in the SVZ might be equivalent until they reach the olfactory bulb and begin to differentiate. However, recent evidence suggests that neuronal progenitors are heterogeneous before reaching the olfactory bulb. It was shown that neuronal precursors in the SVZ generated mostly granule cells (GCs) in the OB while precursors located in the RMS gave rise to mostly periglomerular cells (PGCs). This means that many periglomerular neuron precursors become fate-restricted at a much more rostral position than granule neuron precursors, indicating a regional-in addition to the temporal-specification of OB interneurons along the rostro-caudal axis, similar as it is seen in the developing telencephalon.

The transcription factors Pax6 and Olig2 are crucial components regulating the commitment of B or C cells towards the status of an A cell. While Olig2 promotes a transit-amplifying precursor state and drives precursors into an oligodendric lineage, Pax6 opposes this role and promotes progression towards the neuronal lineage. Moreover, Pax6 was shown to be downregulated during postmitotic differentiation of GCs while PGCs maintained Pax6 expression in the OB even after final differentiation [113]. These data not only provide deeper understanding of the regional specification of neuronal precursor fates but also allows speculation about the lineage commitment of interneurons exiting the SVZ-RMS axis.

In a similar study it was recently shown that postnatal stem cells in different regions of the SVZ produce different types of neurons. Although they retain the potential to produce astrocytes, oligodendrocytes and neurons, they are restricted in the types of neurons they can generate [7]. This suggests that neural stem cells, against all previous assumptions, rather than being

homogenous, are a restricted and diverse population resembling a mosaic organization in the adult mammalian brain.

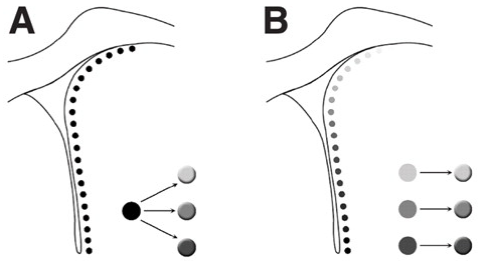

Figure 14: Model for the regional specification of adult neural stem cells. (A) In the classical view of stem cell biology one equivalent stem cell (black dot) gives rise to all other neuronal lineages, **(B)** while recent data suggests a diverse stem cell population that regionally specifies neuronal lineages along the SVZ. Taken from [7].

3.4.3 Postnatal neuronal migration towards the olfactory bulb

3.4.3.1 In the SVZ

As mentioned earlier, neuronal precursors (type A cells) originating in the SVZ, migrate rostral as cellular chains to the most anterior structure of the brain, the olfactory bulb (OB) [110]. This stream of migrating neuronal precursors forms the rostral migratory stream (RMS). The movement of these cells is highly directed without any dispersion of migrating cells into the surrounding tissue, implying the existence of several attracting, repelling and migratory cues or even structural boundaries. The RMS was found to be ensheathed by GFAP positive astrocytes conferring a tube like structure that was originally thought to serve as guidance pattern, preventing diffusion of migrating cells [112]. In an *in vitro* system, perfectly mimicking the migration of neuronal precursors in the RMS *in vivo,* chain migration was observed in the absence of GFAP positive astrocytes [114], demonstrating that SVZ neuronal precursors migrate along each other without the assistance of astrocytes, leaving the function of the glial tube still largely unknown. However, factors secreted by astrocytes, like migration-inducing activity (MIA), appear to enhance the migration of the SVZ neuronal precursors having a direct effect on the number of migrating cells and on the distance they move [115]. Additionally, it is believed that migrating

neuronal precursors coming into contact with the glial tube are induced to switch from a motile phase into a mitotic phase through contact mediated mechanisms.

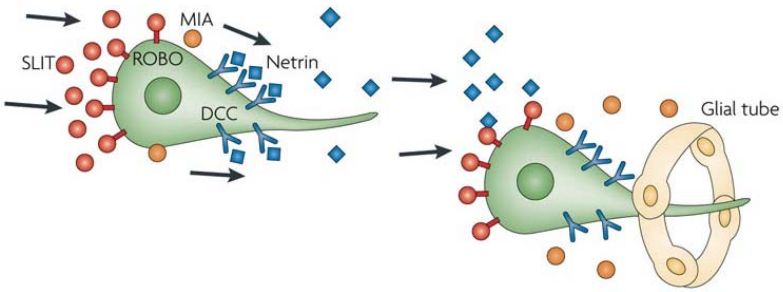

Fig 15: Initiation of migration. The initiation of migration in the adult SVZ is mediated by a combination of chemo-attractive (netrin and DCC), chemo-repellent (ROBO and SLIT) and motogenic (MIA) signals away from the SVZ towards the RMS (indicated by arrows). Taken from [4].

The molecular factors involved in mediating movement along the RMS are only beginning to be identified, but it is likely that a dynamic balance of chemo-attractants and -repellents emanating from the SVZ milieu and RMS are key determinants of this process. The chemo-repulsive molecule SLIT, which is secreted by cells surrounding the SVZ, has been shown to repulse neuronal progenitors from the SVZ into the direction of the OB [116]. The membrane protein ROBO is expressed by neuronal progenitors in the SVZ and functions as receptor for SLIT proteins. Upon binding of SLIT to ROBO, precursors in the SVZ orient away from the SVZ and the surrounding striatal/septal areas, towards the olfactory bulb. “Deleted in colorectal carcinoma” (DCC) possibly through an interaction with netrin-1, also contributes to the direction of migration by regulating the formation of directed protrusions, thereby functioning as a weak chemo-attractive cue [117].

3.4.3.2 Moving along the RMS

Next to chemo-repulsive and -attractive signals a highly coordinated interplay between extracellular cues and cell adhesion molecules, is required for the maintenance of migration in the adult forebrain.

Neural cell adhesion molecule NCAM is a glycoprotein highly expressed on the surface of migrating neuronal precursors in the RMS. Genetic ablation of the protein leads to an accumulation of precursors in the subependymal zone of the SVZ and an undersized olfactory bulb [118]. The polysialated form of the neural cell adhesion molecule NCAM (PSA-NCAM) was also shown to be of significant importance in mediating organization of chain formation in the RMS. Enzymatic removal of PSA resulted in the same phenotype that was observed in the NCAM mutants [119].

Grafting experiments further elucidated the mode of action of PSA-NCAM. PSA-NCAM mutant cells in a wildtype SVZ were able to move toward the olfactory bulb, whereas wild-type cells grafted into a mutant SVZ failed to initiate migration. These experiments provided a clue that a particular migration environment of the SVZ is more critical in generation of the mutant phenotype than a cell autonomous effect [120]. The neuregulin receptor ErbB4 was also shown to promote tangential migration in the adult RMS, since conditional ablation of ErbB4 in the SVZ and RMS lead to altered chain organization and migration and deficits in the placement and differentiation of olfactory interneurons [121].

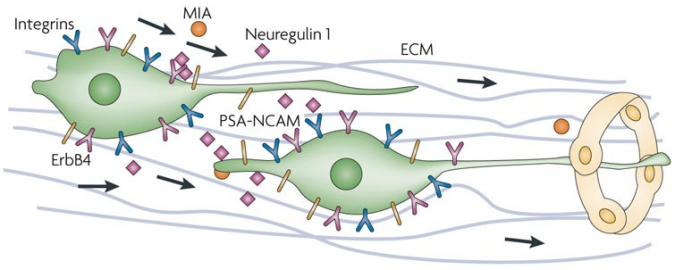

Fig 16: Maintenance of migration. Maintenance of chain migration is dependent on a combination of ECM-integrin interactions. PSA-NCAM mediated adhesion, motogenic (MIA) signals and netrin-ErbB4 interactions. Arrows indicate migration towards the OB. Taken from [4].

Using fibered confocal microendoscopy, it has been estimated that neuronal precursors migrate at speeds of 40 -80 µm / h *in vivo* [122]. This requires rapid remodeling of the cytoskeleton and efficient turnover of cytoskeleton and microtubule associated proteins. Recently, doublecortin (DCX), a microtubule-associated protein was shown to have a direct role in the intrinsic mechanisms

modulating RMS neuroblast migration [123]. Mutation of *Dcx* decreased the velocity of migration, disrupted branching of leading processes, and nuclear translocation towards the centrosome in the direction of migration [124].
As the OB is the only known target for SVZ neuronal precursors, an interesting observation was made when bulbectomy, the elimination of the OB, did not impede the rostral migration of precursors along the RMS [125]. This implied that short distance cues rather than chemo-attractants over long distances are the main mediators of stream formation.

3.4.3.3 Entering the OB

Once in the olfactory bulb, neuronal precursors cease tangential migration and disperse radially to reach the outer layers of the OB. Direct evidence for molecules mediating the switch from tangential to radial migration are still unknown, but two ECM proteins have been implicated in this process: One is Reelin, which is expressed by mitral cells in the OB and in *in vitro* assays was shown to induce detachment of postnatal neuronal precursors from their chains during tangential migration [126]. A second ECM protein, Tenascin R, was found to be expressed in the granule cell layer of the OB. It not only induces detachment of neuronal precursors from their chains, like Reelin does, but also initiates radial migration into the superficial layers of the OB. Grafting of tenascin R secreting cells into regions that normally do not express this protein even redirected the migration of neuronal precursors into these areas [127].

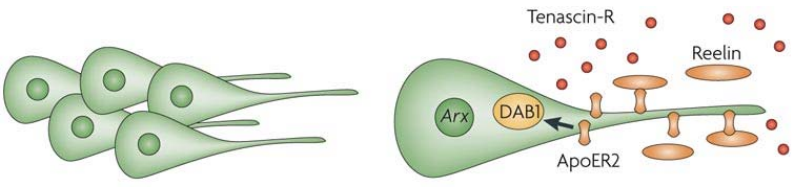

Fig 17: Termination of migration. Termination of migration in the OB is initiated by Reelin and its downstream effectors ApoER2 and Dab1. Tenascin-R mediates the detachment of neuronal precursors from chains and radial migration into the deeper layers of the OB. Taken from [4].

3.4.3.4 Differentiation in the OB

Once detached in the OB, neuronal precursors differentiate into two principal subtypes of inhibitory interneurons: granule cells (GC) found in the granule cell layer (GCL), and periglomerular cells (PGC) located in the glomerular layer (GL).

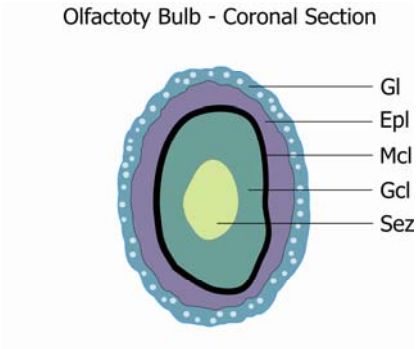

Figure 18: Anatomy of the olfactory bulb. The image depicts a coronal section with the respective laminated structures of the olfactory bulb. Gl glomerular layer,Epl ependymal layer, Mcl mitral cell layer, Gcl granule cell layer, Sez subependymal zone)

Around 95% of SVZ derived interneurons differentiate into GABA-containing granule cells, which, according to their morphological criteria, can further be subdivided into deep GCs and superificial GCs. The minority of the olfactory bulb interneurons differentiate into GABA expressing periglomerular cells (PGC) [128]. Based on their immunoreactivity, PGCs can also be further subdivided into PGCs positive for the dopamine-synthesizing hormone tyrosine hydroxylase (TH), the calcium-binding proteins calbindin or calretinin, and neurocalcin [129].

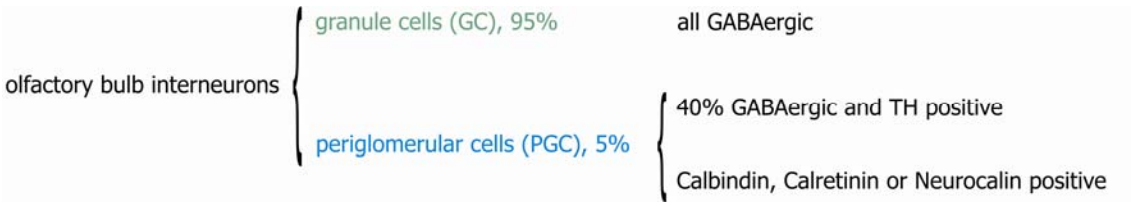

The majority of interneurons in the olfactory bulb are generated postnatally and the general consensus used to be that specification of these neurons to a certain interneuron lineage would occur in the OB itself. It is now becoming evident however, that neuronal precursors migrating along the RMS are

already, to a certain degree, committed to an interneuronal lineage within the OB. It was shown that precursors in the RMS acquire a GABAergic phenotype before reaching the OB [130] and retroviral lineage tracing showed that RMS precursors give rise to a larger population of PG neurons whereas SVZ precursors generate few PG cells and more GCs [113]. (see also section 3.4.2). These findings clearly emphasize that neuronal precursors are subject to a spatial and temporal lineage separation and that their final fate is most likely a trade off between intrinsic signals like the expression of specific transcription factors and extracellular stimuli encountered at different points during migration. It should also be noted that quite interestingly, a small proportion of early born postnatal OB interneurons are produced locally within the OB [131]

3.4.3.5 Life and death in the OB

Not all the newly generated neurons arriving in the OB are functionally integrated into the preexisting olfactory circuit as one subset is integrated while the remaining newborn cells are eliminated. Until now it remains unclear why the OB is chosen as the specific region in the adult brain to receive this tremendous input of newly generated neurons every day, only to send an estimated 50 % into programmed cell death. A few years ago it was shown that sensory input can regulate the survival of newborn neurons [132, 133]. Granule cells subjected to modulation by environmental cues maintained a constitutive turnover of granule cells which could be associated with improved olfactory memory. Moreover, mice that were exposed to an odor-enriched environment showed significantly less precursor cell death within the OB and displayed improved olfactory memory when compared to control populations [133]. It therefore seems that survival of OB interneurons depends on the level of activity that they receive.

3.4.3.6 Wiring the OB

Odor discrimination within the OB begins upon binding of an odor molecule to a specific olfactory receptor located in the nasal epithelium. Only one type of

olfactory receptor is expressed by each olfactory sensory neuron (OSN). However, several distinct receptors expressed by different olfactory sensory neurons can bind the same set of odors. The axons from all cells expressing receptors that bind the same odor converge onto one glomerulus (GL) in the OB. The nearly 2000 glomeruli function as essential crossroads in the rodent OB as they not only gather incoming information from the OSN but are also contacted by the apical dendrites of the mitral cells as well as axon and dendrites from PGCs. Mitral cells in turn project axons outside the OB into the olfactory cortex initiating odor discrimination. While superficial GCS primarily make contact with tufted cells which mediate the initial perception of odorants, deep GCs mostly contact the dendrites of mitral cells [134-136].

This highly complex and intricate network forms the basis of odor perception and the formation of olfactory memory.

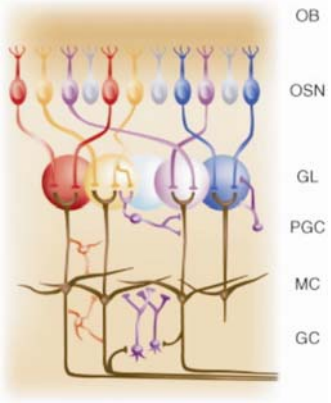

Fig 19: Schematic representation of the cellular architecture of the OB. Olfactory sensory neurons (OSN) are the first cells of the OB to perceive an odor. OSNs binding the same odor then extend their axons onto one glomeruls (GL). This GL also receives input from periglomerular cells (PGCs) and mitral cells which in turn receive information from granule cells (GC) and extend axons to the olfactory cortex initiating olfactory discrimination. Taken from [2].

3.4.4 The Reelin pathway in postnatal neuronal migration

Recently components of the Reelin signaling pathway were shown to be essential for the initiation of migration in the postnatal RMS. Mice lacking Reelin, both ApoER2 and VLDLR or Dab1 displayed massive accumulation of neuronal precursors in the SVZ unable to initiate migration along the RMS.

Activation of the signaling pathway was shown to be essential as 5F-Dab1 mice, lacking Reelin inducable tyrosine phosphorylation sites, displayed the same phenotype [11].

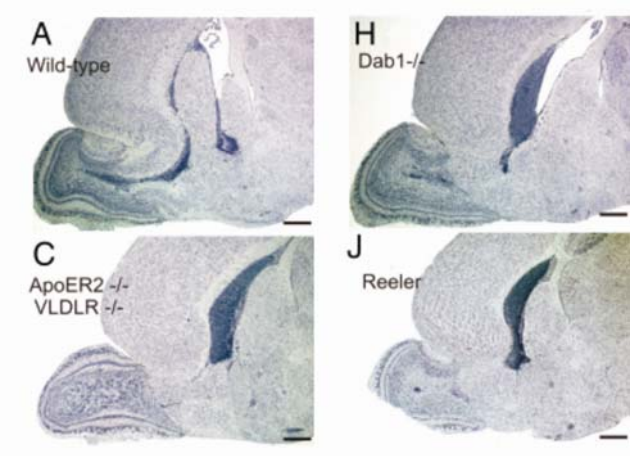

Fig 20: Ablation of Reelin pathway components results in failure to initiate migration along th RMS. Hematoxylin stained sagittal sections of the forebrains of **(*A*)** Wild-type, **(*C*)** *ApoER2*$^{-/-}$/*VLDLR*$^{-/-}$, **(*H*)** *Dab1*$^{-/-}$ and **(*J*)** *Reeler* mice at P17 cells. Taken from [11].

Interestingly Reelin, the only known functional ligand for the pathway is not expressed in the SVZ or in the RMS, indicating that other, as yet unidentified ligands have to activate the signaling cascade via ApoER2, VLDLR and Dab1 to initiate postnatal precursor migration.

3.5 Thrombopsondin-1 (THBS-1)

3.5.1 Thrombospondins

Thrombospondins (THBSs), like Reelin, are large secreted ECM proteins expressed in a vast array of different tissues. They comprise a subgroup of glycoproteins with five family members identified so far: THBS-1, -2, -3, -4 and THBS-5 (also referred to as cartilage oligomeric matrix protein, COMP).
According to their structure and oligomerization status, there are two main classifications of THBSs, subgroup A and B THBSs.

Subgroup A

Members of this group comprise THBS-1 and THBS-2. *In vivo,* they form homo-trimers with a relative molecular mass (M_r) of 170 for each monomer.

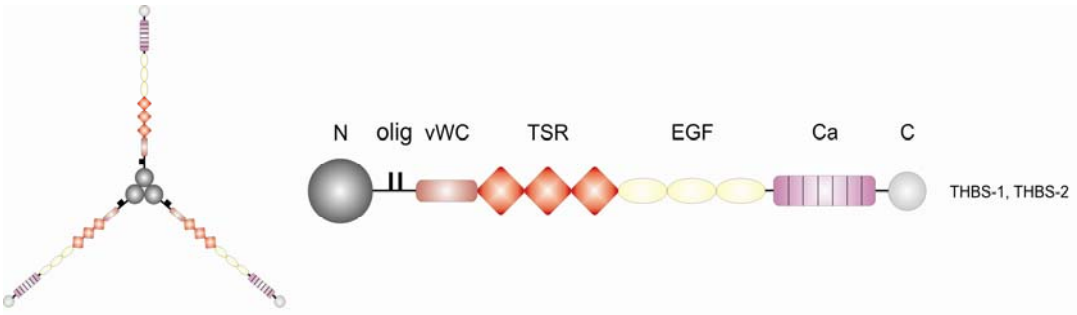

Fig 21: Schematic representation of THBS-1 and-2. Subgroup A family members form trimers *in vivo*. N= NH2 terminal domain, olig= oligomerization domain, vWC= von Willebrand factor type C domain, TSR= Thrombospondin type I repeat domain, EGF= EGF-like repeat/type II repeats domain, Ca= Calcium binding wire/ type III repeat domain. Adapted from [3].

Each monomer has a characteristic architecture of domains:

- N-terminal domain/THBS-N. Amongst its many binding partners this domain is best known for its heparin binding ability [5].
- Oligomerization domain. Responsible for homo-trimer formation via intermolecular disulfide-bonds [137].
- Von Willebrand Factor type C domain (vWC). Group A THBSs contain one vWC module consisting of ten cysteine rich residues which all form

disulfide bonds stabilising the protein.

- Thrombospondin type I repeat (TSR) domain. This region is unique to group A THBSs and links them to an ECM protein group referred to as the TSR superfamily. Associated function to this region are protein interactions, cell attachment and inhibition of angiogenesis [5].
- EGF-like repeat/type II repeats. They consist of three tandem motifs including one calcium binding motif, with currently unknown function.
- Calcium binding wire/ type III repeats comprising 13 calcium repeats are involved in cell interactions.
- Lektin-like module/cell binding domain [3].

Subgroup B

Members in this group, THBS-3 to -5, are pentamers with a subunit relative molecular mass of about 100.

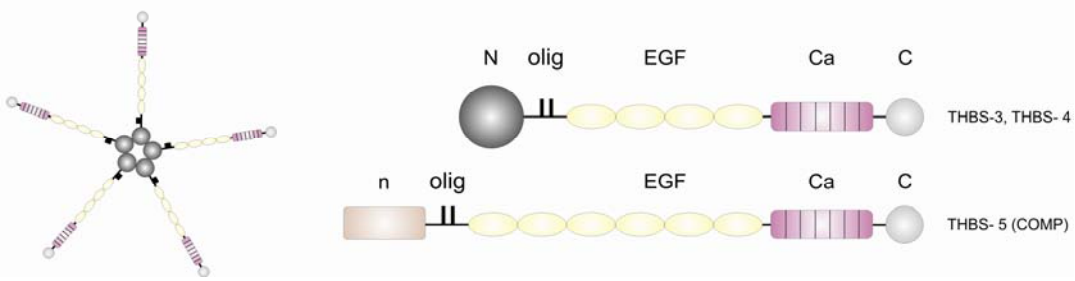

Fig 22: Schematic representation of THBS-3-4 and COMP. Subgroup B family members form pentamers *in vivo*. N= NH2 terminal domain, olig= oligomerization domain, EGF= EGF-like repeat/type II repeats domain, Ca= Calcium binding wire/ type III repeat domain, n= unique region to THBS-5. Adapted from [3].

They lack the vWC and TSR domain but have additional EGF-like repeats. THBS-5 also lacks the distinctive N-terminal domain.

3.5.2 Expression pattern

Each THBS has a unique spatial and temporal expression pattern even though many tissues show expression of more than one family member at the same time but often not in the same cellular population. Further, the expression level

of THBS-1, have been shown to be drastically altered in some pathological conditions.

Protein	Major sites of expression[a]		
	Embryonic	Adult	Pathophysiological
TSP-1	Widespread, especially heart, lung, intestinal epithelium, skeletal muscle (m), CNS, cartilage (ch), Floorplate (ch, X)	Platelet α granules (h, m) activated endothelium, fibroblasts, monocytes (h, m), corneal endothelium (b, h), lens epithelium (b)	Component of fibrin clot (h, m) Healing wounds of skin, skeletal muscle, nerve, atherosclerotic lesions, intimal hyperplasia (h, m), corneal fibroblasts of pseudoexfoliation syndrome (h)
TSP-2	Cartilage, growth zone (ch, h, m), tendon (ch), adrenal, skeletal muscle, kidney (m)	Adrenal cortex (b, m), Leydig and Purkinje cells, marrow stromal cells (m)	Fibroblasts of healing skin wounds (m)
TSP-3	CNS, spinal cord, lung, bone (ch, m), kidney (h), notocord (X)	Endocrine, kidney, uterus, muscle (h), CNS, gut, lung (m)	
TSP-4	Early osteogenesis, cornea (ch), somites, skeletal muscle (X)	Heart, skeletal muscle (h), neuromuscular junction (m), cerebellum, retina (m), tendon (b)	Increased in dystrophic muscle (h)
COMP/ TSP- 5	Articular cartilage (m, p)	Articular cartilage, tendon, synovium (p, b, m, h), testis (m), arteries (h)	Mutations lead to bone dysplasias, PSACH and MED (h). Increased in serum and synovial fluid in joint injury, osteoarthritis and rheumatoid arthritis (h)

Table 2: Expression and distribution of thrombospondins. [a] compiled from tissue Northern Blot, in situ hybridization and immunostaing data, species: b=bovine, ch=chick, h=human, m= mouse or rat, p=porcine, X=*Xenopus*. Taken from ShuShun Li, “Thrombospondin 1, an autocrine regulator in T cell adhesion & migration”, Karolinska Institute, Sweden, 2005.

THBS-1 can be detected as early as E10 and shows high expression levels in the nervous system, heart, lung, kidney, liver, skeletal muscle and cartilage on both protein and RNA level. In the developing brain, expression is tightly regulated with highest levels seen at E11 and E12 [138]. This time frame is highly intriguing as it coincides with the splitting of the cortical preplate and marks a significant switch from the phase of progenitor proliferation, to expand the neural stem cell pool, to the phase of active radial migration of mostly postmitotic projection neurons, establishing the cortical layers. This might functionally implicate THBS-1 in proliferation of progenitor cells in the developing cortex, which remains to be investigated.

3.5.3 Functions

Thrombospondin-1 (THBS-1) was first described in 1978 as “a high molecular

weight glycoprotein released by platelets in response to thrombin treatment and is proteolyzed when left in the presence of platelets after liberation.“ [139]. It was the first THBS family member to be identified and since its first identification as molecule involved in platelet aggregation and clot formation, THBS-1 has been shown to be involved in multiple biological processes including apoptosis [140], activation of latent TGFβ [141, 142], inhibition of angiogenesis [143, 144], inhibition or promotion of cell proliferation according to cell type [145], motility [145], neurite outgrowth [146-148], synaptogenesis [149], and VLDLR-mediated inhibition of cell division [150], to name only a few.

Functions	TSP-1	TSP-2	TSP-3	TSP-4	TSP-5/COMP
Calcium-binding	+	+	+	+	+
Cell attachment	+	+	+	+	
Cell spreading/cytoskeletal organization*	+	+	NT	+	-/+
Cell motility*	+	+	NT	NT	NT
Cell proliferation*	S/I	+	NT	NT	NT
Neurite outgrowth	+	NT	NT	+	NT
Apoptosis*	+	+	NT	NT	NT
Phagocytosis*	+	NT	NT	NT	NT
Binding other ECM	+	+	NT	+	+
ECM assembly	-	+	NT	NT	+
Binding/regulating Protease*	+	+	NT	NT	+
Activation of TGF-β	+	-	NT	NT	NT
Platelet aggregation	+	+	NT	NT	NT
Cell-cell interaction*	+	+	NT	+	NT
Inhibition of angiogenesis	+	+	NT	NT	-

Table 3: Known functions of thrombospondins. Presence (+), or absence of activity (-). S: stimulation, I: inhibition and depends on the cell-type. NT: not tested. Underlined properties are known to be mediated by the type 1 repeats and are therefore unlikely to be shared in pentameric TSPs by the same mechanism. (*): Indicates function is cell-type dependent. Taken from ShuShun Li, “Thrombospondin 1, an autocrine regulator in T cell adhesion & migration”, Karolinska Institute, Sweden, 2005

The diversity of processes and the specific effects THBS-1 exerts on various cell types depends mainly on the repertoire of receptors expressed, and suggests that THBS-1 is involved in events which require a broad tissue distribution and highly regulated temporal expression.

3.5.3.1 THBS-1 knockout

In spite of its abundant expression in the developing CNS and significant presence in the adult brain, THBS-1$^{-/-}$ mice show no gross brain abnormalities. They are viable and fertile and merely have an increase in inflammatory cell infiltrates in the lung and a curvature of the spine [151]. The lack of obvious developmental defects may partly be ascribed to a functional redundancy between THBS-1 and its most close relative, THBS-2. However, mutants for both molecules [152] or THBS-2 alone [152] are still devoid of any obvious brain defects. This is in line with knockout lines generated for other adhesive ECM molecules that all display a surprisingly mild phenotype [153].

3.5.3.2 The TSR repeat superfamily

As mentioned earlier, the TSR domain unites subgroup A THBSs into a family termed the TSR superfamily, with many of its members being expressed in the nervous system [154]. Several of the known functions for THBS-1 can be attributed to the TSR domain in the central region of the protein [154]. TSR repeats are exclusively present in eukaryotic organisms and have been identified in 41 different human proteins [155]. In THBS-1, this region becomes glycosylated by addition of mannose and fructose residues on conserved amino acid positions, thereby mediating ECM and cell surface interactions. The best characterized members are the cell adhesion molecule F-Spondin, most prominently expressed in the floor plate of the developing vertebrate CNS and in peripheral nerves promoting neurite outgrowth [156], SCO-Spondin, which contains a massive 25 TSRs and is exclusively expressed in the roof of the third brain ventricle with currently unknown function [157], and the metalloproteinases ADAMTS (“ADAM-like” proteins with TS repeats).

3.5.4 THBS-1 receptors

The binding of a variety of receptors to different domains of THBS-1 induce various functional responses and are most likely responsible for the vast

functional diversity reported for THBS-1.

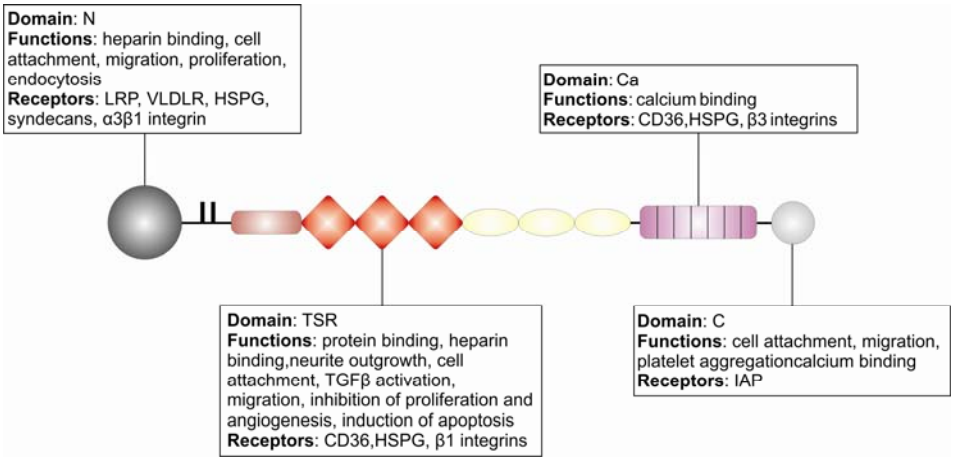

Fig 23: Functional domains of THBS-1 and their receptors. Based on proteoloytic fragment analysis, blocking antibodies or synthetic peptides. Adapted from [5].

Integrins

Integrins comprise a large family of hetero-dimeric cell surface receptor molecules that are involved in ECM as well as cell-cell interactions. THBS-1 is a ligand for several integrins mediating a vast diversity of cellular responses on different target cells. The interaction with α3β1 integrin is of specific interest. It was shown that α3β1 functions as neuronal receptor for THBS-1, mediating neurite outgrowth on rat sympathetic neurons *in vitro* [158]. This finding is consistent with other reports, confirming THBS-1 to induce neurite outgrowth in various neuronal cell types [42]. Also during cortical development, THBS-1 was shown to mediate neurite outgrowth while located in the proliferative VZ, which seemed to depend on binding of THBS-1 to α3β1 integrin and implies a functional significance of this integrin in maintaining correct cortical lamination. This function is further strengthened by analysis of postnatal β1 integrin mutant mouse brains which show a defect in neuronal chain formation in the RMS, due to a lack of neuron to neuron adhesion within the stream.

LRP

Most commonly ECM proteins are catabolized via extracellular proteolysis [159]. THBS-1 protein levels however were shown to be regulated by cell-

mediated uptake and lysosomal degradation [160]. In 1995, two independent groups reported LRP as a receptor mediating THBS-1 catabolism. In a fibroblast cell system, Mikhailenko and colleagues could nicely demonstrate that LRP is responsible for the cellular uptake and subsequent degradation of THBS-1, as treatment of cells with a function blocking anti-LRP antibody or the inhibitor RAP virtually abolished THBS-1 catabolism. Notably, this effect was dependent on the presence of cell surface proteoglycans, as heparitinase treatment markedly reduced the extent of LRP-mediated uptake and degradation [161]. Later the region of THBS-1 binding to LRP was determined to reside in the N-terminal heparin binding domain [68]. While the previously mentioned findings were confirmed and also reproduced in smooth muscle cells, additional experiments performed in endothelial cells failed to link LRP as main catabolic receptor to THBS-1 binding and degradation, most likely due to lack of expression of the receptor. As RAP, a common ligand and competitor for all LDLR-family member ligands, however maintained its antagonistic function in these epithelial cells, it was proposed that LDLR family members other than LRP are involved in THBS-1 catabolism.

VLDLR

While analyzing the domains responsible for THBS-1 catabolism in fibroblasts it was shown that VLDLR, with a similar efficiency as seen for LRP, mediates cellular degradation of THBS-1 [68]. Recent work on the regulation of cell cyle progression in microvascular endothelial cells firmly established a functional link between THBS-1 and -2 and VLDLR. Using surface plasmon resonance they were able to determine Kd values for the binding of THBS-1 and -2 to VLDLR of 11 nM and 21 nM respectively, values similar to those obtained in [11]. Further, they were able to show that purified THBS-2 inhibited VEGF induced proliferation of cells and reduced phosphorylation levels of AKT and MAPK probably by inhibiting the PI3K pathway. The reduction of phosphorylation levels were not shown for THBS-1 [150].

CD36

CD36 is a major scavenger receptor that has also been shown to have adhesive properties for the binding of collagens and THBS-1 [162]. The interaction between THBS-1 and CD36 has been implicated in platelet-tumor cell adhesion, platelet aggregation, and the anti-angiogenic effect in endothelial cells [5]. Purified THBS-1 was also shown to bind to a CD36 binding motif in the HIV envelope protein gp120, which inhibited HIV infection of peripheral blood mononuclear cells and transformed T and promonocytic cell lines [163].

3.5.5 THBS-1 in the developing and adult nervous sytem

During embryogenesis, THBS-1 was shown to be expressed in the leading edge of migrating granule cells in the developing cerebellum. Treatment of explant-cultures with anti-THBS antibodies led to a dose dependent effect in the inhibition of migration of these granule cells [164]. Follow up work performed in the early 1990s further supported these previous studies demonstrating that THBS-1 propagated neurite extension and adhesion of dorsal root ganglia, spinal cord neurons, and PC12 cells in an *in vitro* model for CNS development and neuronal migration [148]. In the adult rat brain, THBS-1 was shown to be secreted by macrophages upon induced injury of the brain and promoted neurite outgrowth and regeneration of cultured CNS neurons [165]. Studies performed in amphibians and fish localized THBS-1 mainly to central nerve tracts capable of regeneration [166] implicating a correlation between the presence of THBS-1 and potentially successful nerve regeneration. However, immunohistochemical analysis of brains of Alzheimer disease patients showed THBS-1 expression in senile plaques and a reduction of expression in a subpopulation of pyramidal neurons that may be vulnerable in Alzheimer's disease [167], thereby linking it to the process of neuronal degeneration and senile plaque formation. Recently, THBS-1 was shown to be secreted from immature astrocytes in culture, promoting CNS synaptogenesis *in vitro* and *in vivo* [149]. A possible model for the induction of synapse formation might be binding of THBS-1 to cell surface receptors concentrated at the synapses

thereby activating a downstream-signaling cascade leading to synaptic adhesion. The receptors involved in this process are currently unknown. However, the Reelin pathway components ApoER2 and Dab1 were recently found to be localized to post synaptic density fractions of rat brain synaptosomes. Here, ApoER2 formed a multiprotein complex with NMDA receptor subunits and the postsynaptic density protein PSD95. [168]. THBS-1 might facilitate its synaptogenic properties by binding to ApoER2 and activating an intracellular signaling cascade via Dab1. This theory is however, highly speculative and remains to be further investigated. As the THBS-1 induced synapses were found to be non-functional, this indicates that more as yet unidentified factors are involved in the generation of functionally active synapses.

Summarizing the functions of THBS-1, it acts as cell surface molecule, bringing together membrane proteins and their ligands to modulate the ECM environment, cellular phenotypes and often their migratory properties.

4 References

1. May, P. and J. Herz, *LDL receptor-related proteins in neurodevelopment.* Traffic, 2003. **4**(5): p. 291-301.
2. Lledo, P.M., F.T. Merkle, and A. Alvarez-Buylla, *Origin and function of olfactory bulb interneuron diversity.* Trends Neurosci, 2008. **31**(8): p. 392-400.
3. Carlson, C.B., J. Lawler, and D.F. Mosher, *Structures of thrombospondins.* Cell Mol Life Sci, 2008. **65**(5): p. 672-86.
4. Ghashghaei, H.T., C. Lai, and E.S. Anton, *Neuronal migration in the adult brain: are we there yet?* Nat Rev Neurosci, 2007. **8**(2): p. 141-51.
5. Chen, H., M.E. Herndon, and J. Lawler, *The cell biology of thrombospondin-1.* Matrix Biol, 2000. **19**(7): p. 597-614.
6. Nadarajah, B. and J.G. Parnavelas, *Modes of neuronal migration in the developing cerebral cortex.* Nat Rev Neurosci, 2002. **3**(6): p. 423-32.
7. Merkle, F.T., Z. Mirzadeh, and A. Alvarez-Buylla, *Mosaic organization of neural stem cells in the adult brain.* Science, 2007. **317**(5836): p. 381-4.
8. Gupta, A., L.H. Tsai, and A. Wynshaw-Boris, *Life is a journey: a genetic look at neocortical development.* Nat Rev Genet, 2002. **3**(5): p. 342-55.
9. Cooper, J.A., *A mechanism for inside-out lamination in the neocortex.* Trends Neurosci, 2008. **31**(3): p. 113-9.
10. Marin, O. and J.L. Rubenstein, *A long, remarkable journey: tangential migration in the telencephalon.* Nat Rev Neurosci, 2001. **2**(11): p. 780-90.
11. Andrade, N., et al., *ApoER2/VLDL receptor and Dab1 in the rostral migratory stream function in postnatal neuronal migration independently of Reelin.* Proc Natl Acad Sci U S A, 2007. **104**(20): p. 8508-13.
12. Trommsdorff, M., et al., *Reeler/Disabled-like disruption of neuronal migration in knockout mice lacking the VLDL receptor and ApoE receptor 2.* Cell, 1999. **97**(6): p. 689-701.

13. Bock, H.H., et al., *Phosphatidylinositol 3-kinase interacts with the adaptor protein Dab1 in response to Reelin signaling and is required for normal cortical lamination.* J Biol Chem, 2003. **278**(40): p. 38772-9.
14. Book, K.J. and D.K. Morest, *Migration of neuroblasts by perikaryal translocation: role of cellular elongation and axonal outgrowth in the acoustic nuclei of the chick embryo medulla.* J Comp Neurol, 1990. **297**(1): p. 55-76.
15. Nadarajah, B., et al., *Neuronal migration in the developing cerebral cortex: observations based on real-time imaging.* Cereb Cortex, 2003. **13**(6): p. 607-11.
16. Stensaas, L.J., *The development of hippocampal and dorsolateral pallial region of the cerebral hemisphere in fetal rabbits. V. Sixty millimeter stage, glial cell morphology.* J Comp Neurol, 1967. **131**(4): p. 423-36.
17. Walsh, C. and C.L. Cepko, *Clonal dispersion in proliferative layers of developing cerebral cortex.* Nature, 1993. **362**(6421): p. 632-5.
18. Tan, S.S., et al., *Cell dispersion patterns in different cortical regions studied with an X-inactivated transgenic marker.* Development, 1995. **121**(4): p. 1029-39.
19. Parnavelas, J.G., et al., *The contribution of the ganglionic eminence to the neuronal cell types of the cerebral cortex.* Novartis Found Symp, 2000. **228**: p. 129-39; discussion 139-47.
20. Frotscher, M., *Cajal-Retzius cells, Reelin, and the formation of layers.* Curr Opin Neurobiol, 1998. **8**(5): p. 570-5.
21. Falconer, D.S., *Two congenital defects of the limb bones in the mouse.* Acta Anat (Basel), 1951. **13**(4): p. 371-8.
22. D'Arcangelo, G., et al., *A protein related to extracellular matrix proteins deleted in the mouse mutant reeler.* Nature, 1995. **374**(6524): p. 719-23.
23. Hong, S.E., et al., *Autosomal recessive lissencephaly with cerebellar hypoplasia is associated with human RELN mutations.* Nat Genet, 2000. **26**(1): p. 93-6.

24. Sheldon, M., et al., *Scrambler and yotari disrupt the disabled gene and produce a reeler-like phenotype in mice.* Nature, 1997. **389**(6652): p. 730-3.
25. Howell, B.W., et al., *Neuronal position in the developing brain is regulated by mouse disabled-1.* Nature, 1997. **389**(6652): p. 733-7.
26. Strasser, V., et al., *Receptor clustering is involved in Reelin signaling.* Mol Cell Biol, 2004. **24**(3): p. 1378-86.
27. Howell, B.W., et al., *The disabled 1 phosphotyrosine-binding domain binds to the internalization signals of transmembrane glycoproteins and to phospholipids.* Mol Cell Biol, 1999. **19**(7): p. 5179-88.
28. Howell, B.W., et al., *Dab1 tyrosine phosphorylation sites relay positional signals during mouse brain development.* Curr Biol, 2000. **10**(15): p. 877-85.
29. Keshvara, L., et al., *Cyclin-dependent kinase 5 phosphorylates disabled 1 independently of Reelin signaling.* J Neurosci, 2002. **22**(12): p. 4869-77.
30. Arnaud, L., et al., *Fyn tyrosine kinase is a critical regulator of disabled-1 during brain development.* Curr Biol, 2003. **13**(1): p. 9-17.
31. Kuo, G., et al., *Absence of Fyn and Src causes a reeler-like phenotype.* J Neurosci, 2005. **25**(37): p. 8578-86.
32. Keshvara, L., et al., *Identification of reelin-induced sites of tyrosyl phosphorylation on disabled 1.* J Biol Chem, 2001. **276**(19): p. 16008-14.
33. Beffert, U., et al., *Reelin-mediated signaling locally regulates protein kinase B/Akt and glycogen synthase kinase 3beta.* J Biol Chem, 2002. **277**(51): p. 49958-64.
34. Assadi, A.H., et al., *Interaction of reelin signaling and Lis1 in brain development.* Nat Genet, 2003. **35**(3): p. 270-6.
35. Pramatarova, A., et al., *Nck beta interacts with tyrosine-phosphorylated disabled 1 and redistributes in Reelin-stimulated neurons.* Mol Cell Biol, 2003. **23**(20): p. 7210-21.
36. Ballif, B.A., et al., *Activation of a Dab1/CrkL/C3G/Rap1 pathway in Reelin-stimulated neurons.* Curr Biol, 2004. **14**(7): p. 606-10.

37. Chen, K., et al., *Interaction between Dab1 and CrkII is promoted by Reelin signaling.* J Cell Sci, 2004. **117**(Pt 19): p. 4527-36.
38. Huang, Y., et al., *Tyrosine phosphorylated Disabled 1 recruits Crk family adapter proteins.* Biochem Biophys Res Commun, 2004. **318**(1): p. 204-12.
39. Suetsugu, S., et al., *Regulation of actin cytoskeleton by mDab1 through N-WASP and ubiquitination of mDab1.* Biochem J, 2004. **384**(Pt 1): p. 1-8.
40. Feng, L., et al., *Cullin 5 regulates Dab1 protein levels and neuron positioning during cortical development.* Genes Dev, 2007. **21**(21): p. 2717-30.
41. Anton, E.S., J.A. Kreidberg, and P. Rakic, *Distinct functions of alpha3 and alpha(v) integrin receptors in neuronal migration and laminar organization of the cerebral cortex.* Neuron, 1999. **22**(2): p. 277-89.
42. Dulabon, L., et al., *Reelin binds alpha3beta1 integrin and inhibits neuronal migration.* Neuron, 2000. **27**(1): p. 33-44.
43. Senzaki, K., M. Ogawa, and T. Yagi, *Proteins of the CNR family are multiple receptors for Reelin.* Cell, 1999. **99**(6): p. 635-47.
44. Herrick, T.M. and J.A. Cooper, *A hypomorphic allele of dab1 reveals regional differences in reelin-Dab1 signaling during brain development.* Development, 2002. **129**(3): p. 787-96.
45. Gotthardt, M., et al., *Interactions of the low density lipoprotein receptor gene family with cytosolic adaptor and scaffold proteins suggest diverse biological functions in cellular communication and signal transduction.* J Biol Chem, 2000. **275**(33): p. 25616-24.
46. Meyer, D., A. Liu, and B. Margolis, *Interaction of c-Jun amino-terminal kinase interacting protein-1 with p190 rhoGEF and its localization in differentiated neurons.* J Biol Chem, 1999. **274**(49): p. 35113-8.
47. Ohkubo, N., et al., *Reelin signals survival through Src-family kinases that inactivate BAD activity.* J Neurochem, 2007. **103**(2): p. 820-30.
48. Frotscher, M., *Dual role of Cajal-Retzius cells and reelin in cortical development.* Cell Tissue Res, 1997. **290**(2): p. 315-22.

49. Schiffmann, S.N., B. Bernier, and A.M. Goffinet, *Reelin mRNA expression during mouse brain development.* Eur J Neurosci, 1997. **9**(5): p. 1055-71.
50. Magdaleno, S., L. Keshvara, and T. Curran, *Rescue of ataxia and preplate splitting by ectopic expression of Reelin in reeler mice.* Neuron, 2002. **33**(4): p. 573-86.
51. Yoshida, M., et al., *Massive loss of Cajal-Retzius cells does not disrupt neocortical layer order.* Development, 2006. **133**(3): p. 537-45.
52. Nadarajah, B., et al., *Two modes of radial migration in early development of the cerebral cortex.* Nat Neurosci, 2001. **4**(2): p. 143-50.
53. Royaux, I., et al., *Genomic organization of the mouse reelin gene.* Genomics, 1997. **46**(2): p. 240-50.
54. D'Arcangelo, G., et al., *Reelin is a secreted glycoprotein recognized by the CR-50 monoclonal antibody.* J Neurosci, 1997. **17**(1): p. 23-31.
55. Lambert de Rouvroit, C., et al., *Reelin, the extracellular matrix protein deficient in reeler mutant mice, is processed by a metalloproteinase.* Exp Neurol, 1999. **156**(1): p. 214-7.
56. D'Arcangelo, G., et al., *Reelin is a ligand for lipoprotein receptors.* Neuron, 1999. **24**(2): p. 471-9.
57. Ignatova, N., C.J. Sindic, and A.M. Goffinet, *Characterization of the various forms of the Reelin protein in the cerebrospinal fluid of normal subjects and in neurological diseases.* Neurobiol Dis, 2004. **15**(2): p. 326-30.
58. Jossin, Y., et al., *The central fragment of Reelin, generated by proteolytic processing in vivo, is critical to its function during cortical plate development.* J Neurosci, 2004. **24**(2): p. 514-21.
59. Smalheiser, N.R., et al., *Expression of reelin in adult mammalian blood, liver, pituitary pars intermedia, and adrenal chromaffin cells.* Proc Natl Acad Sci U S A, 2000. **97**(3): p. 1281-6.
60. Quattrocchi, C.C., et al., *Reelin is a serine protease of the extracellular matrix.* J Biol Chem, 2002. **277**(1): p. 303-9.

61. Hiesberger, T., et al., *Direct binding of Reelin to VLDL receptor and ApoE receptor 2 induces tyrosine phosphorylation of disabled-1 and modulates tau phosphorylation.* Neuron, 1999. **24**(2): p. 481-9.
62. Tissir, F. and A.M. Goffinet, *Reelin and brain development.* Nat Rev Neurosci, 2003. **4**(6): p. 496-505.
63. Takahashi, S., et al., *Rabbit very low density lipoprotein receptor: a low density lipoprotein receptor-like protein with distinct ligand specificity.* Proc Natl Acad Sci U S A, 1992. **89**(19): p. 9252-6.
64. Webb, J.C., et al., *Characterization and tissue-specific expression of the human 'very low density lipoprotein (VLDL) receptor' mRNA.* Hum Mol Genet, 1994. **3**(4): p. 531-7.
65. Christie, R.H., et al., *Expression of the very low-density lipoprotein receptor (VLDL-r), an apolipoprotein-E receptor, in the central nervous system and in Alzheimer's disease.* J Neuropathol Exp Neurol, 1996. **55**(4): p. 491-8.
66. Frykman, P.K., et al., *Normal plasma lipoproteins and fertility in gene-targeted mice homozygous for a disruption in the gene encoding very low density lipoprotein receptor.* Proc Natl Acad Sci U S A, 1995. **92**(18): p. 8453-7.
67. Argraves, K.M., et al., *The very low density lipoprotein receptor mediates the cellular catabolism of lipoprotein lipase and urokinase-plasminogen activator inhibitor type I complexes.* J Biol Chem, 1995. **270**(44): p. 26550-7.
68. Mikhailenko, I., et al., *Cellular internalization and degradation of thrombospondin-1 is mediated by the amino-terminal heparin binding domain (HBD). High affinity interaction of dimeric HBD with the low density lipoprotein receptor-related protein.* J Biol Chem, 1997. **272**(10): p. 6784-91.
69. Brandes, C., et al., *Avian and murine LR8B and human apolipoprotein E receptor 2: differentially spliced products from corresponding genes.* Genomics, 1997. **42**(2): p. 185-91.

70. Brandes, C., et al., *Alternative splicing in the ligand binding domain of mouse ApoE receptor-2 produces receptor variants binding reelin but not alpha 2-macroglobulin.* J Biol Chem, 2001. **276**(25): p. 22160-9.
71. Koch, S., et al., *A secreted soluble form of ApoE receptor 2 acts as a dominant-negative receptor and inhibits Reelin signaling.* Embo J, 2002. **21**(22): p. 5996-6004.
72. Yasuda, J., et al., *The JIP group of mitogen-activated protein kinase scaffold proteins.* Mol Cell Biol, 1999. **19**(10): p. 7245-54.
73. Stockinger, W., et al., *The reelin receptor ApoER2 recruits JNK-interacting proteins-1 and -2.* J Biol Chem, 2000. **275**(33): p. 25625-32.
74. Herz, J., M. Gotthardt, and T.E. Willnow, *Cellular signalling by lipoprotein receptors.* Curr Opin Lipidol, 2000. **11**(2): p. 161-6.
75. Trommsdorff, M., et al., *Interaction of cytosolic adaptor proteins with neuronal apolipoprotein E receptors and the amyloid precursor protein.* J Biol Chem, 1998. **273**(50): p. 33556-60.
76. Davis, C.G., et al., *The low density lipoprotein receptor. Identification of amino acids in cytoplasmic domain required for rapid endocytosis.* J Biol Chem, 1987. **262**(9): p. 4075-82.
77. Magrane, J., et al., *The role of O-linked sugars in determining the very low density lipoprotein receptor stability or release from the cell.* FEBS Lett, 1999. **451**(1): p. 56-62.
78. Krieger, M. and J. Herz, *Structures and functions of multiligand lipoprotein receptors: macrophage scavenger receptors and LDL receptor-related protein (LRP).* Annu Rev Biochem, 1994. **63**: p. 601-37.
79. Hussain, M.M., D.K. Strickland, and A. Bakillah, *The mammalian low-density lipoprotein receptor family.* Annu Rev Nutr, 1999. **19**: p. 141-72.
80. Chen, W.J., J.L. Goldstein, and M.S. Brown, *NPXY, a sequence often found in cytoplasmic tails, is required for coated pit-mediated internalization of the low density lipoprotein receptor.* J Biol Chem, 1990. **265**(6): p. 3116-23.

81. Willnow, T.E., et al., *RAP, a specialized chaperone, prevents ligand-induced ER retention and degradation of LDL receptor-related endocytic receptors.* Embo J, 1996. **15**(11): p. 2632-9.
82. Bu, G., *Receptor-associated protein: a specialized chaperone and antagonist for members of the LDL receptor gene family.* Curr Opin Lipidol, 1998. **9**(2): p. 149-55.
83. Schneider, W.J. and J. Nimpf, *LDL receptor relatives at the crossroad of endocytosis and signaling.* Cell Mol Life Sci, 2003. **60**(5): p. 892-903.
84. Nimpf, J. and W.J. Schneider, *From cholesterol transport to signal transduction: low density lipoprotein receptor, very low density lipoprotein receptor, and apolipoprotein E receptor-2.* Biochim Biophys Acta, 2000. **1529**(1-3): p. 287-98.
85. Herz, J., *The LDL receptor gene family: (un)expected signal transducers in the brain.* Neuron, 2001. **29**(3): p. 571-81.
86. Rohlmann, A., et al., *Inducible inactivation of hepatic LRP gene by cre-mediated recombination confirms role of LRP in clearance of chylomicron remnants.* J Clin Invest, 1998. **101**(3): p. 689-95.
87. Kounnas, M.Z., et al., *Cellular internalization and degradation of antithrombin III-thrombin, heparin cofactor II-thrombin, and alpha 1-antitrypsin-trypsin complexes is mediated by the low density lipoprotein receptor-related protein.* J Biol Chem, 1996. **271**(11): p. 6523-9.
88. Kounnas, M.Z., et al., *Low density lipoprotein receptor-related protein/alpha 2-macroglobulin receptor mediates cellular uptake of pro-urokinase.* J Biol Chem, 1993. **268**(29): p. 21862-7.
89. Qiu, Z., et al., *alpha 2-Macroglobulin exposure reduces calcium responses to N-methyl-D-aspartate via low density lipoprotein receptor-related protein in cultured hippocampal neurons.* J Biol Chem, 2002. **277**(17): p. 14458-66.
90. Herz, J., D.E. Clouthier, and R.E. Hammer, *LDL receptor-related protein internalizes and degrades uPA-PAI-1 complexes and is essential for embryo implantation.* Cell, 1992. **71**(3): p. 411-21.

91. Liu, C.X., et al., *LRP-DIT, a putative endocytic receptor gene, is frequently inactivated in non-small cell lung cancer cell lines.* Cancer Res, 2000. **60**(7): p. 1961-7.
92. Li, Y., W. Lu, and G. Bu, *Striking differences of LDL receptor-related protein 1B expression in mouse and human.* Biochem Biophys Res Commun, 2005. **333**(3): p. 868-73.
93. Nielsen, R., et al., *Transcellular transport of vitamin B(12) in LLC-PK1 renal proximal tubule cells.* J Am Soc Nephrol, 2001. **12**(6): p. 1099-106.
94. Marino, M. and R.T. McCluskey, *Megalin-mediated transcytosis of thyroglobulin by thyroid cells is a calmodulin-dependent process.* Thyroid, 2000. **10**(6): p. 461-9.
95. Marino, M., et al., *Transcytosis of retinol-binding protein across renal proximal tubule cells after megalin (gp 330)-mediated endocytosis.* J Am Soc Nephrol, 2001. **12**(4): p. 637-48.
96. Willnow, T.E., et al., *Defective forebrain development in mice lacking gp330/megalin.* Proc Natl Acad Sci U S A, 1996. **93**(16): p. 8460-4.
97. Nakayama, M., et al., *Identification of high-molecular-weight proteins with multiple EGF-like motifs by motif-trap screening.* Genomics, 1998. **51**(1): p. 27-34.
98. Paton, J.A. and F.N. Nottebohm, *Neurons generated in the adult brain are recruited into functional circuits.* Science, 1984. **225**(4666): p. 1046-8.
99. Harzsch, S. and R.R. Dawirs, *Neurogenesis in the developing crab brain: postembryonic generation of neurons persists beyond metamorphosis.* J Neurobiol, 1996. **29**(3): p. 384-98.
100. Font, E., et al., *Neurogenesis and neuronal regeneration in the adult reptilian brain.* Brain Behav Evol, 2001. **58**(5): p. 276-95.
101. Kaas, J.H., *Plasticity of sensory and motor maps in adult mammals.* Annu Rev Neurosci, 1991. **14**: p. 137-67.
102. Gould, E., et al., *Proliferation of granule cell precursors in the dentate gyrus of adult monkeys is diminished by stress.* Proc Natl Acad Sci U S A, 1998. **95**(6): p. 3168-71.

103. Eriksson, P.S., et al., *Neurogenesis in the adult human hippocampus.* Nat Med, 1998. **4**(11): p. 1313-7.
104. Doetsch, F., et al., *Subventricular zone astrocytes are neural stem cells in the adult mammalian brain.* Cell, 1999. **97**(6): p. 703-16.
105. Seri, B., et al., *Astrocytes give rise to new neurons in the adult mammalian hippocampus.* J Neurosci, 2001. **21**(18): p. 7153-60.
106. Seri, B., et al., *Composition and organization of the SCZ: a large germinal layer containing neural stem cells in the adult mammalian brain.* Cereb Cortex, 2006. **16 Suppl 1**: p. i103-11.
107. Lee, A., et al., *Isolation of neural stem cells from the postnatal cerebellum.* Nat Neurosci, 2005. **8**(6): p. 723-9.
108. Johansson, C.B., et al., *Identification of a neural stem cell in the adult mammalian central nervous system.* Cell, 1999. **96**(1): p. 25-34.
109. Luskin, M.B., *Restricted proliferation and migration of postnatally generated neurons derived from the forebrain subventricular zone.* Neuron, 1993. **11**(1): p. 173-89.
110. Alvarez-Buylla, A. and D.A. Lim, *For the long run: maintaining germinal niches in the adult brain.* Neuron, 2004. **41**(5): p. 683-6.
111. Altman, J., *Autoradiographic and histological studies of postnatal neurogenesis. IV. Cell proliferation and migration in the anterior forebrain, with special reference to persisting neurogenesis in the olfactory bulb.* J Comp Neurol, 1969. **137**(4): p. 433-57.
112. Lois, C. and A. Alvarez-Buylla, *Long-distance neuronal migration in the adult mammalian brain.* Science, 1994. **264**(5162): p. 1145-8.
113. Hack, M.A., et al., *Neuronal fate determinants of adult olfactory bulb neurogenesis.* Nat Neurosci, 2005. **8**(7): p. 865-72.
114. Wichterle, H., J.M. Garcia-Verdugo, and A. Alvarez-Buylla, *Direct evidence for homotypic, glia-independent neuronal migration.* Neuron, 1997. **18**(5): p. 779-91.
115. Mason, H.A., S. Ito, and G. Corfas, *Extracellular signals that regulate the tangential migration of olfactory bulb neuronal precursors: inducers, inhibitors, and repellents.* J Neurosci, 2001. **21**(19): p. 7654-63.

116. Wu, W., et al., *Directional guidance of neuronal migration in the olfactory system by the protein Slit.* Nature, 1999. **400**(6742): p. 331-6.
117. Murase, S. and A.F. Horwitz, *Deleted in colorectal carcinoma and differentially expressed integrins mediate the directional migration of neural precursors in the rostral migratory stream.* J Neurosci, 2002. **22**(9): p. 3568-79.
118. Cremer, H., et al., *Inactivation of the N-CAM gene in mice results in size reduction of the olfactory bulb and deficits in spatial learning.* Nature, 1994. **367**(6462): p. 455-9.
119. Ono, K., et al., *N-CAM mutation inhibits tangential neuronal migration and is phenocopied by enzymatic removal of polysialic acid.* Neuron, 1994. **13**(3): p. 595-609.
120. Hu, H., et al., *The role of polysialic acid in migration of olfactory bulb interneuron precursors in the subventricular zone.* Neuron, 1996. **16**(4): p. 735-43.
121. Anton, E.S., et al., *Receptor tyrosine kinase ErbB4 modulates neuroblast migration and placement in the adult forebrain.* Nat Neurosci, 2004. **7**(12): p. 1319-28.
122. Davenne, M., et al., *In vivo imaging of migrating neurons in the mammalian forebrain.* Chem Senses, 2005. **30 Suppl 1**: p. i115-6.
123. Koizumi, H., et al., *Doublecortin maintains bipolar shape and nuclear translocation during migration in the adult forebrain.* Nat Neurosci, 2006. **9**(6): p. 779-86.
124. Kappeler, C., et al., *Branching and nucleokinesis defects in migrating interneurons derived from doublecortin knockout mice.* Hum Mol Genet, 2006. **15**(9): p. 1387-400.
125. Kirschenbaum, B., et al., *Adult subventricular zone neuronal precursors continue to proliferate and migrate in the absence of the olfactory bulb.* J Neurosci, 1999. **19**(6): p. 2171-80.
126. Hack, I., et al., *Reelin is a detachment signal in tangential chain-migration during postnatal neurogenesis.* Nat Neurosci, 2002. **5**(10): p. 939-45.

127. Saghatelyan, A., et al., *Tenascin-R mediates activity-dependent recruitment of neuroblasts in the adult mouse forebrain.* Nat Neurosci, 2004. **7**(4): p. 347-56.
128. Betarbet, R., et al., *Dopaminergic and GABAergic interneurons of the olfactory bulb are derived from the neonatal subventricular zone.* Int J Dev Neurosci, 1996. **14**(7-8): p. 921-30.
129. Parrish-Aungst, S., et al., *Quantitative analysis of neuronal diversity in the mouse olfactory bulb.* J Comp Neurol, 2007. **501**(6): p. 825-36.
130. De Marchis, S., et al., *GABAergic phenotypic differentiation of a subpopulation of subventricular derived migrating progenitors.* Eur J Neurosci, 2004. **20**(5): p. 1307-17.
131. Lemasson, M., et al., *Neonatal and adult neurogenesis provide two distinct populations of newborn neurons to the mouse olfactory bulb.* J Neurosci, 2005. **25**(29): p. 6816-25.
132. Petreanu, L. and A. Alvarez-Buylla, *Maturation and death of adult-born olfactory bulb granule neurons: role of olfaction.* J Neurosci, 2002. **22**(14): p. 6106-13.
133. Rochefort, C., et al., *Enriched odor exposure increases the number of newborn neurons in the adult olfactory bulb and improves odor memory.* J Neurosci, 2002. **22**(7): p. 2679-89.
134. Orona, E., J.W. Scott, and E.C. Rainer, *Different granule cell populations innervate superficial and deep regions of the external plexiform layer in rat olfactory bulb.* J Comp Neurol, 1983. **217**(2): p. 227-37.
135. Lledo, P.M. and A. Saghatelyan, *Integrating new neurons into the adult olfactory bulb: joining the network, life-death decisions, and the effects of sensory experience.* Trends Neurosci, 2005. **28**(5): p. 248-54.
136. Lledo, P.M. and S. Lagier, *Adjusting neurophysiological computations in the adult olfactory bulb.* Semin Cell Dev Biol, 2006. **17**(4): p. 443-53.
137. Sottile, J., J. Selegue, and D.F. Mosher, *Synthesis of truncated amino-terminal trimers of thrombospondin.* Biochemistry, 1991. **30**(26): p. 6556-62.

138. Iruela-Arispe, M.L., et al., *Differential expression of thrombospondin 1, 2, and 3 during murine development.* Dev Dyn, 1993. **197**(1): p. 40-56.
139. Lawler, J.W., H.S. Slayter, and J.E. Coligan, *Isolation and characterization of a high molecular weight glycoprotein from human blood platelets.* J Biol Chem, 1978. **253**(23): p. 8609-16.
140. Chandrasekaran, S., et al., *Pro-adhesive and chemotactic activities of thrombospondin-1 for breast carcinoma cells are mediated by alpha3beta1 integrin and regulated by insulin-like growth factor-1 and CD98.* J Biol Chem, 1999. **274**(16): p. 11408-16.
141. Murphy-Ullrich, J.E., S. Schultz-Cherry, and M. Hook, *Transforming growth factor-beta complexes with thrombospondin.* Mol Biol Cell, 1992. **3**(2): p. 181-8.
142. Schultz-Cherry, S., et al., *Thrombospondin binds and activates the small and large forms of latent transforming growth factor-beta in a chemically defined system.* J Biol Chem, 1994. **269**(43): p. 26775-82.
143. Tolsma, S.S., et al., *Peptides derived from two separate domains of the matrix protein thrombospondin-1 have anti-angiogenic activity.* J Cell Biol, 1993. **122**(2): p. 497-511.
144. Rege, T.A., et al., *Thy-1, via its GPI anchor, modulates Src family kinase and focal adhesion kinase phosphorylation and subcellular localization, and fibroblast migration, in response to thrombospondin-1/hep I.* Exp Cell Res, 2006. **312**(19): p. 3752-67.
145. Adams, J.C. and J. Lawler, *The thrombospondins.* Int J Biochem Cell Biol, 2004. **36**(6): p. 961-8.
146. Neugebauer, K.M., et al., *Vitronectin and thrombospondin promote retinal neurite outgrowth: developmental regulation and role of integrins.* Neuron, 1991. **6**(3): p. 345-58.
147. Osterhout, D.J., W.A. Frazier, and D. Higgins, *Thrombospondin promotes process outgrowth in neurons from the peripheral and central nervous systems.* Dev Biol, 1992. **150**(2): p. 256-65.
148. O'Shea, K.S., L.H. Liu, and V.M. Dixit, *Thrombospondin and a 140 kd fragment promote adhesion and neurite outgrowth from embryonic*

central and peripheral neurons and from PC12 cells. Neuron, 1991. **7**(2): p. 231-7.

149. Christopherson, K.S., et al., *Thrombospondins are astrocyte-secreted proteins that promote CNS synaptogenesis.* Cell, 2005. **120**(3): p. 421-33.
150. Oganesian, A., et al., *Thrombospondins use the VLDL receptor and a nonapoptotic pathway to inhibit cell division in microvascular endothelial cells.* Mol Biol Cell, 2008. **19**(2): p. 563-71.
151. Crawford, S.E., et al., *Thrombospondin-1 is a major activator of TGF-beta1 in vivo.* Cell, 1998. **93**(7): p. 1159-70.
152. Agah, A., et al., *The lack of thrombospondin-1 (TSP1) dictates the course of wound healing in double-TSP1/TSP2-null mice.* Am J Pathol, 2002. **161**(3): p. 831-9.
153. Hynes, R.O., *Targeted mutations in cell adhesion genes: what have we learned from them?* Dev Biol, 1996. **180**(2): p. 402-12.
154. Adams, J.C. and R.P. Tucker, *The thrombospondin type 1 repeat (TSR) superfamily: diverse proteins with related roles in neuronal development.* Dev Dyn, 2000. **218**(2): p. 280-99.
155. Tan, K., et al., *Crystal structure of the TSP-1 type 1 repeats: a novel layered fold and its biological implication.* J Cell Biol, 2002. **159**(2): p. 373-82.
156. Klar, A., M. Baldassare, and T.M. Jessell, *F-spondin: a gene expressed at high levels in the floor plate encodes a secreted protein that promotes neural cell adhesion and neurite extension.* Cell, 1992. **69**(1): p. 95-110.
157. Gobron, S., et al., *SCO-spondin: a new member of the thrombospondin family secreted by the subcommissural organ is a candidate in the modulation of neuronal aggregation.* J Cell Sci, 1996. **109 (Pt 5)**: p. 1053-61.
158. DeFreitas, M.F., et al., *Identification of integrin alpha 3 beta 1 as a neuronal thrombospondin receptor mediating neurite outgrowth.* Neuron, 1995. **15**(2): p. 333-43.

159. Tryggvason, K., M. Hoyhtya, and T. Salo, *Proteolytic degradation of extracellular matrix in tumor invasion.* Biochim Biophys Acta, 1987. **907**(3): p. 191-217.
160. McKeown-Longo, P.J., R. Hanning, and D.F. Mosher, *Binding and degradation of platelet thrombospondin by cultured fibroblasts.* J Cell Biol, 1984. **98**(1): p. 22-8.
161. Mikhailenko, I., M.Z. Kounnas, and D.K. Strickland, *Low density lipoprotein receptor-related protein/alpha 2-macroglobulin receptor mediates the cellular internalization and degradation of thrombospondin. A process facilitated by cell-surface proteoglycans.* J Biol Chem, 1995. **270**(16): p. 9543-9.
162. Daviet, L. and J.L. McGregor, *Vascular biology of CD36: roles of this new adhesion molecule family in different disease states.* Thromb Haemost, 1997. **78**(1): p. 65-9.
163. Crombie, R., et al., *Identification of a CD36-related thrombospondin 1-binding domain in HIV-1 envelope glycoprotein gp120: relationship to HIV-1-specific inhibitory factors in human saliva.* J Exp Med, 1998. **187**(1): p. 25-35.
164. O'Shea, K.S., J.S. Rheinheimer, and V.M. Dixit, *Deposition and role of thrombospondin in the histogenesis of the cerebellar cortex.* J Cell Biol, 1990. **110**(4): p. 1275-83.
165. Chamak, B., A. Dobbertin, and M. Mallat, *Immunohistochemical detection of thrombospondin in microglia in the developing rat brain.* Neuroscience, 1995. **69**(1): p. 177-87.
166. Hoffman, J.R., V.M. Dixit, and K.S. O'Shea, *Expression of thrombospondin in the adult nervous system.* J Comp Neurol, 1994. **340**(1): p. 126-39.
167. Buee, L., et al., *Immunohistochemical identification of thrombospondin in normal human brain and in Alzheimer's disease.* Am J Pathol, 1992. **141**(4): p. 783-8.

168. Beffert, U., et al., *Modulation of synaptic plasticity and memory by Reelin involves differential splicing of the lipoprotein receptor Apoer2.* Neuron, 2005. **47**(4): p. 567-79.

5 Results and Discussion

5.1 “Thrombospondin-1 binds to ApoER2 and VLDL receptor and functions in postnatal neuronal migration”

The EMBO Journal (2008), 1–12 | © 2008 European Molecular Biology Organization | All Rights Reserved 0261-4189/08
www.embojournal.org

THE
EMBO
JOURNAL

Thrombospondin-1 binds to ApoER2 and VLDL receptor and functions in postnatal neuronal migration

Sophia M Blake, Vera Strasser, Nuno Andrade, Sarah Duit, Reinhold Hofbauer, Wolfgang J Schneider and Johannes Nimpf*

Department of Medical Biochemistry, Max F Perutz Laboratories, Medical University Vienna, Vienna, Austria

Apolipoprotein E receptor 2 (ApoER2), very low-density lipoprotein receptor (VLDLR), and Dab1 are the main components of the Reelin signalling cascade. Reelin is the sole ligand defined so far in signalling through this pathway. Postnatal migration of neuronal precursors from the subventricular zone (SVZ) to the olfactory bulb (OB), however, depends on ApoER2 and Dab1, but functions independently of Reelin. Here, we show that thrombospondin-1 (THBS-1) is a novel physiological ligand for ApoER2 and VLDLR. THBS-1 is present in the SVZ and along the entire rostral migratory stream (RMS). It binds to ApoER2 and VLDLR and induces phosphorylation of Dab1. In contrast to Reelin, it does not induce Dab1 degradation or Akt phosphorylation, but stabilizes neuronal precursor chains derived from subventricular explants. Lack of THBS-1 results in anatomical abnormalities of the RMS and leads to a reduction of postnatal neuronal precursors entering the OB.

The EMBO Journal advance online publication, 23 October 2008; doi:10.1038/emboj.2008.223
Subject Categories: signal transduction; neuroscience
Keywords: postnatal neuronal migration; Reelin receptors; rostral migratory stream; thrombospondin-1

Introduction

The Reelin signalling pathway is indispensable for the development of laminated structures in the brain (Tissir and Goffinet, 2003). The best studied role of Reelin is its function in radial neuronal migration during development of the neocortex and positioning of granule cells in the hippocampus (Forster *et al*, 2006). Key players of the Reelin signalling pathway are apolipoprotein E receptor 2 (ApoER2) and very low-density lipoprotein receptor (VLDLR) that relay the Reelin signal into radially migrating neurons. The molecular basis of this signalling cascade was recently summarized (Herz and Chen, 2006) and involves binding of oligomeric Reelin to ApoER2 and/or VLDLR, subsequent activation of Src family kinases, and phosphorylation of Disabled 1 (Dab1).

Reelin also has an important function in the integration of neuronal precursors into the olfactory bulb (OB) during postnatal development of the olfactory system in rodents. Neuronal precursors within the subventricular zone (SVZ) migrate tangentially through the rostral migratory stream (RMS) towards the OB forming chains ensheathed by glial cells (Lois *et al*, 1996). Reelin produced by mitral cells in the OB promotes the detachment of neuronal precursors from the incoming chains so as to allow proper radial migration of the precursors within the bulb (Hack *et al*, 2002). As recently discovered in our laboratory, however, ApoER2 and Dab1 within the RMS function independently of Reelin in postnatal tangential neuronal migration (Andrade *et al*, 2007). In mice lacking either ApoER2 or Dab1, chain formation is severely compromised, and neuronal precursors accumulate in the SVZ unable to migrate into the OB and thereby failing to form an RMS. As Reelin-producing cells are absent from both the SVZ and the RMS, it seems likely that ligands other than Reelin interact with ApoER2. The following observations prompted us to consider thrombospondin-1 (THBS-1) as such a ligand. THBSs are widely expressed in the developing central nervous system (O'Shea and Dixit, 1988; O'Shea *et al*, 1990). Cell culture experiments demonstrated that THBS-1 promotes neurite outgrowth from cultured neurons (O'Shea *et al*, 1991), and antibodies against THBSs block migration of cerebellar granule cells *in vitro*, suggesting that THBSs might be involved in neuronal migration (O'Shea *et al*, 1990). Despite these *in vitro* data, the function of THBS-1 in the central nervous system at the cellular level remained largely unknown mostly because mice lacking either THBS-1 (Lawler *et al*, 1998) or THBS-2 (Kyriakides *et al*, 1998) or both (Agah *et al*, 2002) did not exhibit an overt phenotype in the brain. THBS-1 belongs to a subfamily of THBSs that form trimers (Carlson *et al*, 2008) and are involved in cell-to-cell and cell-to-matrix communications (Lawler, 2000; Bornstein, 2001). They interact with membrane proteins such as integrins, CD47, CD36, proteoglycans, and low-density lipoprotein receptor-related protein 1 (LRP1) as well as with growth factors such as TGFβ and PDGF. The interaction of THBS-1 with LRP1 (Godyna *et al*, 1995) is of specific interest as ApoER2, VLDLR, and LRP1 belong to the same receptor family and share many ligands (Schneider and Nimpf, 2003). Here, we have identified THBS-1 as a component of the SVZ and RMS that binds to ApoER2 and VLDLR and stabilizes neuronal precursor chains without inducing the canonical Reelin signalling pathway.

Our findings demonstrate a hitherto unknown function of THBS-1 in the plasticity of neuronal precursor chains in the postnatal brain within the RMS. This function is mediated by ApoER2 and depends on the presence of Dab1, but stands

*Corresponding author. Department of Medical Biochemistry, Max F Perutz Laboratories, Medical University of Vienna, Dr Bohrgasse 9/2, 1030 Vienna, Austria. Tel.: +43 1 4277 61808; Fax: +43 1 4277 9618; E-mail: Johannes.Nimpf @meduniwien.ac.at

Received: 5 May 2008; accepted: 26 September 2008

in clear contrast to the Reelin signal that promotes disintegration of neuronal precursor chains.

Results

THBS-1 is expressed in the RMS of postnatal mice

ApoER2 and Dab1 knockout mice display phenotypes in the postnatal brain, where formation of neuronal precursor chains is severely compromised and the RMS is absent (Andrade *et al*, 2007). This effect cannot easily be ascribed to disruption of the Reelin signalling pathway, as Reelin, the only known physiological signalling ligand for ApoER2 and VLDLR to date, is absent from both the RMS and the SVZ. ApoER2 and VLDLR belong to the LDL receptor family and share many ligands with LRP1 (a comprehensive list of ligands of LRP1 can be found in Herz and Strickland, 2001). Screening the Allen Brain Atlas (Lein *et al*, 2007) for the expression of those candidate ligands revealed the presence of transcripts for THBS-1 in the RMS. THBS-1 belongs to a superfamily of proteins involved in neuronal development (Adams and Tucker, 2000) and has been shown to bind to LRP1 (Godyna *et al*, 1995).

To confirm the presence of THBS-1 protein within the RMS, we performed immunohistochemical studies on sagittal sections of forebrains of P17 mice using a specific antibody against THBS-1. As demonstrated in Figure 1A, consistent staining for THBS-1 is present not only throughout the entire RMS but also in the SVZ. Higher magnification suggested that THBS-1 is associated with cells within the chains of migrating neurons forming the RMS (Figure 1B). Immunohistochemistry of a corresponding section derived from *THBS-1*$^{-/-}$ mice as a control (Figure 1C) verified the specificity of the staining shown in Figure 1A and B. It has been proposed that THBS-1 expression is downregulated after birth (Iruela-Arispe *et al*, 1993). Western blots performed using total brain extracts derived from postnatal brain and embryonic brain from wt mice, however, demonstrated that THBS-1 protein is present before and after birth (Figure 1D). A prominent band with an M_r (relative molecular mass) of 170×10^3 (under reducing conditions) is present in postnatal (P17, lane 1) and embryonic brain (E17, lane 2) from wt mice, but not in the brain of a *THBS-1*$^{-/-}$ mouse (P17, lane 3). This protein migrates with the same M_r as purified THBS-1 (lane 4).

THBS-1 binds to ApoER2 and VLDLR

Having revealed the presence of a candidate ligand for ApoER2 and VLDLR within the RMS, we tested whether THBS-1 indeed binds to both receptors. We purified THBS-1 from human platelets and performed an ELISA-based binding assay using recombinant ligand-binding domains of ApoER2 and VLDLR (Koch *et al*, 2002) (Figure 2). THBS-1 is a homotrimeric glycoprotein that migrates under non-reducing conditions with an M_r of 450×10^3 and with an M_r of 170×10^3 under reducing conditions (Figure 2D). As demonstrated in Figure 2A, purified THBS-1 binds with high affinity to both Reelin receptors. The affinities (K_d values) of THBS-1 were determined to be 32 nM for ApoER2 and 14 nM for VLDLR. Binding of THBS-1 to both receptors is inhibited by Reelin (Figure 2B) and receptor-associated protein (myc–RAP) (Figure 2C). RAP associates with most members of the LDL receptor family and inhibits the interaction with their cognate ligands (Willnow, 1998). These results demonstrate that the modes of interaction of THBS-1 and Reelin with ApoER2 and VLDLR are qualitatively and quantitatively similar.

THBS-1 induces Dab1 phosphorylation in primary neurons, but does not stimulate other key events of the Reelin signalling cascade

As recently demonstrated, receptor clustering by multivalent ligands, such as Reelin, is sufficient to promote Dab1 phosphorylation (Strasser *et al*, 2004). As THBS-1 forms homotrimers, it is a prime candidate for signalling through ApoER2 and VLDLR. We tested whether purified THBS-1 triggers Dab1 phosphorylation in primary neurons. Primary mouse E16 neurons were treated with purified THBS-1 or Reelin-conditioned medium (RCM) as a control. As shown in Figure 3A (lane 3), neurons respond to THBS-1 (10 μg/ml) with a robust phosphorylation of Dab1 similar to that induced by RCM (lane 1). The effect of THBS-1 was dose dependent, leading to maximal Dab1 phosphorylation at 10–20 μg/ml with a decrease at higher concentrations (data not shown). Dab1 phosphorylation is most likely mediated by interaction of THBS-1 with ApoER2 and VLDLR, as it is abolished by the addition of myc–RAP (lane 4). myc–RAP even suppressed phosphorylation levels below the background (compare lane 4 to 2 and 5), which has been shown to be caused by small amounts of endogenous Reelin consistently present in the preparation of primary neurons (Koch

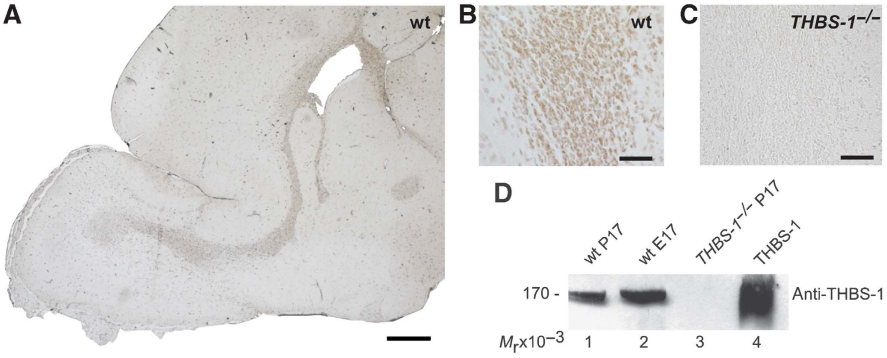

Figure 1 Thrombospondin-1 is expressed in the RMS and the SVZ of postnatal mice. Sagittal sections (6 μm) of the forebrains from (**A**, **B**) wt and (**C**) *THBS-1*$^{-/-}$ mice were immunostained with a monoclonal antibody against THBS-1. (**D**) Total protein extracts from wt P17 (lane 1), wt E17 (lane 2), and *THBS-1*$^{-/-}$ P17 brains (lane 3) were prepared. The samples (20 μg of total protein lysate per lane) and purified THBS-1 (0.5 μg, lane 4) were subjected to 6% SDS–PAGE under reducing conditions, and subsequent western blot analysis was performed using a monoclonal antibody against THBS-1 and an appropriate HRP-conjugated secondary antibody. Scale bars: (A) 500 μm; (B, C) 50 μm.

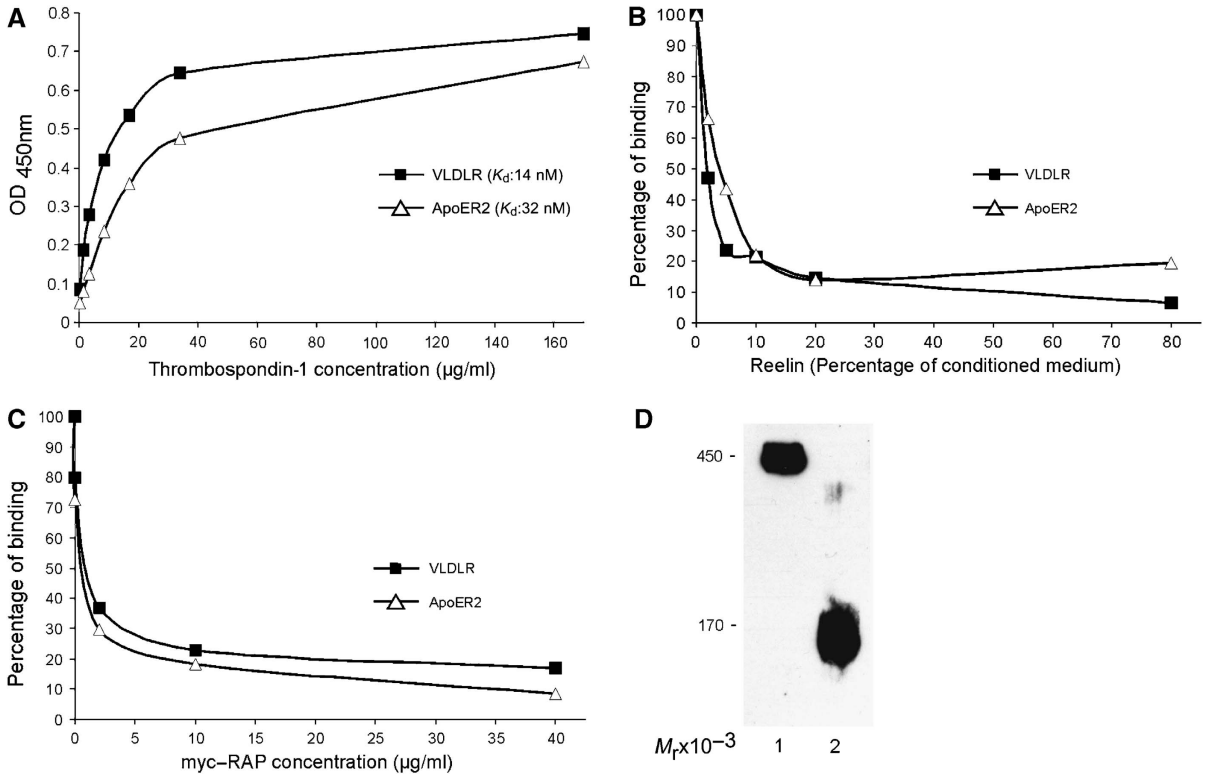

Figure 2 Thrombospondin-1 binds to ApoER2 and VLDLR. (**A**) Microtitre plates were coated with recombinant ligand-binding domains of ApoER2 and VLDLR (ApoER2Δ4-6-MBP/His and VLDLR1-8-MBP/His, respectively) and incubated with the indicated amounts of THBS-1. (**B**, **C**) Microtitre plates were coated with ApoER2Δ4-6-MBP/His or VLDLR1-8-MBP/His, and incubated with THBS-1 (15 μg/ml for ApoER2 and 6.5 μg/ml for VLDLR) in the presence of increasing amounts of Reelin-conditioned medium (B) or myc-tagged RAP (myc–RAP) (C). Bound THBS-1 was detected with a monoclonal anti-THBS-1 antibody and an appropriate HRP-conjugated secondary antibody. OD_{450}, optical density at 450 nm. K_d, dissociation constant. In each case (A–C), the results of a representative experiment are shown. K_d values have been calculated from three independent experiments. (**D**) Western blot analysis of purified THBS-1. THBS-1 was purified from human plasma as described in Materials and methods and subjected to 6% SDS–PAGE (0.5 μg of protein per lane) under non-reducing (lane 1) and reducing conditions (lane 2) and subsequent western blot analysis using a monoclonal antibody against THBS-1 and an appropriate HRP-conjugated secondary antibody.

et al, 2002). To further support the notion that the effect of THBS-1 is mediated by ApoER2/VLDLR, we used primary E16 neurons derived from mouse embryos lacking both receptor genes (*ApoER2*$^{-/-}$/*VLDLR*$^{-/-}$) (Trommsdorff *et al*, 1999). In sharp contrast to neurons derived from wt mice, these neurons neither responded to Reelin nor to THBS-1 with phosphorylation of Dab1 (Figure 3B, lanes 3–6). Again, due to the lack of the receptors, these neurons do not even exhibit background levels of Dab1 phosphorylation.

Another important effect of the Reelin signalling pathway is the proteasome-dependent degradation of Dab1 (Arnaud *et al*, 2003; Bock *et al*, 2004). As recently demonstrated, this effect is an important regulator for correct positioning of radially migrating neurons during cortical development (Feng *et al*, 2007). Thus, we tested whether THBS-1 causes Dab1 degradation in primary neurons (Figure 3C). In contrast to Reelin (Figure 3C, lane 1), which causes significant loss of total Dab1 protein, THBS-1 treatment did not result in a detectable reduction of this protein even after 6 h (Figure 3C, lane 3). The surprising result that THBS-1 triggers Dab1 phosphorylation but not Dab1 degradation led us to examine whether Akt phosphorylation, another downstream event of Reelin-induced Dab1 phosphorylation, can be induced by THBS-1. Using primary neurons, Reelin-induced Akt phosphorylation is not as dramatic as can be seen using fibroblasts expressing ApoER2 and Dab1 (Mayer *et al*, 2006) (Figure 3D, lanes 1 and 2). Again, this is due to the presence of endogenous Reelin in such cultures, which results in detectable background phosphorylation of Akt. Addition of myc–RAP, which blocks the effect of Reelin by competing for the Reelin receptors, strongly reduced Akt phosphorylation (lane 3). Addition of THBS-1 also diminished Akt phosphorylation (lanes 4 and 5), demonstrating that THBS-1-induced Dab1 phosphorylation does not trigger Akt phosphorylation, but most likely inhibits background activation by competing with Reelin for the receptors.

Taken together, these results demonstrate that THBS-1 is present in the RMS, binds to both Reelin receptors, phosphorylates Dab1, but does not elicit cellular responses downstream of Dab1 similar to those of Reelin.

THBS-1 stabilizes neuronal chains produced by SVZ explants in vitro

As neuronal precursors migrating along the RMS express ApoER2 (Andrade *et al*, 2007) and Dab1 (Hack *et al*, 2002), we next investigated the role of THBS-1 on migratory neuronal precursors. We used cultured SVZ explants in a three-dimensional matrix, a system where chain migration of neuronal precursors can be studied *in vitro* (Wichterle *et al*,

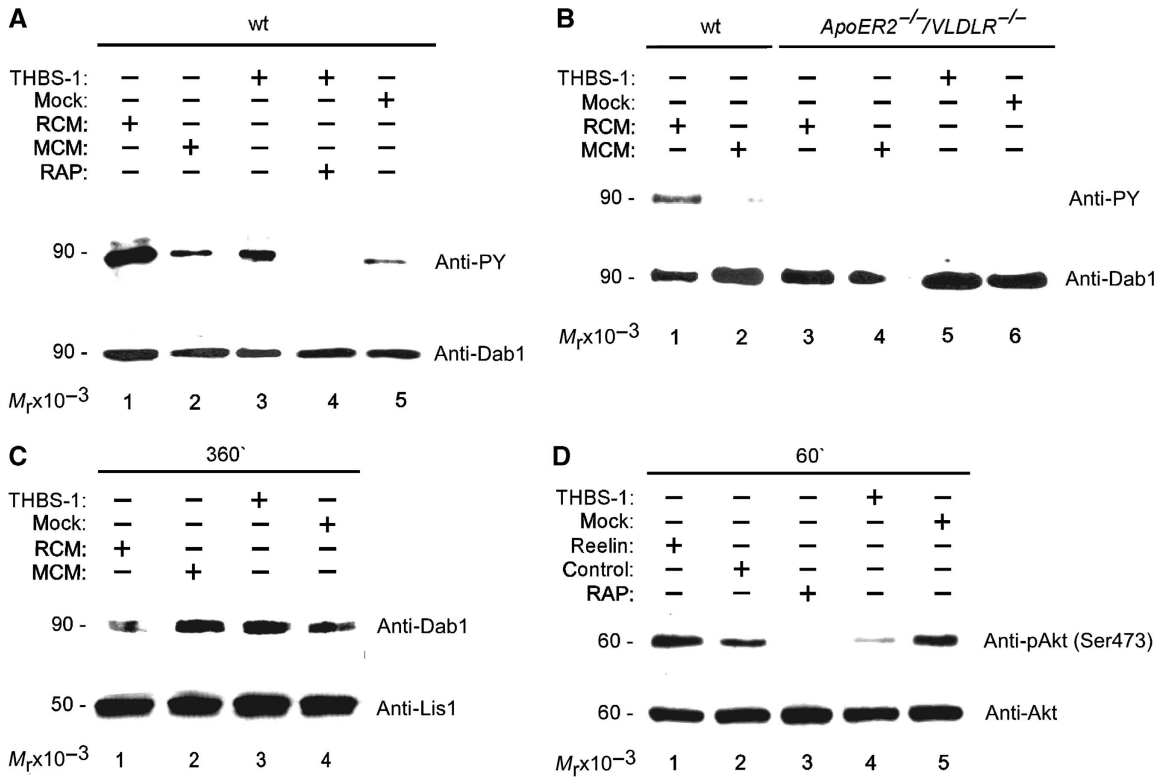

Figure 3 Thrombospondin-1 induces Dab1 phosphorylation but not Dab1 degradation and Akt phosphorylation in primary embryonic neurons. (**A**) Primary mouse E16 wt neurons were incubated with Reelin-conditioned medium (RCM, lane 1), mock-conditioned medium (MCM, lane 2), purified THBS-1 (10 μg/ml, lane 3), THBS-1 in the presence of myc–RAP (lane 4), and mock medium (lane 5). Cells were processed for immunoprecipitation of Dab1, and western blotting was subsequently performed using antiphosphotyrosine (PY) or anti-Dab1 (Dab1) antibody as indicated. (**B**) Primary mouse E16 wt and primary E16 *ApoER2*$^{-/-}$/*VLDLR*$^{-/-}$ neurons were incubated with RCM (lanes 1 and 3), MCM (lanes 2 and 4), purified THBS-1 (lane 5) and mock medium (lane 6). Dab1 phosphorylation was measured as indicated above. (**C**) Primary mouse E16 wt neurons were incubated with RCM (lane 1), MCM (lane 2), purified THBS-1 (10 μg/ml, lane 3), and mock medium (lane 4) for 6 h. Total cell extracts were prepared and western blotting was performed using anti-Dab1 and anti-Lis1 antibodies. (**D**) Primary mouse E16 wt neurons were incubated with Reelin (lane 1), control medium (lane 2), control medium and myc–RAP (lane 3), purified THBS-1 (10 μg/ml, lane 4), and mock medium (lane 5) for 1 h. Cell extracts were prepared and western blotting was performed using anti-phospho-Akt and anti-Akt antibodies.

1997). SVZ explants were prepared from wt mice, and chain development was monitored with and without the addition of Reelin or THBS-1. In the absence of exogenous Reelin or THBS-1, typical chains were formed 2 days after the start of the experiment (Figure 4A). Addition of Reelin caused disassembly of the chains (Figure 4I) and a dramatic increase of individual cells (Figure 4L) as described (Hack *et al*, 2002). In sharp contrast, addition of THBS-1 did not dissolve the chains, but significantly increased the chain length (Figure 4K) when compared with the mock condition (Figure 4A and E) and there was no increase in the number of individual cells (Figure 4L). In accordance with previous experiments (Wichterle *et al*, 1997), longer incubation of the explants for 5 days led to disassembly of the chains (Figure 4B) and a dramatic increase in the number of dissociated cells even in the absence of Reelin (Figure 4M). Explants treated for 5 days with THBS-1 exhibited a significantly different behaviour. They retained the ability to form robust neuronal precursor chains (Figure 4F), and the number of detached cells was dramatically reduced in comparison to the mock situation (Figure 4M, control). Staining for Tuj1, a neuron-specific beta tubulin (Wichterle *et al*, 1997), demonstrated that the cells present within the chains of mock- and THBS-1-treated explants after 5 days are migrating neuronal precursors, which express the same marker as the precursors *in vivo* (Figure 4D and H). The effect of THBS-1 on the explants was completely abolished in the presence of myc–RAP (Figure 4J and M).

The results from these experiments, together with the finding that THBS-1 does not induce Dab1 degradation and Akt phosphorylation, strongly suggest that THBS-1 and Reelin have different physiological effects on migrating neuronal precursors. As Reelin binds with higher affinity to the receptors than THBS-1 does, we expected the effect of Reelin to be dominant over THBS-1. When SVZ explants were treated with a combination of both ligands, Reelin-promoted destabilization of the chains at day 2 was only partially inhibited by the addition of an excess of THBS-1 (Figure 4L). On the other hand, THBS-1-induced stabilization after 5 days of incubation was significantly reduced in the presence of Reelin (Figure 4M). It is to be noted here that Reelin was added as a component of RCM, and its estimated concentration was below that of THBS-1.

Next, we tested whether the effect of THBS-1 is indeed mediated by ApoER2/VLDLR as suggested by the RAP experiments described above. Explants from *ApoER2*$^{-/-}$/*VLDLR*$^{-/-}$ mice were treated with THBS-1 and chain formation was monitored. As demonstrated in Figure 5A and B, addition of THBS-1 did not rescue the inability of those explants to form neuronal precursor chains.

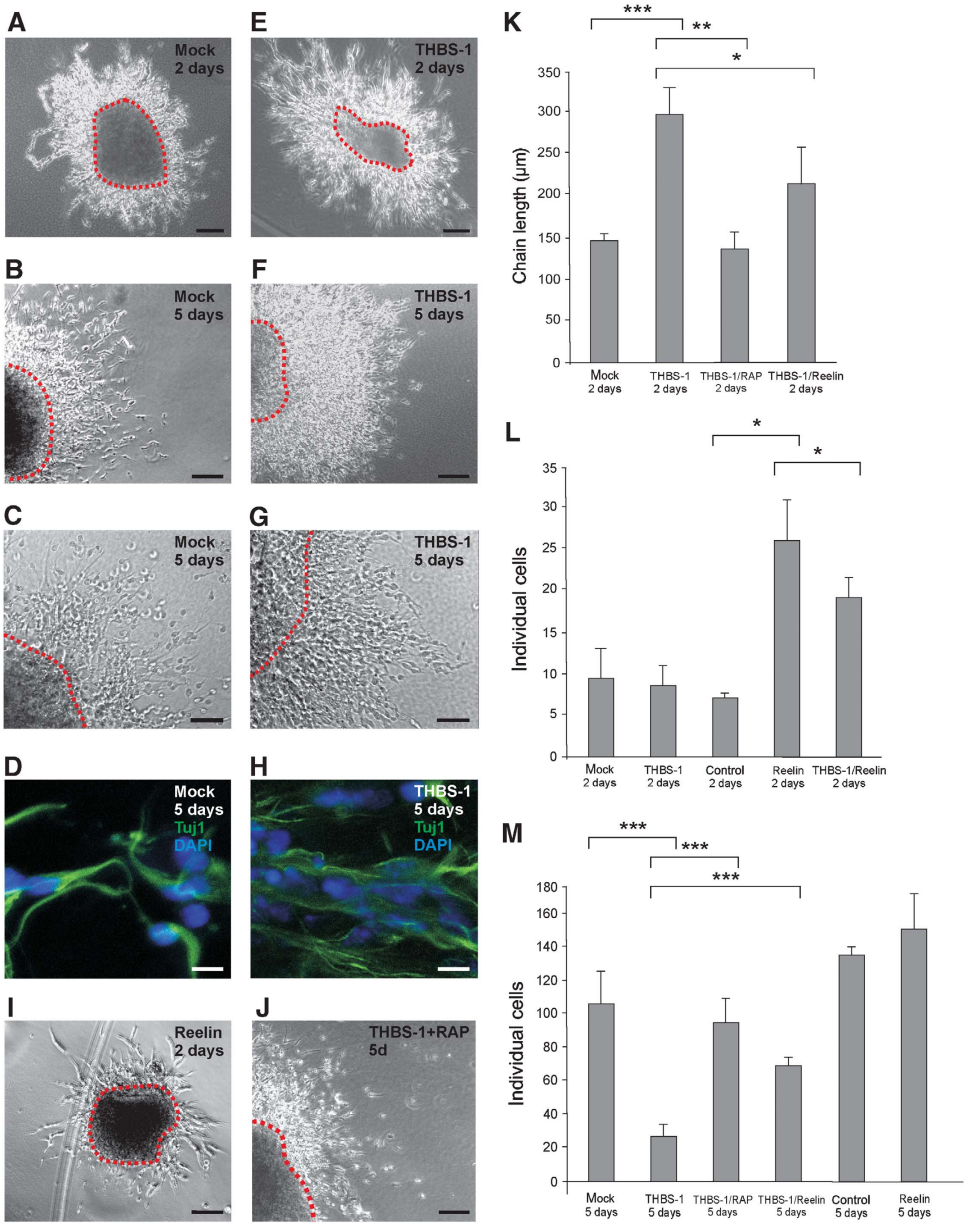

Figure 4 Thrombospondin-1 stabilizes chains of migratory neuronal precursors from explants of the SVZ. (**A**–**D**) SVZ explants were prepared from P7 wt mice and treated with mock medium, or (**E**–**H**) cultivated in the presence of 4 µg/ml purified THBS-1, (**I**) Reelin or (**J**) THBS-1 in the presence of myc–RAP for 2 days (A, E, I) or 5 days (B, C, D, F, G, H, J), respectively. (D, H) Explants were immunostained using antibodies against Tuj1 with the appropriate secondary Alexa-Fluor antibody and DAPI. Representative explants are shown. (**K**) Explants were analysed by measuring the length of migratory chains after 2 days in culture and the number of individual cells per field after (**L**) 2 days and after (**M**) 5 days in culture (chain length 2 days: mock: $n=8$, THBS-1: $n=13$, THBS-1/myc–RAP: $n=7$, THBS-1/Reelin: $n=6$; dissociated neurons 2 days: mock: $n=5$, THBS-1: $n=7$, control: $n=2$, Reelin: $n=2$, THBS-1/Reelin: $n=4$; dissociated neurons 5 days: mock: $n=6$, THBS-1: $n=28$, THBS-1/myc–RAP: $n=6$, THBS-1/Reelin: $n=6$, control: $n=4$, Reelin: $n=4$; individual explants were derived from at least four different wt mice). Plots show average + s.e.m.; $^{***}P<0.001$; $^{**}P<0.01$; $^{*}P<0.05$ (Student's *t*-test); scale bars: (A, B, E, F, I, J) 100 µm; (C, G) 50 µm; (D, H) 10 µm.

To confirm an intrinsic function of THBS-1 in chain formation and stabilization, we first confirmed the presence of THBS-1 in SVZ explants and tested whether it is involved in the initial formation of neuronal precursor chains. As demonstrated by western blot analysis (Figure 5C), THBS-1 is indeed expressed by explants used for the assays. Comparing chain formation in explants derived from *THBS-1*$^{-/-}$ mice (Figure 5E) with those from wt mice (Figure 5D) clearly showed that initial chain formation as judged by chain length (Figure 5H) appeared normal. Counting individual cells, however, revealed a significant increase in explants from *THBS-1*$^{-/-}$ mice (Figure 5I). This phenotype became even more evident after 2 days in culture, when a dramatic increase in individual cells was apparent in *THBS-1*$^{-/-}$ explants (Figure 5I). After 3 days, chains derived from *THBS-1*$^{-/-}$ explants were completely disintegrated and closely resembled wt explants after 5 days in culture (not shown). To test whether other THBSs might be upregulated in the *THBS-1*$^{-/-}$ situation, expression of THBS-2 was evaluated by western blotting. THBS-2 could be detected neither in

explants from wt nor from *THBS-1*$^{-/-}$ mice (data not shown). In total brain extracts and extracts derived from OBs, THBS-2 expression was not different between wt and *THBS-1*$^{-/-}$ mice. q-PCR experiments using mRNA derived from total brain demonstrated that levels of THBS-2, -3, and -4 transcripts were not upregulated in *THBS-1*$^{-/-}$ mice (data not shown).

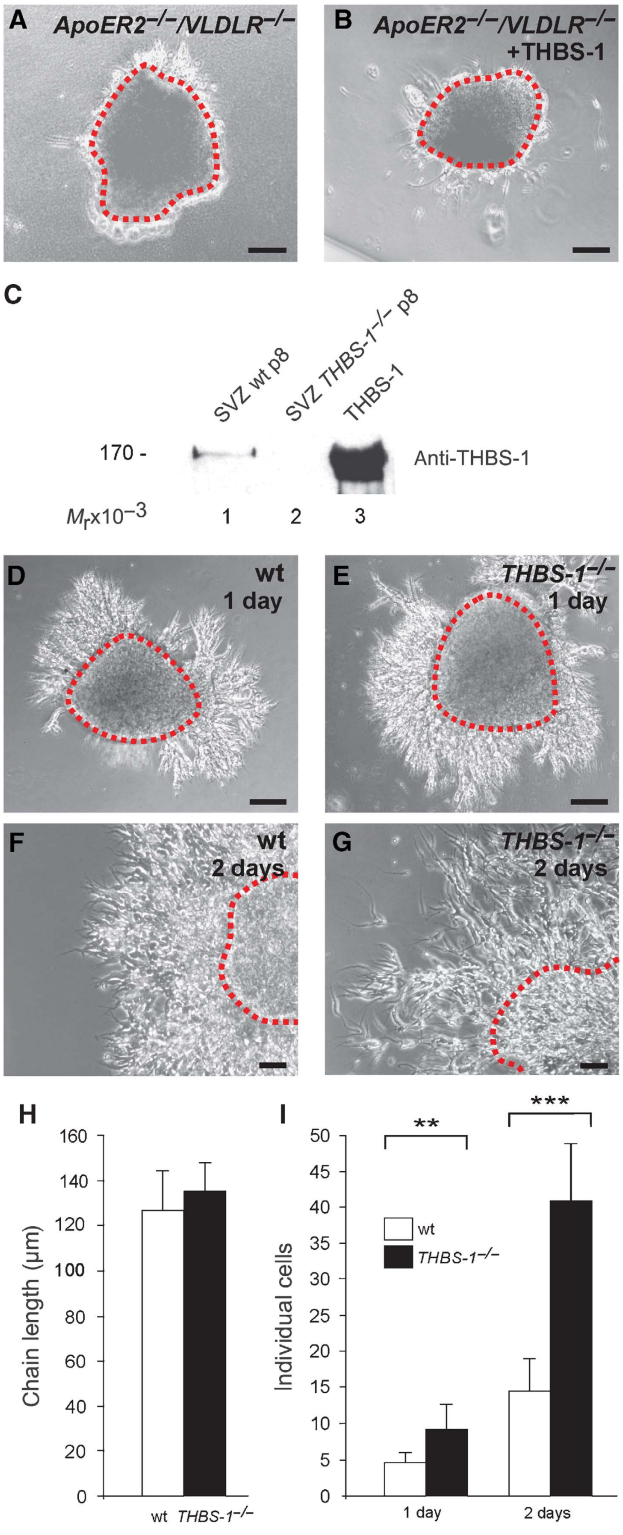

Lack of THBS-1 leads to a widening of the RMS and to a reduction of neuronal precursors integrated into the postnatal OB

To assess the effect of THBS-1 *in vivo*, we examined the RMS of *THBS-1*$^{-/-}$ mice (Figure 6). Haematoxylin and eosin staining of sagittal sections derived from *THBS-1*$^{-/-}$ mice showed that the RMS is present, but exhibits an altered morphology at the entrance point to the OB (Figure 6A and E). In this area, the stream appears much wider and less focused. Closer examination of the RMS using immunofluorescence to stain for cells present in this area (DAPI) and for migrating neuronal precursors (doublecortin, DCX) demonstrated that the widening of the stream is due to less densely packed cells forming the RMS in *THBS-1*$^{-/-}$ mice (Figure 6F–H) when compared with cells forming the wt RMS (Figure 6B–D).

To further investigate and quantify the observation that *THBS-1*$^{-/-}$ mice have a wider and less compact stream architecture at the area proximal to the entrance point into the OB, serial sagittal sections derived from wt and *THBS-1*$^{-/-}$ mice were prepared, and the width of the RMS was measured at three defined positions in every section (Figure 6I; all measurements were performed blind to the genotype, see Materials and methods). These points are situated at the beginning of the stream (elbow 1), in the middle of the stream (elbow 2), and at the entrance point to the OB (straight arm). Comparison of the mean values derived from four wt and eight *THBS-1*$^{-/-}$ mice in the same genetic background showed a significant widening (34%) of the stream in the area between elbow 2 and the entrance point to the OB in *THBS-1*$^{-/-}$ mice (Figure 6I). Measuring the actual size of the respective OBs did not reveal a significant difference between wt and *THBS-1*$^{-/-}$ mice.

To test whether the widening of the RMS at the entrance point to the OB leads to fewer postnatal neuronal precursors reaching the OB, BrdU labelling experiments were performed. wt and *THBS-1*$^{-/-}$ animals were injected at P12, and the number of BrdU-positive cells present in the SVZ, along the RMS and in the layers of the OB were determined 5 days after BrdU administration (P17). As demonstrated in Figure 7C, there was no significant difference between wt and *THBS-1*$^{-/-}$ animals in the number of newly generated neuronal precursors present in the SVZ and along the RMS. Within the OB, however, significantly fewer BrdU-positive cells (47%) were detected in the mitral cell layer, the ependymal layer, and

Figure 5 Stability of SVZ explants is dependent on THBS-1. (**A**) P7 *ApoER2*$^{-/-}$/*VLDLR*$^{-/-}$ SVZ explants were treated with control medium or (**B**) cultivated in the presence of 4 µg/ml purified THBS-1 for 2 days. (**C**) Protein extracts (45 µg) from SVZ explants from wt (lane 1), *THBS-1*$^{-/-}$ (lane 2) mice, and purified THBS-1 (0.5 µg) were subjected to 6% SDS–PAGE under reducing conditions. Subsequent western blot analysis was performed using a monoclonal antibody against THBS-1 and an appropriate HRP-conjugated secondary antibody. (**D**, **F**) SVZ explants were prepared from P7 wt and (**E**, **G**) *THBS-1*$^{-/-}$ mice and kept in culture for 1 day (D, E) and 2 days (F,G). Representative explants are shown. (**H**) Explants were analysed by measuring the length of migratory chains after 2 days in culture and (**I**) the number of individual cells per field after 1 and 2 days (chain length 2 days: wt: $n=5$, *THBS-1*$^{-/-}$: $n=6$; individual neurons 1 day: wt: $n=7$, *THBS-1*$^{-/-}$: $n=7$; individual neurons 2 days: wt: $n=17$, *THBS-1*$^{-/-}$: $n=10$; individual explants were derived from at least five different wt and *THBS-1*$^{-/-}$ mice). Plots show average + s.e.m.; ***$P<0.001$; **$P<0.01$; (Student's *t*-test); scale bars: (A, B, D, E) 100 µm; (F, G) 50 µm.

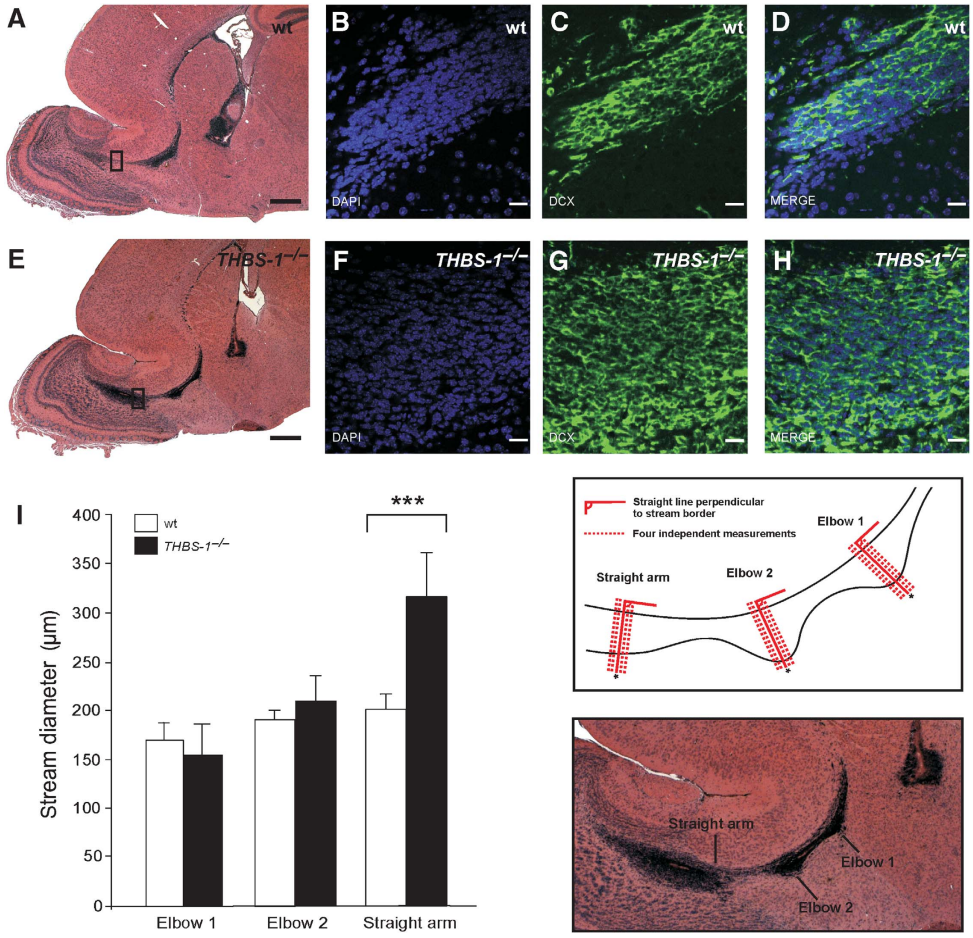

Figure 6 The architecture of the RMS of *THBS-1*$^{-/-}$ mice is altered. (**A–D**) Matched sagittal sections (6 μm) of the forebrains from wt mice and (**E–H**) *THBS-1*$^{-/-}$ mice were stained with (A, E) haematoxylin and eosin, (B, F) DAPI, or (C, G) immunostained with anti-doublecortin (DCX). (**I**) Measurement of the width of the RMS from wt mice (empty bars) and *THBS-1*$^{-/-}$ mice (black bars). Matched serial sections from (P17) wt ($n=4$) and *THBS-1*$^{-/-}$ mice ($n=8$) were used to measure the width of the RMS at three defined sites as described in Materials and methods. Plots show average + s.e.m., ***$P<0.001$ (Student's *t*-test); scale bars: (A, E) 500 μm; (B–D, F–H) 20 μm.

glomerular layer of *THBS-1*$^{-/-}$ animals than in the corresponding structures of wt animals (Figure 7A, B and D). To assess the possibility that the observed difference in the number of newly arrived precursors within the OB might be caused by an interference of THBS-1 with neuronal precursor production in the SVZ, a very short BrdU pulse (2 h) was performed to label only actively proliferating cells in the SVZ. As demonstrated in Figure 7E, there is no overt effect of THBS-1 on neurogenesis that could account for fewer neuronal precursors reaching the OB. In addition, the number of apoptotic cells in these structures (assessed by TUNEL stainings) was indistinguishable between the two genotypes (data not shown).

Taken together, these results strongly suggest that lack of THBS-1 leads to a widening of the RMS and consequently allows fewer neuronal precursors to reach the OB. In turn, this reduction might have an impact on the fate determination and/or life expectancy of these neuronal precursors.

Discussion

THBS-1 is expressed in the SVZ and RMS of postnatal mice and binds to ApoER2 and VLDLR receptor

The finding that ApoER2 functions independently of Reelin in the postnatal RMS (Andrade *et al*, 2007) prompted us to search for alternative ligands for ApoER2 and VLDLR. ApoER2 belongs to the LDL receptor family and is expected to share many of the ligands that bind to VLDLR or LRP1. From a list of potential ligands, THBS-1 was identified as a very interesting candidate present in the entire RMS and the SVZ, but not in the OB. THBS-1 has been described to bind to LRP1 (Godyna *et al*, 1995) and belongs to a family of proteins, the members of which are known to be involved in neuronal development (Adams and Tucker, 2000).

As demonstrated here, THBS-1 binds to ApoER2 and VLDLR and competes for binding with both Reelin and myc–RAP, demonstrating that similar or overlapping binding sites are involved. The affinity of THBS-1 to both receptors is lower than that of Reelin (Koch *et al*, 2002; Strasser *et al*, 2004), but still in the range to be considered high affinity. Although the local concentration of THBS-1 present within the RMS and the SVZ cannot be assessed, functional *in vitro* analysis of THBS-1 demonstrated that Dab1 phosphorylation in primary neurons is triggered by THBS-1. This is in agreement with previous observations that receptor clustering is the key event in inducing Dab1 phosphorylation (Strasser *et al*, 2004). As THBS-1 forms homo-trimers *in vivo*, it is possible that this complex binds up to three receptor molecules simultaneously. The effect of THBS-1 was dose depen-

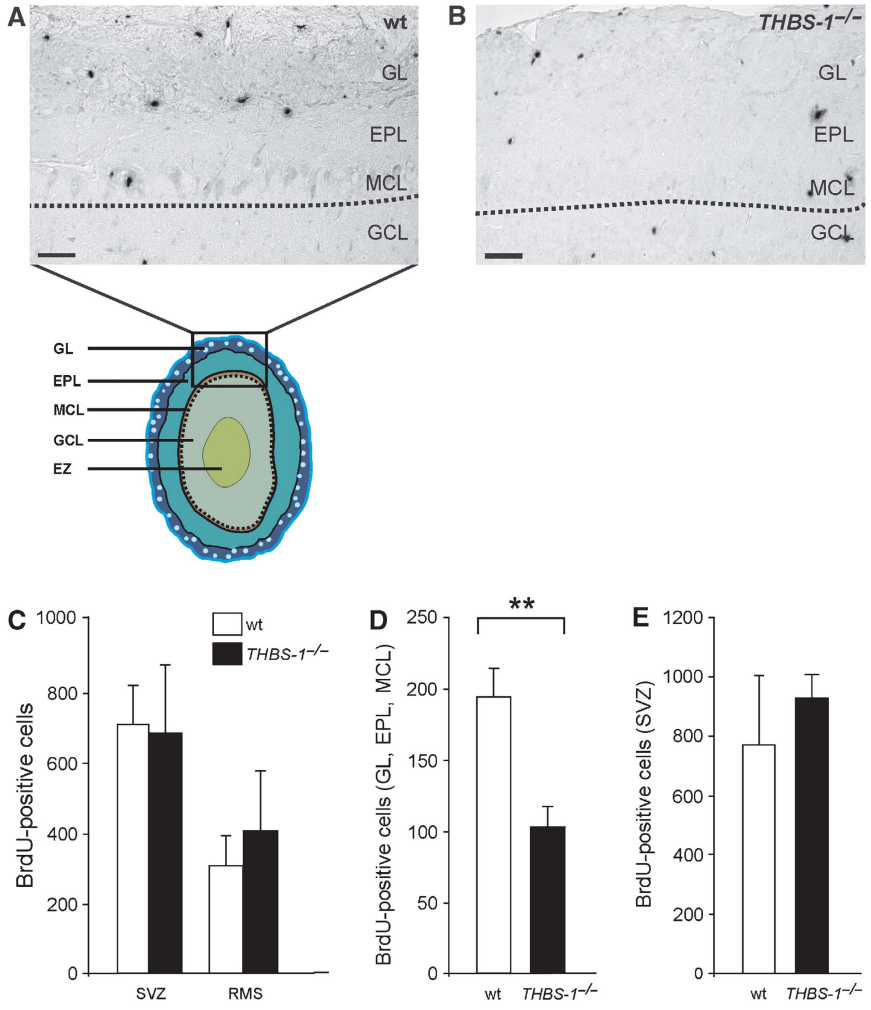

Figure 7 Number of newly generated neuronal precursors derived from the RMS is reduced in the OB of *THBS-1*$^{-/-}$ mice. (**A**) wt and (**B**) *THBS-1*$^{-/-}$ mice received a BrdU pulse at P12, and brains were collected at P17. Matched sagittal sections of the forebrains were stained for BrdU-positive cells. Borders between granule cell layer (GCL) and mitral cell layer (MCL) are marked by dotted lines. (**C**) Quantification of BrdU-positive cells in the SVZ and RMS. (**D**) Quantification of BrdU-positive cells in the glomerular layer (GL), ependymal layer (EPL), and MCL of wt (empty bar) and *THBS-1*$^{-/-}$ mice (black bar). (**E**) Quantification of BrdU-positive cells in the SVZ after a 2 h BrdU pulse. Representative sections are shown (wt mice: empty bars, *THBS-1*$^{-/-}$ mice: black bars; BrdU 5 days, SVZ and RMS: wt: $n=4$, *THBS-1*$^{-/-}$ $n=4$; BrdU 5 days, GL, EPL, and MCL: wt: $n=3$, *THBS-1*$^{-/-}$ $n=6$; BrdU 2 h, SVZ: wt: $n=4$, *THBS-1*$^{-/-}$: $n=3$). Plots show average + s.e.m., $^{**}P<0.01$ (Student's *t*-test); scale bars: 50 μm.

dent with maximal Dab1 phosphorylation at concentrations between 10 and 20 μg/ml, the range at which according to our studies considerable ligand occupation of the receptors is achieved. At higher concentrations (five times higher or more), the effect decreased. Such kinetics are typical for a multivalent ligand that functions through forming higher order complexes with the interacting partner (receptor) (Strasser *et al*, 2004). At non-stoichiometric concentrations, the effect decreases by dilution. Several observations suggest that the effect of THBS-1 is indeed mediated by specific binding to ApoER2 and/or VLDLR. First, the maximal effect occurred at concentrations in the range between the K_d values and maximal saturation of both receptors. Second, THBS-1-mediated Dab1 phosphorylation does not occur in primary neurons lacking both receptors (Figure 3B), and third, the effect is inhibited by myc–RAP (Figure 3A). Dab1 phosphorylation in primary neurons triggered with THBS-1, however, does not lead to Dab1 degradation and Akt phosphorylation, both intricate events of the Reelin signalling pathway. These results further strengthen the hypothesis that Dab1 phosphorylation is necessary but not sufficient to trigger the complete Reelin response in neurons (Jossin *et al*, 2004). In summary, these experiments demonstrate that we have found the first alternative physiological ligand for ApoER2 and VLDLR capable of elucidating Dab1 phosphorylation but not other key events of the Reelin signalling pathway.

Disassembly of neuronal precursor chains in vitro is prevented by THBS-1

In addition to Reelin's role to orchestrate radial migration of neuronal precursors during cortical development, it was also shown to be important for the development of the OB (Hack *et al*, 2002). Reelin was reported to induce the switch from tangential to radial migration of neuronal precursors in the

postnatal OB. Reelin is produced by mitral cells and is believed to function as detachment signal for neuronal precursors entering the OB within chains moving along the RMS. This effect was corroborated *in vitro*, as Reelin was shown to dissolve neuronal precursor chains produced by SVZ explants in three-dimensional Matrigel cultures (Hack *et al*, 2002). Here, we show that THBS-1, however, has the opposite effect on such cultures. It increases chain length and stabilizes the structure of established chains. Incubation of SVZ explants in the presence of THBS-1 prevents the disassembly of neuronal precursor chains after 5 days in culture and increases chain stability with significantly fewer dissociated cells than in the mock situation. This is in accordance with previous findings (Wichterle *et al*, 1997). Apparently, after an initial period during which neuronal precursors form chains and migrate away from the explant, after 4–5 days in culture the chains disintegrate. Furthermore, explants from *THBS-1*$^{-/-}$ mice initially form neuronal precursor chains, which are not significantly different from those produced from wt explants. These chains, however, start to disintegrate significantly earlier (2 days after starting the experiment, a significant portion of the chains is already dispersed). As revealed by competition experiments, even small amounts of Reelin were able to partially revert the effect of THBS-1, in agreement with our binding data, which demonstrate that Reelin has higher affinity for the receptors than THBS-1. Considering that the initial molecular event produced by Reelin and THBS-1 is identical (i.e. Dab1 phosphorylation), this finding is very intriguing. Most likely, this observation can be explained by one or more parallel pathways for the two signalling molecules. One possibility might be the co-receptor concept originally put forward for the action of Reelin, which is based on the finding that Reelin also binds to CNR (Senzaki *et al*, 1999) and $\alpha_3\beta_1$ integrin (Dulabon *et al*, 2000). The interaction of Reelin with $\alpha_3\beta_1$ integrin is of particular interest as it might also serve as intracellular binding site for Dab1 (Calderwood *et al*, 2003) and, under some circumstances, might interact with THBS-1 (Chandrasekaran *et al*, 2000). Although the interaction of Reelin with CNRs or $\alpha_3\beta_1$ integrin or an hitherto unknown receptor is not required for promoting Dab1 phosphorylation, such interaction might promote a 'full-blown' Reelin effect, in which Dab1 phosphorylation is necessary but not sufficient (Jossin *et al*, 2004). In such a scenario, THBS-1 could interact either with another co-receptor not involved in the Reelin action or with ApoER2 and/or VLDLR only, which although promoting Dab1 phosphorylation would elicit a different overall cellular response. On the basis of the results of our competition experiments, we envision an alternate mode of action of THBS-1 and Reelin along the RMS. THBS-1 binding to ApoER2 stabilizes the neuronal precursor chains along the RMS without activation of the canonical Reelin signalling pathway. Reelin present in the OB does not dissolve the chains actively by triggering the Reelin signalling cascade, but in displacing THBS-1 from the receptor it would dissolve the chains and consequently promote correct positioning achieved by radial migration within the OB. Although Dab1 is present in the RMS (Hack *et al*, 2002) and becomes phosphorylated *in vitro* by THBS-1, it is not clear yet whether Dab1 is phosphorylated *in vivo* within the RMS and whether it is involved in the chain stabilizing effect of THBS-1.

Postnatal THBS-1$^{-/-}$ *mice display an altered morphology of the RMS and a decrease of postnatal neurons in the OB*

The concept of THBS-1 stabilizing neuronal precursor chains within the RMS is in agreement with previous findings that THBS-1 promotes adhesion of central and peripheral neurons and PC12 cells (O'Shea *et al*, 1991). As demonstrated here, lack of THBS-1 leads to an altered morphology of the stream and to a decrease of postnatal neuronal precursors derived from the SVZ reaching the OB. Although the SVZ and the proximal part of the RMS appear unchanged (which is in agreement with the results obtained using SVZ explants, where lack of THBS-1 alters neither neurogenesis nor the primary formation of chains), the distal part of the RMS is significantly wider at the entrance point to the OB. This is most likely due to the fact that in the absence of THBS-1 the neuronal precursors present at this point of the RMS are significantly less densely packed. In addition, and possibly as a result of this altered structure of the RMS, fewer precursors and subsequently interneurons become integrated into the peripheral layers of the OB. This phenotype is less severe than that of mice lacking both ApoER2 and VLDLR, where chain formation is virtually absent. Most likely, ApoER2 and VLDLR integrate the signals from other signalling molecules in addition to THBS-1, which might also be present in the SVZ and RMS, like F-Spondin (Andrade *et al*, 2007).

Materials and methods

Animals

wt mice, *ApoER2*$^{-/-}$*/VLDLR*$^{-/-}$ mice and *THBS-1*$^{-/-}$ mice on a C57BL6/J background were housed under standard conditions.

Antibodies

Polyclonal anti-Dab1 antibody (anti-54) was raised in rabbits against a glutathione *S*-transferase fusion protein containing the first 180 amino acids of the short splice variant of murine Dab1. Monoclonal mouse anti-Dab1 (D4) was obtained from Andre Goffinet (University of Louvain, Belgium) and monoclonal mouse anti-Lis1 was obtained from Orly Reiner (Weizmann Institute of Science, Israel). The following antibodies were purchased from the indicated sources: anti-THBS-1 (mouse monoclonal; Abcam), anti-THBS-2 (mouse monoclonal; BD Bioscience), anti-phosphotyrosine (mouse monoclonal; Santa Cruz Biotechnology), anti-Akt (rabbit polyclonal; Cell Signaling), anti-phospho Akt (rabbit polyclonal; Cell Signaling), anti-doublecortin C18 (goat polyclonal; Santa Cruz Biotechnology), anti-Tuj1 (mouse monoclonal; Santa Cruz Biotechnology), and anti-BrdU (mouse monoclonal; Becton Dickinson, Mountain View).

THBS purification

THBS-1 purification was performed as described (Roberts *et al*, 1994) with some minor modifications. The THBS-1-containing solution was brought to 20% (w/v) with ultrapure sucrose. Before use, sucrose was removed by dialysis against TBS by means of a Dialysis Cassette with 20 kDa molecular weight cutoff (Pierce). The purity of THBS-1 following dialysis was checked by Coomassie staining after SDS–PAGE.

Expression of recombinant proteins, preparation of cell extracts, electrophoresis, and western blotting

Reelin was expressed in stably transfected 293 cells, and conditioned medium was prepared as described earlier (Brandes *et al*, 2001). RCM was concentrated by ultra-centrifugation for 2 h. The resulting pellet was dissolved and enrichment estimated on a Coomassie gel to be 20-fold.

Preparation of MBP fusion proteins containing the ligand-binding domain of ApoER2 (ApoER2Δ4-6-MBP/His), VLDLR

(VLDLR 1-8-MBP/His), and of myc–RAP were performed as described earlier (Koch *et al*, 2002).

Total cell extracts from primary neuronal cultures, isolated SVZ, and OBs were obtained after washing twice with PBS and scraping or homogenizing in Hunt buffer with protease inhibitor cocktail (Roche), 50 mM NaF and 10 mM Na_3VO_4 and centrifugation for 15 min at 20 000 *g*.

SDS–PAGE was performed according to the method of Laemmli (1970), and proteins were transferred onto nitrocellulose membranes by semidry blotting. For western blotting, nitrocellulose membranes were blocked for 1 h in PBS–0.1% Tween-20 containing 5% bovine serum albumin. Primary antibodies were used at the following dilutions: D4 1:7500, PY99 1:750, Akt 1:1000, phospho-Akt 1:1000, Lis1 1:15000, THBS-1 1:1000, and THBS-2 1:250. Appropriate horseradish peroxidase-conjugated antibodies (1:10 000; Jackson ImmunoResearch) were used for detection with enhanced chemiluminescence (Pierce).

Solid-phase binding assay

The solid-phase binding assay was essentially performed as described in Koch *et al* (2002) and Bajari *et al* (2005). Here, 100 µl TBS-C (2 mM $CaCl_2$) containing 10 µg/ml of ApoER2Δ4-6-MBP/His or VLDLR 1-8-MBP/His were incubated on a 96-well plate overnight at 4°C. All further incubations were carried out at room temperature for 1 h, and ligands or antibodies were diluted in blocking solution (2% BSA in TBS-C and 0.05% Tween). After blocking and binding of THBS-1, anti-THBS-1 antibody followed by HRP-conjugated secondary antibody was used for the detection of bound THBS-1. For the colour reaction, 0.1 mg/ml 3,3′,5,5′-tetramethylbenzidine in 0.1 M sodium acetate, pH 6.0 containing 10 mM H_2O_2 was used. The reaction was stopped after 5 min by the addition of 0.3 M H_2SO_4, and the resulting yellow product was measured at 450 nm. For the competition assay, plates were coated with ApoER2Δ4-6-MBP/His or VLDLR 1-8-MBP/His as described above. Plates were overlaid with 14 or 32 nM THBS-1 for VLDLR or ApoER2, respectively, in the presence of increasing amounts of either RCM or myc–RAP. Bound THBS-1 was detected by the addition of an antibody against THBS-1 followed by HRP-conjugated secondary antibody.

Dab1 phosphorylation and degradation assay

The Dab1 phosphorylation assay was essentially performed as described (Hiesberger *et al*, 1999). Briefly, brains from embryonic day 16 (E16) wt mouse embryos or E16 *ApoER2*$^{-/-}$/*VLDLR*$^{-/-}$ mouse embryos were homogenized in HBSS, centrifuged (1200 r.p.m., 2 min), resuspended in Dulbecco's modified Eagle's medium F-12 (DMEM-F12; Gibco) containing B27 supplement (Gibco), 2 mM L-glutamine, 100 U/ml penicillin, and 100 U/ml streptomycin sulphate, and subsequently plated on tissue culture dishes coated with 150 µg/ml poly-L-ornithine. Cells were grown at 37°C in a humidified environment and 5% CO_2. After 3 days in culture, the cells were washed with PBS and subsequently incubated with different media containing the indicated ligands (see Figure 3A and B). After 20 min at 37°C, cells were lysed in Hunt buffer and the supernatants were immediately used for immunoprecipitation of Dab1 using 5 µl of anti-Dab1 antiserum. After overnight incubation at 4°C, 40 µl of a suspension containing protein A beads (Amersham) was added, and the mixture was incubated for 2 h at 4°C. The beads were washed with Hunt buffer and boiled in reducing Laemmli buffer prior to SDS–PAGE and western blotting.

To analyse Dab1 degradation, primary neuronal cultures were washed with PBS and subsequently incubated with different media containing the indicated ligands (see Figure 3C) for 360 min and total cell extracts were prepared as described earlier.

Akt phosphorylation

Phosphorylation of Akt was measured directly in total cell extracts derived from stimulated E16 neurons. After 3 days in culture, the cells were starved overnight using plain DMEM-F12 to reduce background phosphorylation of Akt, washed with PBS, and subsequently incubated with different media containing the indicated ligands (see Figure 3D). Equal amounts of protein from cell lysates were separated by SDS–PAGE and immunoblotted using an antibody directed against phospho-Akt and Akt.

Histology, immunohistochemistry, and immunofluorescence

Postnatal day 17 (P17) animals were anaesthetized with a combination of xylazine–ketamine (10 and 75 mg/kg respectively) in 0.9% NaCl, and immediately perfused with 4% paraformaldehyde (PFA) in PBS at 4°C. Brains were dehydrated and embedded in paraffin according to standard protocols. Serial sagittal paraffin sections (6 µm) were obtained. For immunohistochemistry, dehydrated paraffin sections were boiled with citrate buffer (10 mM sodium citrate, 0.05% Tween-20, pH 6.0) for 20 min to unmask antigenic epitopes. Endogenous peroxidase activity was blocked by adding 3% H_2O_2 for 10 min. Anti-THBS-1 (mouse monoclonal; Abcam) was used to detect endogenous THBS-1 in tissue sections. Primary antibody was visualized using the Vecta Stain Elite ABC Kit and Peroxidase Substrate Kit DAB (both from Vector Laboratories).

For immunofluorescence, tissue was prepared as described above. Dehydrated paraffin sections were incubated with anti-doublecortin antibody and DAPI and visualized using the TSA Plus Kit (Perkin Elmer).

SVZ explants

SVZ explants were prepared as reported (Andrade *et al*, 2007). Briefly, newborn pups were killed at P7 by decapitation. Brains were dissected and placed in cold OptiMEM medium (Gibco). Here, 250 µm slices were obtained using a Vibratome (Leica). The SVZ was dissected from the lateral wall of the anterior horn of the lateral ventricle and cut into pieces of 250–350 µm in diameter. The explants were mixed with Matrigel (BD Bioscience) and cultured in four-well dishes. After polymerization (20 min), 500 µl of serum-free neurobasal A medium (Gibco), supplemented with B-27 (Gibco-Invitrogen), insulin (50 ng/ml; Novo Nordisk), putrescine (100 µM; Sigma), progesterone (1 nM; Sigma), glutamine and penicillin/streptomycin (Gibco) containing either purified THBS-1 (3 µg/ml in TBS), TBS alone (mock), concentrated RCM (Reelin), concentrated MCM (control), or 50 µg/ml myc–RAP. Cultures were maintained in a humidified, 5% CO_2, 37°C incubator. After 2 and 5 days, the explants were monitored and the length of migratory chains and the number of individual neurons per field were determined using AxioVision software (Zeiss).

Migratory chain length was determined by dividing each explant into quadrants, with each quadrant receiving two measurements. All measurements from one explant were averaged and the resulting chain length was referred to as the mean chain length of a given explant. The mean chain length of all explants from one experimental group was then averaged for *n* explants. All measurements and subsequent evaluation were performed blind.

For immunofluorescence analysis, tissue explants were treated as described (Lois and Alvarez-Buylla, 1993). Briefly, explants were fixed in 4% PFA for 10 min, rinsed in PBS and cells were permeabilized with 0.25% Triton X-100 for 5 min. After incubation with a blocking solution containing 10% BSA/PBS for 20 min, explants were incubated for 24 h at 4°C with primary antibodies against Tuj1 (dilution 1:50) diluted in 3% BSA/PBS. After rinsing in PBS, samples were incubated for 1 h at room temperature with the appropriate secondary Alexa-Fluor antibody and DAPI diluted in 3% BSA/PBS.

For western blot analysis, tissue explants were homogenized in Hunt buffer using a 26 G needle immediately after dissection and total cell extracts were prepared as described earlier.

Measurement of RMS width

To determine the width of the RMS in *THBS-1*$^{-/-}$ and control mice, three characteristic morphological features (elbow 1, elbow 2, and straight arm shown in Figure 6I) of the stream were defined and used to measure the width of the RMS. 'Elbow 1' was defined as the characteristic elbow-like prominence situated at the base of the RMS. 'Elbow 2' was defined as the second characteristic elbow-like prominence situated in the central part of the RMS and 'straight arm' as the site where the stream widens at the entrance point to the OB at the end of the RMS. Serial sagittal sections of P17 *THBS-1*$^{-/-}$ and P17 control mice were stained for haematoxylin and eosin to visualize nuclei. The diameter of the stream was measured in every consecutive section as follows (see cartoon in Figure 6I): through each of the characteristic morphological features, a straight line perpendicular to the clearly defined stream border was set. Two measurements on either side of each straight line, in total four measurements per straight line and feature, were averaged and used for analysis. Consecutive slices were taken from each brain.

Measurements were performed on each slice, and the biggest average width value from each feature was used for statistical analysis. All measurements and subsequent evaluation were performed blind to the mouse genotype. To exclude strain-specific phenotypes, *THBS-1*$^{-/-}$ mice on a C57BL6/J background were backcrossed for at least four generations with wt C57BL6/J mice.

BrdU experiments

Animals were injected i.p. with BrdU (50 mg/kg of body weight; Sigma) dissolved in 0.9% NaCl at P12 or P17 and were killed 5 days or 2 h later, respectively. BrdU-positive cells were quantified in three distinct areas: The SVZ, defined as the area between ventricle and elbow 1 and the RMS defined as the area between elbow 1 and elbow 2. In the OB, only BrdU-positive cells within the mitral cell layer, ependymal layer, and glomerular layer were quantified. BrdU stainings were performed on paraffin sections (6 μm) after 20 min of boiling in citrate buffer (pH 6) for antigen retrieval using anti-BrdU antibodies diluted 1:50 in 1% BSA/0.1% gelatine in PBS. Quantification of BrdU-positive cells was carried out blind to the mouse genotype.

Microscopy

Confocal images were acquired using a Zeiss LSM 5 system and LSM 5 software (Zeiss). DIC and phase contrast images were acquired using an Apotome system or an Axiovert 135 system and AxioVision software (Zeiss).

Acknowledgements

This study was supported by the 'Fonds zur Förderung der Wissenschaftlichen Forschung, FWF', Austria, grants P16872-B09, and P19611-B09, and the Herzfelder'sche Familienstiftung. We thank Christoph Daniel for *THBS-1*$^{-/-}$ mice. We appreciate the technical assistance of Harald Rumpler, Vukoslav Komnenovic, Thomas Sauer and Stephan Weinhart and thank Stefan Stricker for critical reading of the paper.

References

Adams JC, Tucker RP (2000) The thrombospondin type 1 repeat (TSR) superfamily: diverse proteins with related roles in neuronal development. *Dev Dyn* **218:** 280–299

Agah A, Kyriakides TR, Lawler J, Bornstein P (2002) The lack of thrombospondin-1 (TSP1) dictates the course of wound healing in double-TSP1/TSP2-null mice. *Am J Pathol* **161:** 831–839

Andrade N, Komnenovic V, Blake SM, Jossin Y, Howell B, Goffinet A, Schneider WJ, Nimpf J (2007) ApoER2/VLDL receptor and Dab1 in the rostral migratory stream function in postnatal neuronal migration independently of Reelin. *Proc Natl Acad Sci USA* **104:** 8508–8513

Arnaud L, Ballif BA, Forster E, Cooper JA (2003) Fyn tyrosine kinase is a critical regulator of Disabled-1 during brain development. *Curr Biol* **13:** 9–17

Bajari TM, Strasser V, Nimpf J, Schneider WJ (2005) LDL receptor family: isolation, production, and ligand binding analysis. *Methods* **36:** 109–116

Bock HH, Jossin Y, May P, Bergner O, Herz J (2004) Apolipoprotein E receptors are required for reelin-induced proteasomal degradation of the neuronal adaptor protein Disabled-1. *J Biol Chem* **279:** 33471–33479

Bornstein P (2001) Thrombospondins as matricellular modulators of cell function. *J Clin Invest* **107:** 929–934

Brandes C, Kahr L, Stockinger W, Hiesberger T, Schneider WJ, Nimpf J (2001) Alternative splicing in the ligand binding domain of mouse ApoE receptor-2 produces receptor variants binding reelin but not alpha2-macroglobulin. *J Biol Chem* **276:** 22160–22169

Calderwood DA, Fujioka Y, de Pereda JM, Garcia-Alvarez B, Nakamoto T, Margolis B, McGlade CJ, Liddington RC, Ginsberg MH (2003) Integrin beta cytoplasmic domain interactions with phosphotyrosine-binding domains: a structural prototype for diversity in integrin signaling. *Proc Natl Acad Sci USA* **100:** 2272–2277

Carlson CB, Lawler J, Mosher DF (2008) Structures of thrombospondins. *Cell Mol Life Sci* **65:** 672–686

Chandrasekaran L, He CZ, Al-Barazi H, Krutzsch HC, Iruela-Arispe ML, Roberts DD (2000) Cell contact-dependent activation of alpha3beta1 integrin modulates endothelial cell responses to thrombospondin-1. *Mol Biol Cell* **11:** 2885–2900

Dulabon L, Olson EC, Taglienti MG, Eisenhuth S, McGrath B, Walsh CA, Kreidberg JA, Anton ES (2000) Reelin binds alpha3beta1 integrin and inhibits neuronal migration. *Neuron* **27:** 33–44

Feng L, Allen NS, Simo S, Cooper JA (2007) Cullin 5 regulates Dab1 protein levels and neuron positioning during cortical development. *Genes Dev* **21:** 2717–2730

Forster E, Zhao S, Frotscher M (2006) Laminating the hippocampus. *Nat Rev Neurosci* **7:** 259–267

Godyna S, Liau G, Popa I, Stefansson S, Argraves WS (1995) Identification of the low density lipoprotein receptor-related protein (LRP) as an endocytic receptor for thrombospondin-1. *J Cell Biol* **129:** 1403–1410

Hack I, Bancila M, Loulier K, Carroll P, Cremer H (2002) Reelin is a detachment signal in tangential chain-migration during postnatal neurogenesis. *Nat Neurosci* **5:** 939–945

Herz J, Chen Y (2006) Reelin, lipoprotein receptors and synaptic plasticity. *Nat Rev Neurosci* **7:** 850–859

Herz J, Strickland DK (2001) LRP: a multifunctional scavenger and signaling receptor. *J Clin Invest* **108:** 779–784

Hiesberger T, Trommsdorff M, Howell BW, Goffinet A, Mumby MC, Cooper JA, Herz J (1999) Direct binding of reelin to VLDL receptor and ApoE receptor 2 induces tyrosin phosphorylation of the adaptor protein disabled-1 and modulates tau phosphorylation. *Neuron* **24:** 481–489

Iruela-Arispe ML, Liska DJ, Sage EH, Bornstein P (1993) Differential expression of thrombospondin 1, 2, and 3 during murine development. *Dev Dyn* **197:** 40–56

Jossin Y, Ignatova N, Hiesberger T, Herz J, Lambert de Rouvroit C, Goffinet AM (2004) The central fragment of Reelin, generated by proteolytic processing *in vivo*, is critical to its function during cortical plate development. *J Neurosci* **24:** 514–521

Koch S, Strasser V, Hauser C, Fasching D, Brandes C, Bajari TM, Schneider WJ, Nimpf J (2002) A secreted soluble form of ApoE receptor 2 acts as dominant negative receptor and inhibits reelin signaling. *EMBO J* **21:** 5996–6004

Kyriakides TR, Zhu YH, Smith LT, Bain SD, Yang Z, Lin MT, Danielson KG, Iozzo RV, LaMarca M, McKinney CE, Ginns EI, Bornstein P (1998) Mice that lack thrombospondin 2 display connective tissue abnormalities that are associated with disordered collagen fibrillogenesis, an increased vascular density, and a bleeding diathesis. *J Cell Biol* **140:** 419–430

Laemmli UK (1970) Cleavage of structural proteins during assembly of the head of the bacteriophage T4. *Nature* **227:** 680–685

Lawler J (2000) The functions of thrombospondin-1 and-2. *Curr Opin Cell Biol* **12:** 634–640

Lawler J, Sunday M, Thibert V, Duquette M, George EL, Rayburn H, Hynes RO (1998) Thrombospondin-1 is required for normal murine pulmonary homeostasis and its absence causes pneumonia. *J Clin Invest* **101:** 982–992

Lein ES, Hawrylycz MJ, Ao N, Ayres M, Bensinger A, Bernard A, Boe AF, Boguski MS, Brockway KS, Byrnes EJ, Chen L, Chen L, Chen TM, Chin MC, Chong J, Crook BE, Czaplinska A, Dang CN, Datta S, Dee NR *et al* (2007) Genome-wide atlas of gene expression in the adult mouse brain. *Nature* **445:** 168–176

Lois C, Alvarez-Buylla A (1993) Proliferating subventricular zone cells in the adult mammalian forebrain can differentiate into neurons and glia. *Proc Natl Acad Sci USA* **90:** 2074–2077

Lois C, Garcia-Verdugo JM, Alvarez-Buylla A (1996) Chain migration of neuronal precursors. *Science* **271:** 978–981

Mayer H, Duit S, Hauser C, Schneider WJ, Nimpf J (2006) Reconstitution of the Reelin signaling pathway in fibroblasts demonstrates that Dab1 phosphorylation is independent of receptor localization in lipid rafts. *Mol Cell Biol* **26:** 19–27

O'Shea KS, Dixit VM (1988) Unique distribution of the extracellular matrix component thrombospondin in the developing mouse embryo. *J Cell Biol* **107** (6 Part 2)**:** 2737–2748

O'Shea KS, Liu LH, Dixit VM (1991) Thrombospondin and a 140 kD fragment promote adhesion and neurite outgrowth from embryonic central and peripheral neurons and from PC12 cells. *Neuron* **7:** 231–237

O'Shea KS, Rheinheimer JS, Dixit VM (1990) Deposition and role of thrombospondin in the histogenesis of the cerebellar cortex. *J Cell Biol* **110:** 1275–1283

Roberts DR, Cashel J, Guo N (1994) Purification of thrombospondin from human platelets. *J Tissue Culture Meth* **16:** 217–222

Schneider WJ, Nimpf J (2003) LDL receptor relatives at the crossroad of endocytosis and signaling. *Cell Mol Life Sci* **60:** 892–903

Senzaki K, Ogawa M, Yagi T (1999) Proteins of the CNR family are multiple receptors for Reelin. *Cell* **99:** 635–647

Strasser V, Fasching D, Hauser C, Mayer H, Bock HH, Hiesberger T, Herz J, Weeber EJ, Sweatt JD, Pramatarova A, Howell B, Schneider WJ, Nimpf J (2004) Receptor clustering is involved in Reelin signaling. *Mol Cell Biol* **24:** 1378–1386

Tissir F, Goffinet AM (2003) Reelin and brain development. *Nat Rev Neurosci* **4:** 496–505

Trommsdorff M, Gotthardt M, Hiesberger T, Shelton J, Stockinger W, Nimpf J, Hammer R, Richardson JA, Herz J (1999) Reeler/Disabled-like disruption of neuronal migration in knock out mice lacking the VLDL receptor and apoE receptor-2. *Cell* **97:** 689–701

Wichterle H, Garcia-Verdugo JM, Alvarez-Buylla A (1997) Direct evidence for homotypic, glia-independent neuronal migration. *Neuron* **18:** 779–791

Willnow TE (1998) Receptor-associated protein (RAP): a specialized chaperone for endocytic receptors. *Biol Chem* **379:** 1025–1031

5.2 “ApoER2/ VLDL receptor and Dab1 in the Rostral Migratory Stream function in postnatal neuronal migration independently of the Reelin signal”

ApoER2/VLDL receptor and Dab1 in the rostral migratory stream function in postnatal neuronal migration independently of Reelin

Nuno Andrade*, Vukoslav Komnenovic†, Sophia M. Blake*, Yves Jossin‡, Brian Howell§, Andre Goffinet‡, Wolfgang J. Schneider*, and Johannes Nimpf*¶

*Max F. Perutz Laboratories, University Departments at the Vienna Biocenter, Department of Medical Biochemistry, Medical University of Vienna, A-1030 Vienna, Austria; †Institute of Molecular Biotechnology, Austrian Academy of Sciences, 1030 Vienna, Austria; ‡Developmental Neurobiology Unit, University of Leuven Medical School, 3000 Leuven, Belgium; and §Neurogenetics Branch, National Institute of Neurological Disorders and Stroke, National Institutes of Health, Bethesda, MD 20892

Edited by Thomas C. Südhof, The University of Texas Southwestern Medical Center, Dallas, TX, and approved March 30, 2007 (received for review December 21, 2006)

Postnatal migration of interneuron precursors from the subventricular zone to the olfactory bulb occurs in chains that form the substrate for the rostral migratory stream. Reelin is suggested to induce detachment of neuroblasts from the chains when they arrive at the olfactory bulb. Here we show that ApoER2 and possibly very-low-density lipoprotein receptor (VLDLR) and their intracellular adapter protein Dab1 are involved in chain formation most likely independent of Reelin. F-spondin, which is present in the stream, may act as ligand for ApoER2 and VLDLR. In mice lacking either both receptors or Dab1 chain formation is severely compromised, and as a consequence the rostral migratory stream is virtually absent and neuroblasts accumulate in the subventricular zone. The mutant animals exhibit severe neuroanatomical defects in the subventricular zone and in the olfactory bulb. These data demonstrate a cell-autonomous function of ApoER2, and most likely VLDLR and Dab1, in postnatal migration of neuroblasts in the forebrain, which is suggested to depend on ligands other than Reelin.

Reelin signaling | postnatal neurogenesis | tangential neuronal migration

The development of the olfactory bulb (OB) in rodents continues after birth. Most interneurons differentiate from neuroblasts generated postnatally in the subventricular zone (SVZ) of the cerebral cortex and migrate to the OB along the so-called "rostral migratory stream" (RMS) (1). Whereas the majority of these neuroblasts originate and migrate during the early postnatal period, the process continues throughout life (2). Neuronal migration in the RMS occurs by formation of chains that are ensheathed by glial cells and their processes (3). In these chains, neuroblasts migrate along each other in a saltatory fashion (4).

Migration along the RMS depends on the transcription factor serum response factor (SRF) (5). In the absence of SRF, cells destined for the OB accumulate in the SVZ because of a cell-autonomous defect that might be caused by down-regulation of actin and gelsolin, impairing the dynamics of actin microfilaments. The polysialylated form of neural cell adhesion molecule (NCAM) (6) mediates the interaction between migrating neuroblasts and their environment (7, 8). Migration in the RMS is guided by the repulsive action of Slit secreted by cells in the lateral septum and the SVZ (9, 10), as well as by Netrin (11). Once in the OB, neuroblasts switch from chain migration to radial migration, integrate into the laminated structure of the bulb, and differentiate into granule and periglomerular interneurons (2, 12). The switch from chain migration to radial migration seems to depend on the Reelin signal that detaches neuroblasts from the chains (13). Reelin is expressed by olfactory mitral cells (14), and Reelin-deficient mice have a diminutive OB because of a reduction of the number of neurons and a disorganization of the granular cell layer (Gcl) (15). Thus, it seems that Reelin also orchestrates the lamination of the OB, as it does in the cerebrum and other laminated structures (for reviews see refs. 16 and 17).

In the cerebrum, Reelin is crucial for correct positioning of radially migrating neuroblasts via its binding to ApoER2 and very-low-density lipoprotein receptor (VLDLR) (18, 19), which triggers tyrosine phosphorylation of the adaptor Dab1 by receptor clustering (20). Binding of Reelin to the receptors and subsequent phosphorylation of Dab1 are consecutive steps of a linear pathway, because disruption of any of the corresponding genes causes identical phenotypes in mice (21–24).

Here we report that the lack of ApoER2/VLDLR or Dab1 leads to a cell-autonomous migration defect in the RMS, which is independent of the Reelin signal. Neuroblasts from mutant mice lacking either receptors or Dab1 are unable to form chains and accumulate in the SVZ. As a consequence, the RMS is missing or is very rudimentary. This leads to severe neuroanatomical defects in the SVZ and in the OB of mutant animals. Reelin is not present in the stream and does not play a role in chain formation, but it seems to be involved in maintenance or architecture of the RMS. F-spondin might be a candidate ligand for ApoER2 and VLDLR in the RMS.

Results

ApoER2 and VLDLR and the associated machinery that transduces the Reelin signal play major roles in allowing neuroblasts to switch from chain migration to tangential migration within the OB (13). Neuroblasts within the RMS expressed the ApoER2 protein (Fig. 1 *A* and *B*), confirming *in situ* hybridization data (13). ApoER2 expression was already prominent in neuroblasts generated in the SVZ (Fig. 1 *A* and *C*, open arrowheads), long before they reach the bulb where the Reelin signal is generated (13). The ApoER2-positive staining is specific, because it is absent in mice deficient in ApoER2 and VLDLR (Fig. 1*D*). Close inspection of these mice, however, indicated that the RMS was absent. To evaluate this further, we examined the RMS in WT mice and mice lacking defined components of the Reelin pathway. Sagittal sections of brains from mice at postnatal day 17 (P17) were stained with hematoxylin and with an antibody against doublecortin, a marker

Author contributions: N.A. and J.N. designed research; N.A., V.K., S.M.B., and Y.J. performed research; B.H. contributed new reagents/analytic tools; N.A., Y.J., B.H., A.G., and W.J.S. analyzed data; and A.G. and J.N. wrote the paper.

The authors declare no conflict of interest.

This article is a PNAS Direct Submission.

Abbreviations: SRF, serum response factor; RMS, rostral migratory stream; SVZ, subventricular zone; OB, olfactory bulb; EZ, ependymal zone; Gcl, granular cell layer; VLDLR, very-low-density lipoprotein receptor; P*n*, postnatal day *n*.

¶To whom correspondence should be addressed. E-mail: johannes.nimpf@meduniwien.ac.at.

This article contains supporting information online at www.pnas.org/cgi/content/full/0611391104/DC1.

www.pnas.org/cgi/doi/10.1073/pnas.0611391104

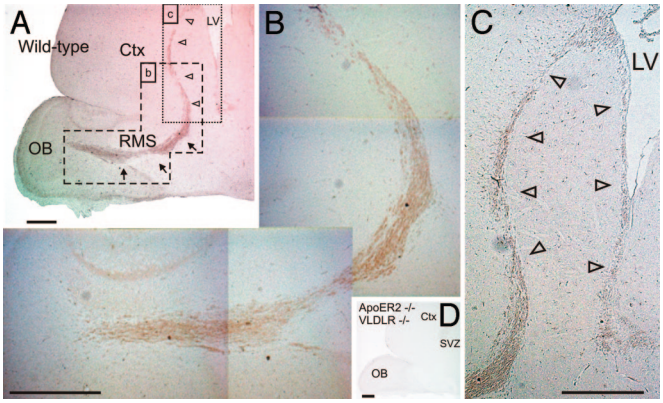

Fig. 1. Neuroblasts migrating within the RMS express ApoER2. Sagittal sections (5 μm) of the forebrains of WT mice (*A–C*) and from *ApoER2*$^{-/-}$/*VLDLR*$^{-/-}$ mice (*D*) were immunostained with a polyclonal antibody against ApoER2. The RMS is highlighted by arrows, and the SVZ is highlighted by open arrowheads. Ctx, cortex; LV, lateral ventricle; St, striatum. (Scale bars: 500 μm.)

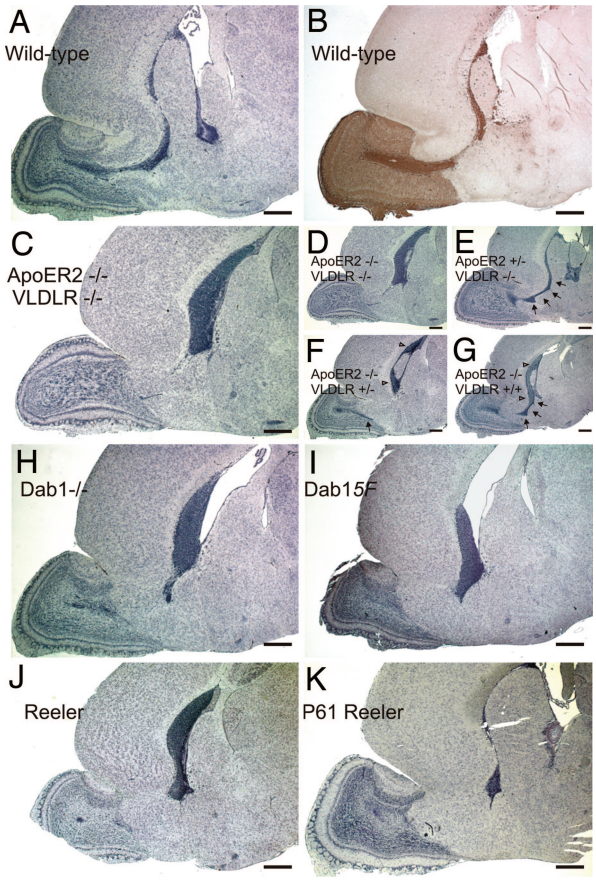

Fig. 2. Ablation of critical components of the Reelin signaling pathway leads to loss of the RMS and accumulation of neuroblasts in the SVZ. Sagittal sections (5 μm) of the forebrains of WT (*A* and *B*), *ApoER2*$^{-/-}$/*VLDLR*$^{-/-}$ (*C* and *D*), *ApoER2*$^{+/-}$/*VLDLR*$^{-/-}$ (*E*), *ApoER2*$^{-/-}$/*VLDLR*$^{+/-}$ (*F*), *ApoER2*$^{-/-}$/*VLDLR*$^{+/+}$ (*G*), *Dab1*$^{-/-}$ (*H*), *Dab1-5F* (*I*), and *reeler* (*J*) mice at P17 and *reeler* mice (*K*) at P61 were stained with hematoxylin (*A* and *C–K*) or with an antibody against doublecortin (*B*). Sections were taken from three to five independent animals from each of the genetic backgrounds, and representative sections are displayed. (Scale bars: 500 μm.) Arrows are used to highlight the RMS.

of the RMS (25); for the mutant animals only sections stained with hematoxylin are shown. In WT mice, a well defined stream of neuroblasts started at the SVZ and ended within the OB defining the RMS (Fig. 2 *A* and *B*). In mice lacking ApoER2 and VLDLR (Fig. 2*C*), Dab1 (Fig. 2*H*), carrying two Dab1 alleles (*Dab1-5F*) in which the critical tyrosine residues are mutated to phenylalanines instead of the WT alleles (26) (Fig. 2*I*), or functional Reelin (Fig. 2*J*), the RMS was severely disrupted and neuroblasts accumulated in the SVZ. The cells accumulating in the SVZ of *reeler* mice and *Dab1*$^{-/-}$ mice still expressed ApoER2 [see supporting information (SI) Fig. 8]. The lack of an RMS seen in *reeler* mice was surprising, because in a previous study a stream that was fanning out just before it reaches the OB was observed in these mice (13). To exclude the possibility that the age of the mice examined made the difference, we also looked at P61 (Fig. 2*K*). Again no stream could be detected, but the accumulation of neuroblasts in the SVZ was less prominent. Serial sagittal sections (5 μm) through the area that would contain the entire RMS revealed that in all mutant animals some patches or solitary individual neuroblasts can be identified migrating from the SVZ toward the OB (data not shown).

Whereas ApoER2 was expressed by neuroblasts in the RMS (Fig. 1), VLDLR was not detected in this structure by *in situ* hybridization (13) or by using a specific antibody (data not shown). Allelic titration of both receptors, however, suggested the presence of VLDLR within the RMS. The presence of one *Apoer2* allele on a *Vldlr*-null background was sufficient to develop an RMS and a SVZ that were indistinguishable from that of WT mice (Fig. 2*E* and SI Fig. 9*B*). The presence of one *Vldlr* allele on an *Apoer2*-null background partially rescued the "RMS-less" phenotype (Fig. 2*F*, black arrow): a faint RMS could be detected by serial sagittal sections. The presence of two WT *Vldlr* alleles almost reestablished the RMS (Fig. 2*G*). Most of the stream was restored, but some neuroblasts still accumulated in the SVZ (SI Fig. 9*D*).

The accumulation of neuroblasts in the SVZ of mice lacking functional Reelin, ApoER2/VLDLR, or Dab1 was also evident in coronal sections (see SI Fig. 10). In comparison to WT mice, where the SVZ appeared as a narrow band of cells, in mutant animals this zone was significantly wider and densely packed with neuroblasts.

To investigate whether the lack of RMS formation also caused accumulation of glial cells in the SVZ, we performed double-staining for GFAP and doublecortin. Numerous GFAP-positive cells were present in the region where neuroblasts accumulated in the mutant mice (SI Fig. 11), indicating that not only neuroblasts, but also accompanying glial cells, accumulated in the SVZ when no RMS was formed. TUNEL analysis disclosed the presence of apoptotic cells within the mass of accumulating neuroblasts (Fig. 3). A 15-fold increase of apoptotic cells was found in the mutant SVZs compared with the WT SVZ (five to eight matched sections from three different animals for each genotype: WT, 0.22 ± 0.2%; *reeler*, 3.42 ± 0.5%; *ApoER2*$^{-/-}$/*VLDLR*$^{-/-}$, 3.56 ± 0.9%; *Dab1*$^{-/-}$, 3.6 ± 1%; ***, $P < 0.0005$). There was no significant difference in apoptosis among the mutant SVZs ($P > 0.1$).

To define the impact of the loss of the RMS on the structure of the OB, we analyzed the mature bulbs of the respective mutant mice. First, we prepared coronal sections as schematized in Fig. 4*J* and estimated the number of cells present in the Gcl including the ependymal zone (EZ) on hematoxylin-stained sections (Fig. 4*I*). The structure of the WT bulb is characterized, from the center to the periphery, by a cell-dense center (EZ), followed by the Gcl, separated from the external plexiform layer by a well defined layer of mitral cells (27). The outermost structure is the glomerular layer that contains calretinin- and calbindin-positive neurons derived from the RMS (1). Hematoxylin (Fig. 4*A*) and immunohistochemical staining for ApoER2 (Fig. 4*E*) of a WT OB confirmed expression of ApoER2 in mitral cells (14) and demonstrated that most cells present in the EZ were immunopositive for ApoER2 (compare to Fig. 1), indicating that these cells derived from the RMS. The OBs from *reeler*, *ApoER2*$^{-/-}$/*VLDLR*$^{-/-}$, and *Dab1*$^{-/-}$ mice contained only 60% of the number of cells in the Gcls

NEUROSCIENCE

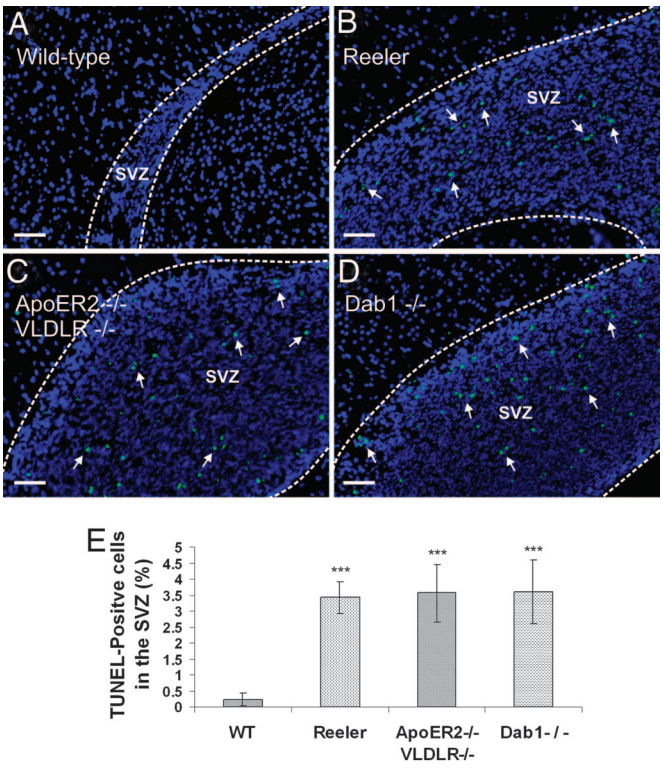

Fig. 3. Cell accumulation in the SVZs of *reeler*, *ApoER2*$^{-/-}$/*VLDLR*$^{-/-}$, and *Dab1*$^{-/-}$ mice leads to increased apoptosis. Sagittal sections (5 μm) prepared from the forebrains of WT (*A*), *reeler* (*B*), *ApoER2*$^{-/-}$/*VLDLR*$^{-/-}$ (*C*), and *Dab1*$^{-/-}$ (*D*) mice were analyzed for the presence of apoptotic cells by TUNEL assays. (*E*) Apoptosis was quantified based on the percentage of TUNEL-positive cells in the SVZ using five to eight matched 5-μm sections from three animals from each genetic background. Plots show average ± SEM. ***, $P <$ 0.0005 (Student's *t* test). (Scale bars: 50 μm.)

compared with their WT counterparts (Fig. 4*I*) (Number of cells in the granular zone in 5-μm sections from two to three animals per background was normalized to the WT values: WT, 1.00 ± 0.07; *reeler*, 0.59 ± 0.05; *ApoER2*$^{-/-}$/*VLDLR*$^{-/-}$, 0.59 ± 0.1; *Dab1*$^{-/-}$ 0.58 ± 0.06; ***, $P <$ 0.0005). This effect was mostly due to a dramatic reduction of cells present in the mutant EZs. This finding was confirmed by BrdU staining. Animals were injected with BrdU at P12, and the SVZ and the OBs were analyzed at P17. In WT mice, the EZ of the OB was filled with BrdU-positive cells (Fig. 5*A*), and the corresponding SVZ was represented by a thin layer of neuroblasts (Fig. 5*a*). In *reeler*, *ApoER2*$^{-/-}$/*VLDLR*$^{-/-}$, and *Dab1*$^{-/-}$ mice, the BrdU-positive staining was dramatically reduced in the EZ of the bulb (Fig. 5 *B–D*) and increased in the respective SVZs (Fig. 5 *b* and *c*). Quantification of calbindin- and calretinin-positive cells (SI Fig. 12) in the glomerular layers disclosed a 3-fold reduction of calbindin-positive cells per glomerulus and an ≈2-fold reduction of calretinin-positive cells in all mutant animals.

To evaluate whether a migration defect was responsible for the lack of the RMS, migration assays in three-dimensional extracellular matrix substrate (Matrigel) of SVZ explants were performed to study chain formation and tangential migration of neuroblasts *in vitro* (4). For quantification of the effects, the average migration distance (length of chains) was measured (Fig. 6*F*), and the number of individual cells per field was counted (Fig. 6*G*). Explants from WT mice extended robust chains consisting of migrating neuroblasts and glial cells (4), which, after 50 h, reached an average length of 262 ± 27 μm (Fig. 6*A*). Under these conditions, very few individual neurons (11.4 ± 7) were present around the explant. Addition of Reelin caused disintegration of the chains, confirming previous observations (13) (data not shown). Chain development and neuronal migration in explants from *reeler* mice (Fig. 6*B*) were indistinguishable from those seen in WT mice (chain length: 266 ± 19 μm; WT, $n = 19$; *reeler*, $n = 16$; explants from at least two animals per genotype; $P > 0.1$), suggesting that Reelin is not crucial for the formation of the chains or for the migration of the cells in chains. In sharp contrast, the development of explants cultured from *ApoER2*$^{-/-}$/*VLDLR*$^{-/-}$ mice was dramatically different (Fig. 6*C*). Only a few neurons left the explants, and the few chains formed were dramatically shorter than those in explants from WT or *reeler* mice (107 ± 47 μm, $n = 20$ explants from two mice; ***, $P < 0.0005$). Explants from *Dab1*$^{-/-}$ mice (Fig. 6*D*) and *Dab1-5F* mice (data not shown) also developed differently from WT explants. A significant number of neurons migrated out and away from the explant, but most of them failed to form chains. These experiments demonstrated that the lack of RMS formation in *reeler* mice is not due to a migration defect of neuroblasts. In mice lacking either ApoER2/VLDLR or Dab1, the absence of the RMS is caused by a migration defect and/or by the inability of neuroblasts to form chains. To define whether this is a cell-autonomous defect, explants from WT animals were infected with an adenovirus to express EGFP and were cocultured with explants derived from *ApoER2*$^{-/-}$/*VLDLR*$^{-/-}$ mice. As demonstrated in Fig. 6*E*, the presence of the WT explant did not induce *ApoER2*$^{-/-}$/*VLDLR*$^{-/-}$ neuroblasts to migrate out of the explant and to form chains. These results demonstrated that the lack of ApoER2 and VLDLR caused a cell-autonomous migration defect that is independent of the presence of Reelin. To support this view, we examined the RMS of WT and *reeler* mice (data not shown) for the presence of Reelin-expressing cells. The *reeler-Orleans* mutant mice used in this study produce a truncated Reelin protein that is not secreted from cells and thus can be readily detected by immunostaining (28). As demonstrated in Fig. 7, we confirmed previous findings that Reelin-expressing cells are present neither at the origin of nor within the RMS (13, 29). However, areas adjacent to the stream contained a significant number of Reelin-producing cells.

What is the ligand for ApoER2 and VLDLR within the stream? Because VLDLR and ApoER2 are promiscuous receptors (30), we tested other ligands for their presence in the RMS. To this end, we could demonstrate that F-spondin, which was recently identified as a ligand for ApoER2 (31), is indeed present in the RMS as shown by immunohistochemistry (Fig. 7*B*). This result was in agreement with the genome-wide *in situ* hybridization results presented in the Allen Brain Atlas (32). The specificity of the staining is further documented by examination of *ApoER2*$^{-/-}$/*VLDLR*$^{-/-}$ mice (Fig. 7*C*). Here F-spondin is confined to the area of accumulating cells destined to form the RMS.

As outlined in the Introduction, mice lacking the gene for SRF exhibit a similar phenotype most likely due to the down-regulation of actin and gelsolin. Thus, we tested whether actin and gelsolin are reduced in the forebrains of our mutants. As demonstrated in SI Fig. 13, the expression levels of actin and gelsolin are not significantly affected in *reeler*, *ApoER2*$^{-/-}$/*VLDLR*$^{-/-}$, or *Dab*$^{-/-}$ mice compared with WT mice.

Discussion

Development of the OB in mice in part depends on postnatal neurogenesis taking place in the SVZ. Tangential migration of neuroblasts along the RMS ensures the integration of these cells into structures of the OB. This mode of migration is characterized by the formation of chains containing migrating neuroblasts and supporting glial cells. Here we have identified ApoER2 and VLDLR as major components of the cellular machinery that supports formation of the chains. In our hands the lack of Dab1 also compromises the formation of chains, which is in contrast to a previous notion (33). Because explants from *Dab1-5F* mice

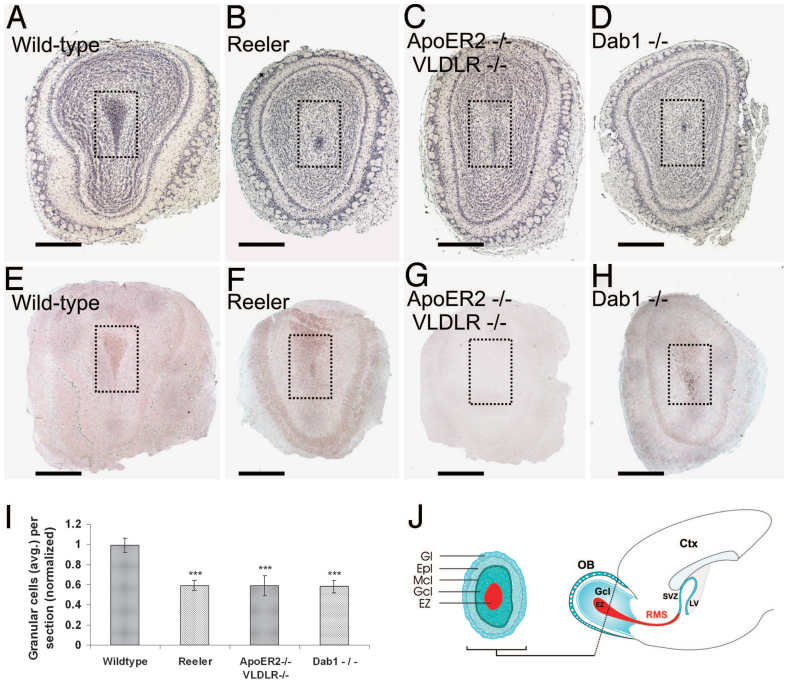

Fig. 4. OBs from *reeler* mice, *ApoER2*$^{-/-}$/*VLDLR*$^{-/-}$ mice, and *Dab1*$^{-/-}$ mice have a reduced or vestigial EZ. Matched coronal sections (5 μm) derived from the OBs of WT mice (*A* and *E*), *reeler* mice (*B* and *F*), *ApoER2*$^{-/-}$/*VLDLR*$^{-/-}$ mice (*C* and *G*), and *Dab1*$^{-/-}$ mice (*D* and *H*) were stained with hematoxylin (*A–D*) or immunostained for ApoER2 (*E–H*). The EZ (darker area inside the doted squares) is drastically reduced in the mutant OBs because of the disruption of the corresponding RMS (*B–D*). (*I*) Quantification of the cell numbers present in the Gcl and EZ (normalized to the cell number in the Gcl of WT mice) displayed a 40% decrease in the mutant OBs. Average cell numbers were calculated from 11 matched sections from two WT mice, 19 matched sections from three *reeler* mice, 18 matched sections from three *ApoER2*$^{-/-}$/*VLDLR*$^{-/-}$ mice, and 18 matched sections from three *Dab1*$^{-/-}$ mice. Plots show average ± SEM. ***, $P < 0.0005$ (Student's *t* test). (*J*) Schematic illustration of a coronal section from an OB (*Left*) and a sagittal section of a forebrain (*Right*). (Scale bars: 500 μm.) Ctx, cortex; LV, lateral ventricle.

have a similar phenotype we are proposing that the whole complex comprising the receptors and Dab1 is involved in chain formation. In mice lacking either both receptors or Dab1, chain formation in the SVZ is defective without compromising the generation of neuroblasts in the SVZ. This leads to an ectopic accumulation of neuroblasts and glial cells in the SVZ accompanied by a significant increase of cell death. For two reasons this defect cannot be due to interference with the classical Reelin signaling pathway: first, SVZ explants derived from *reeler* mice produced chains indistinguishable from those in WT explants; second, activation of the pathway by Reelin *in vitro* leads to disintegration of the chains (13).

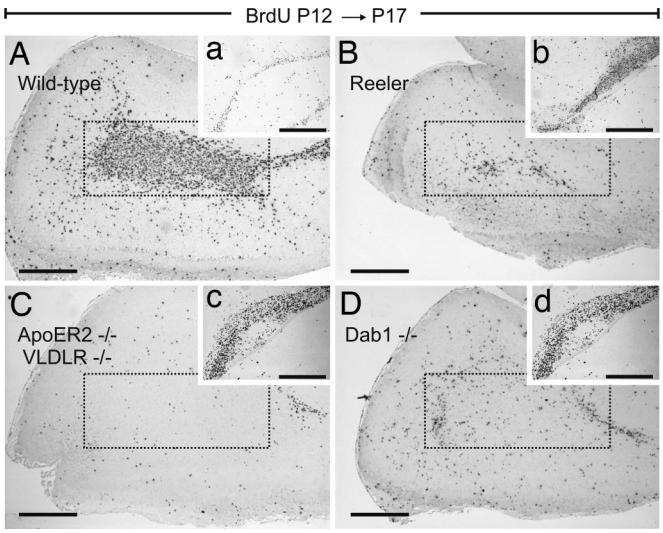

Fig. 5. Migration of newly generated neuroblasts is affected in the forebrains of mice carrying mutations in the Reelin signaling pathway. WT (*A*), *reeler* (*B*), *ApoER2*$^{-/-}$/*VLDLR*$^{-/-}$ (*C*), and *Dab1*$^{-/-}$ (*D*) mice received a BrdU pulse at P12, and brains were collected at P17. Matched sagittal sections of the forebrains were stained for BrdU-positive cells. Areas corresponding to the EZs are marked by dotted frames. (*a–d*) BrdU staining of the corresponding SVZs. (Scale bars: 500 μm.)

Interestingly, the RMS of *reeler* mice is affected similarly, and the observed phenotype seems to be more severe than previously described (13). There, the *reeler* RMS was found to be normal from its origin at the SVZ until shortly before it reaches the entrance point of the OB, where it became wider and less defined. This difference is presumably neither due to differences in genetic backgrounds, because the same strain of *reeler* mutants was used in both studies, nor related to the different ages of the animals analyzed (adult animals versus P17 in our study), because in *reeler* mice at P61 still no RMS could be found, although accumulation of neuroblasts in the SVZ was significantly reduced compared with P17, most likely because of apoptosis.

These results suggest a subdivision of the RMS formation into four mechanistically distinct phases. First is formation of neuroblasts and accompanying glial cells in the SVZ from respective precursor cells. This does not seem to be compromised by the lack of Reelin or the "receptor/adapter" machinery. Second is formation of chains, the substrate for the specific mode of neuronal migration within the RMS. This step depends on the presence of the receptor/adapter machinery but is independent of Reelin, because regular chains are formed by *reeler* explants in *vitro*. Third is bundling of the chains into a stream, and fourth is maintenance and elongation of a defined RMS, in which Reelin, expressed by cells in the vicinity of the stream, appears to play an important role. Whether the entire Reelin-signaling pathway is involved at this point cannot be answered from these

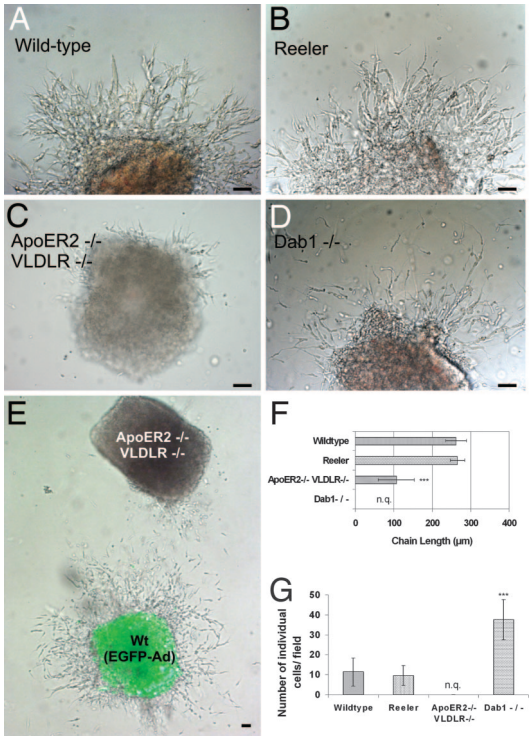

Fig. 6. Chain formation from explants of the SVZ is normal in *reeler* but severely disturbed in *ApoER2*$^{-/-}$/*VLDLR*$^{-/-}$ and *Dab1*$^{-/-}$ mice. SVZ explants were prepared from P5 WT (*A*), *reeler* (*B*), *ApoER2*$^{-/-}$/*VLDLR*$^{-/-}$ (*C*), and *Dab1*$^{-/-}$ (*D*) mice and analyzed after 50 h in culture by measuring the length of migratory chains (*F*, distance between the bases to the tips of the chains) and the number of individual cells per field (*G*). For quantification 19 WT, 16 *reeler*, 20 *ApoER2*$^{-/-}$/*VLDLR*$^{-/-}$, and 21 *Dab1*$^{-/-}$ explants from two mice of each phenotype were used. Plots show average ± SEM. ***, $P < 0.0001$ (Student's *t* test). (*E*) WT SVZ explants infected with EGFP adenovirus were cocultured with explants from *ApoER2*$^{-/-}$/*VLDLR*$^{-/-}$ mice. n.q., not quantified. (Scale bar: 50 μm.)

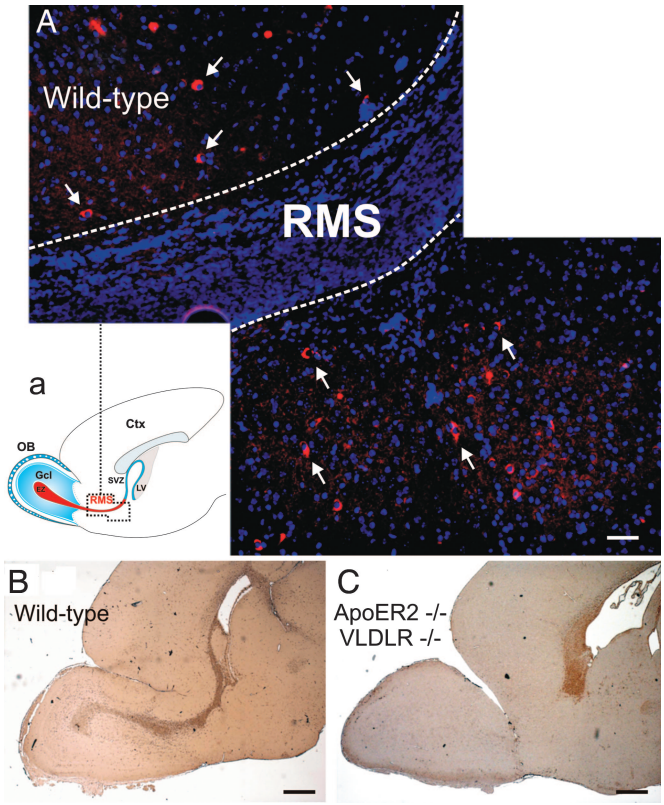

Fig. 7. Expression of Reelin and F-spondin in the RMS. (*A*) Reelin-positive cells accompany the RMS. Sagittal sections (5 μm) prepared from the forebrains of WT mice were immunostained with an antibody against Reelin. The RMS is highlighted by dotted lines. Reelin-positive cells are indicated by arrows. (*a*) Schematic representation of the area shown in *A*. (Scale bar: 50 μm.) (*B* and *C*) F-spondin is present in the RMS and accumulates in the SVZ of *ApoER2*$^{-/-}$/*VLDLR*$^{-/-}$ mice. Sagittal sections (5 μm) prepared from the forebrains of WT (*B*) and *ApoER2*$^{-/-}$/*VLDLR*$^{-/-}$ (*C*) mice were immunostained with an antibody against F-spondin. (Scale bar: 500 μm.)

experiments, because chains are not formed in *ApoER2*$^{-/-}$/*VLDLR*$^{-/-}$ and Dab$^{-/-}$ mice.

Because Reelin is not present in the SVZ or at the origin of the RMS, the inability of neuroblasts lacking ApoER2 and VLDLR to form chains must be Reelin-independent. This notion is in agreement with the explant assays performed here (Fig. 6). Interestingly, not only ApoER2 and/or VLDLR, but also their intracellular adapter Dab1 and at least one of the tyrosines that are phosphorylated upon Reelin stimulation, are needed for this function. Whether phosphorylation of Dab1 is necessary for proper chain formation or for other functions such as the ability of Dab1 to regulate cell surface expression of ApoER2 and VLDLR (34) is not clear yet. Mice lacking both receptors, lacking Dab1, or carrying the *Dab1-5F* alleles have identical phenotypes, characterized by massive accumulation of neuroblasts in the SVZ and the lack of stream formation, but development of the respective explants in Matrigel is different. A significant number of neuroblasts lacking Dab1 do migrate out of the explants but fail to form chains, whereas hardly any neuroblasts leave the explant derived from receptor-deficient mice, and the few chains formed are very short. This indicates that Dab1 is dispensable for migration but necessary for chain formation. Coculturing WT with *ApoER2*$^{-/-}$/*VLDLR*$^{-/-}$ explants demonstrated that (*i*) the presence of the WT explant did not alter the behavior of the mutant explant and (*ii*) none of the few cells leaving the mutant explant is incorporated into WT chains.

An important question concerns the putative ligands of this Reelin-independent function of the "receptor/Dab1" machinery in chain formation and/or migration. Such a ligand would be predicted not to act exactly like Reelin, because activation of the classical Reelin signaling pathway leads to dissociation of the chains (13). Here we have characterized F-spondin as an alternative ligand for ApoER2 and VLDLR present in the RMS. Whether it stimulates Dab1 phosphorylation like Reelin does, but lacks additional activity necessary for the full-blown Reelin signal (35), or whether it acts as substrate for neuroblasts to adhere to each other remains to be established.

The phenotype produced by the loss of components of the ApoER2/VLDLR/Dab1 complex is very similar to that seen in mice lacking SRF (5), in terms of both neuroanatomical abnormalities and the inability of SVZ explants to produce chains. *Srf*-negative mice show a dramatic reduction in brain levels of actin and gelsolin. Because none of the mice lacking components of the Reelin pathway exhibit altered levels of actin or gelsolin, we assume that the defect described here is independent of that produced by the lack of SRF.

In summary, we have identified a function of the ApoER2/VLDLR/Dab1 machinery that is independent of Reelin and mediates neuroblast migration and chain formation in the SVZ. Disruption of the machinery blocks postnatal neuronal migration from the SVZ to the OB and results in severe neuroanatomical defects in the OBs of affected mice.

Materials and Methods

Animals. WT mice on C57BL6/J or BalbC background, *reeler-Orleans* mice on a BalbC background (36), *Dab*$^{-/-}$ mice on a

C57Bl6/129Sv or BalbC background (22), *Dab1-5F* mice on a C57Bl6/129Sv or BalbC background (26), and *ApoER2*$^{-/-}$, *VLDLR*$^{-/-}$, and *ApoER2*$^{-/-}$/*VLDLR*$^{-/-}$ mice on a C57BL/6J/129Sv background were housed under standard conditions.

Histology and Immunohistochemistry. Animals were anesthetized with a combination of xylazine/ketamine (10 mg/kg and 75 mg/kg, respectively) in 0.9% NaCl and immediately perfused with 4% paraformaldehyde in PBS at 4°C. Brains were dehydrated and embedded in paraffin according to standard protocols. Serial coronal and sagittal paraffin sections (5 μm) were obtained and stained with hematoxylin following standard protocols. For immunohistochemistry dehydrated paraffin sections were heat-treated with EDTA buffer-CC1 (Ventana, Tucson, AZ) (pH 8.0) for 38 min at 95°C and incubated with the Discovery System (Ventana) to expose antigenic epitopes. The following primary antibodies were used: anti-doublecortin (C-18 goat polyclonal, 1:1,000; Santa Cruz Biotechnology, Santa Cruz, CA), anti-GFAP (rabbit polyclonal, 1:500; Dako, Glostrup, Denmark), anti-ApoER2 (no. 186 rabbit polyclonal, 1:1,000) (20), anti-calretinin and anti-calbindin (1:500; Sigma, St. Louis, MO), and anti-F-spondin (R2 and R4; a kind gift from Avihu Klar, Hebrew University, Hadassah Medical School, Jerusalem, Israel). Endogenous peroxidase activity was blocked, and chromogenic detection reaction was performed by using the DAB-Map kit (Ventana). Primary antibodies were visualized by incubating the sections with the respective antibodies for 1 h at room temperature [anti-goat secondary probe Alexa Fluor 488 (Molecular Probes) diluted 1:500 in PBS, anti-mouse Texas red (Molecular Probes) diluted 1:500 in PBS, and anti-rabbit Alexa Fluor 594 (Molecular Probes) diluted 1:500 in PBS].

Microscopy. Confocal images were acquired by using an LSM 5 system and LSM 5 software (Zeiss, Göttingen, Germany). Fluorescence and DIC images were acquired by using an Axiovert 135 system and AxioVision software (Zeiss).

BrdU Experiments and TUNEL Assay. Animals (P12) were injected i.p. with BrdU (50 mg/kg of body weight; Sigma) dissolved in 0.9% NaCl and killed at P17. BrdU stainings were performed on matched paraffin sections (5 μm) after 20 min of boiling in citrate buffer (pH 6) for antigen retrieval using anti-BrdU antibodies (Becton Dickinson, Mountain View, CA) diluted 1:50 in antibody dilution buffer (1% BSA/0.1% gelatin in PBS, pH 7.2). TUNEL assays were performed with the *In Situ* Cell Death Detection Kit (Roche Applied Biosciences).

SVZ Explants. SVZ explants were prepared as reported (4). Briefly, newborn pups were genotyped at P2–P3 and killed at P5 by decapitation. Brains were dissected and placed in cold OptiMEM (Gibco–Invitrogen, Carlsbad, CA). Slices (350 μm) were obtained by using a vibratome (Leica, Wetzlar, Germany). The SVZ was dissected from the lateral wall of the anterior horn of the lateral ventricle and cut into pieces of 250–350 μm in diameter. The explants were mixed with Matrigel (Becton Dickinson) and cultured in four-well dishes. After polymerization (20 min) 500 μl of serum-free medium supplemented with B-27 (Gibco–Invitrogen), 50 ng/ml insulin (Novo Nordisk, Graz, Austria), 100 μM putrescine (Sigma), 1 nM progesterone (Sigma), and glutamine and penicillin/Streptomycin (Gibco–Invitrogen) was added. Cultures were maintained in a humidified, 5% CO_2, 37°C incubator. After 50 h explants were monitored and the number of individual neurons per field and the length of migratory chains were measured by using AxioVision software (Zeiss). SVZ explants from WT mice were infected with Ad5CMV-eGFP (Gene Transfer Vector Core, University of Iowa, Iowa City, IA) with a titer of 1×10^{10} viral particles per milliliter in OptiMEM for 1 h in a humidified, 5% CO_2, 37°C incubator. Infected explants where washed three times with 10 volumes of OptiMEM, mixed with *ApoER2*$^{-/-}$/*VLDLR*$^{-/-}$ explants, and kept in culture under the same conditions described above.

Western Blots. Total protein extracts (20 μg) from forebrains (P17, derived from two mice each) were resolved by SDS/PAGE, and Western blotting was performed by using anti-gelsolin (goat polyclonal, 1:500; Santa Cruz Biotechnology), anti-actin (mouse monoclonal, 1:1,000; a kind gift from Vic Small, Institute of Molecular Biotechnology, Austrian Academy of Science, Vienna, Austria), and anti-Erk 1/2 (rabbit polyclonal, 1:10,000; Sigma) antibodies.

We thank Juan Guinea Viniegra for help with the TUNEL assay. This work was supported by the Fonds zur Förderung der Wissenschaftlichen Forschung Grants P16872-B09 and P19611-B09 and the Herzfelder'sche Familienstiftung.

1. Luskin MB (1993) *Neuron* 11:173–189.
2. Lois C, Alvarez-Buylla A (1994) *Science* 264:1145–1148.
3. Lois C, Garcia-Verdugo JM, Alvarez-Buylla A (1996) *Science* 271:978–981.
4. Wichterle H, Garcia-Verdugo JM, Alvarez-Buylla A (1997) *Neuron* 18:779–791.
5. Alberti S, Krause SM, Kretz O, Philippar U, Lemberger T, Casanova E, Wiebel FF, Schwarz H, Frotscher M, Schutz G, Nordheim A (2005) *Proc Natl Acad Sci USA* 102:6148–6153.
6. Tomasiewicz H, Ono K, Yee D, Thompson C, Goridis C, Rutishauser U, Magnuson T (1993) *Neuron* 11:1163–1174.
7. Chazal G, Durbec P, Jankovski A, Rougon G, Cremer H (2000) *J Neurosci* 20:1446–1457.
8. Hu H, Tomasiewicz H, Magnuson T, Rutishauser U (1996) *Neuron* 16:735–743.
9. Nguyen-Ba-Charvet KT, Picard-Riera N, Tessier-Lavigne M, Baron-Van Evercooren A, Sotelo C, Chedotal A (2004) *J Neurosci* 24:1497–1506.
10. Wu W, Wong K, Chen J, Jiang Z, Dupuis S, Wu JY, Rao Y (1999) *Nature* 400:331–336.
11. Murase S, Horwitz AF (2002) *J Neurosci* 22:3568–3579.
12. Petreanu L, Alvarez-Buylla A (2002) *J Neurosci* 22:6106–6113.
13. Hack I, Bancila M, Loulier K, Carroll P, Cremer H (2002) *Nat Neurosci* 5:939–945.
14. Perez-Garcia CG, Tissir F, Goffinet AM, Meyer G (2004) *Eur J Neurosci* 20:2827–2832.
15. Wyss JM, Stanfield BB, Cowan WM (1980) *Brain Res* 188:566–571.
16. Rice DS, Curran T (2001) *Annu Rev Neurosci* 24:1005–1039.
17. Tissir F, Goffinet AM (2003) *Nat Rev Neurosci* 4:496–505.
18. D'Arcangelo G, Homayoundi R, Keshvara L, Rice DS, Sheldon M, Curran T (1999) *Neuron* 24:471–479.
19. Hiesberger T, Trommsdorff M, Howell BW, Goffinet A, Mumby MC, Cooper JA, Herz J (1999) *Neuron* 24:481–489.
20. Strasser V, Fasching D, Hauser C, Mayer H, Bock HH, Hiesberger T, Herz J, Weeber EJ, Sweatt JD, Pramatarova A, *et al.* (2004) *Mol Cell Biol* 24:1378–1386.
21. D'Arcangelo G, Miao GG, Chen SC, Soares HD, Morgan JI, Curran T (1995) *Nature* 374:719–723.
22. Howell BW, Hawkes R, Soriano P, Cooper JA (1997) *Nature* 389:733–737.
23. Sheldon M, Rice DS, D'Arcangelo G, Yoneshima H, Nakajima K, Mikoshiba K, Howell BW, Cooper JA, Goldowitz D, Curran T (1997) *Nature* 389:730–733.
24. Trommsdorff M, Gotthardt M, Hiesberger T, Shelton J, Stockinger W, Nimpf J, Hammer R, Richardson JA, Herz J (1999) *Cell* 97:689–701.
25. Koizumi H, Higginbotham H, Poon T, Tanaka T, Brinkman BC, Gleeson JG (2006) *Nat Neurosci* 9:779–786.
26. Howell BW, Herrick TM, Hildebrand JD, Zhang Y, Cooper JA (2000) *Curr Biol* 10:877–885.
27. Paxinos G, Franklin KBJ (2003) *The Mouse Brain in Stereotaxic Coordinates* (Elsevier Academic, Amsterdam).
28. Takahara T, Ohsumi T, Kuromitsu J, Shibata K, Sasaki N, Okazaki Y, Shibata H, Sato S, Yoshiki A, Kusakabe M, Muramatsu M, *et al.* (1996) *Hum Mol Genet* 5:989–993.
29. Alcantara S, Ruiz M, D'Arcangelo G, Ezan F, de Lecea L, Curran T, Sotelo C, Soriano E (1998) *J Neurosci* 18:7779–7799.
30. Nimpf J, Schneider WJ (2000) *Biochim Biophys Acta* 1529:287–298.
31. Hoe HS, Wessner D, Beffert U, Becker AG, Matsuoka Y, Rebeck GW (2005) *Mol Cell Biol* 25:9259–9268.
32. Lein ES, Hawrylycz MJ, Ao N, Ayres M, Bensinger A, Bernard A, Boe AF, Boguski MS, Brockway KS, Byrnes EJ, *et al.* (2007) *Nature* 445:168–176.
33. Simo S, Pujadas L, Segura MF, La Torre A, Del Rio JA, Urena JM, Comella JX, Soriano E (2007) *Cereb Cortex* 17:294–303.
34. Morimura T, Hattori M, Ogawa M, Mikoshiba K (2005) *J Biol Chem* 280:16901–16908.
35. Jossin Y, Ignatova N, Hiesberger T, Herz J, Lambert de Rouvroit C, Goffinet AM (2004) *J Neurosci* 24:514–521.
36. de Bergeyck V, Nakajima K, Lambert de Rouvroit C, Naerhuyzen B, Goffinet AM, Miyata T, Ogawa M, Mikoshiba K (1997) *Brain Res Mol Brain Res* 50:85–90.

6 Curriculum Vitae

I -Biographical Data

Name: Sophia Maria Blake

Birth Date: August 25th 1982

Birth Place: Düsseldorf, Germany

Nationality: Austria, United Kingdom

Address: Lessinggasse 3/18
1020 Vienna
Austria

Max F. Perutz Laboratories
Department of Medical Biochemistry
Division of Molecular Genetics
Dr. Bohrgasse 9/2
1030 Vienna
Austria

Telephone: +43 650 9304980 (mobile)
+43 1 4277 61809 (workplace)

E – mail: sophia.blake@meduniwien.ac.at

II – Education

January 2006 Performing PhD Thesis in the lab of Prof. Johannes Nimpf
Max F. Perutz Laboratories, Austria
PhD thesis title: *Characterization of the Reelin Signaling Pathway in postnatal neuronal migration*

November 2005 Master examination with honours in the group of
Prof. Annemarie Frischauf, University of Salzburg, Austria
Master of Science in Genetics and Biotechnology
Master thesis title: *Inhibition of Gli mediated transcriptional activation by dominant negatives*

September 2005 Selected from the Vienna Biocenter International PhD program in Vienna, Austria
(participating Institutes: IMP/IMBA/MFPL/GMI)

October 2003 Bachelor of Science in Genetics and Molecular Biology at the University of Salzburg, Austria

July 2000 High School Graduation with honours, High School for Music and Performing Arts, Salzburg, Austria

III – Participation in Scientific Meetings

Attended, poster, talk:

- 13th IMP Spring Conference and IMBA Inaugural Conference, Vienna, Austria
- 5th Forum of European Neuroscience, Vienna, Austria
- 10th International Neuroscience Winter Conference, 2007, Sölden, Austria
- PhD Student Conference Cancer Research UK, 2007, Cambridge, UK
- 32nd FEBS Congress Molecular Machines, Vienna, Austria
- 4th International PhD Student Symposium, 2007, Göttingen, Germany
- FENS 4th Neurotrain Training Course, Innsbruck, Austria
- Gordon Research Conference, Molecular & Cellular Neurobiology, Hong Kong University of Science and Technology, Hong Kong, China
- 8th FEBS Young Scientist Forum – YSF, Loutraki, Greece
- 33rd FEBS Congress -Biochemistry of Cell Regulation, Athens , Greece
- 6th Forum of European Neuroscience, Geneva, Switzerland

IV – Short visits

September 2006 – Ecole Polytechnique Fédérale de Lausanne (EPFL), Brain Mind Institute, Lausanne, Switzerland, Jean-Charles Bensadoun, PhD
Subject : Stereotaxic injection in rodents

V – Publications

- Nuno Andrade, Vukoslav Komnenovic, **Sophia M. Blake**, Yves Jossin, Brian Howell, Andre Goffinet, Wolfgang J. Schneider, Johannes Nimpf
  "ApoER2/ VLDL receptor and Dab1 in the Rostral Migratory Stream function in postnatal neuronal migration independently of the Reelin signal"
  PNAS, May 15th 2007, Vol.104

- **Sophia M. Blake**, Vera Strasser, Nuno Andrade, Reinhold Hofbauer , Wolfgang J. Schneider, Johannes Nimpf
  "Thrombospondin 1 signals via ApoER2 and VLDL receptor and functions in postnatal neuronal migration"
  EMBO Journal, 2008 Oct 23, Epub ahead of print

VI – Grants and Scholarships

- Excellence scholarship from the Paris Lodron University, Salzburg, Austria for Master Thesis, September 2005
- Participation and successful selection from the International PhD Program of the Vienna Biocenter, Vienna, Austria, September 2005
- EU funded scholarship to attend the 4th Neurotrain Training Course in Innsbruck, Austria
- Selected to attend the FEBS sponsored 8th FEBS Young Scientist Forum -YSF2008 -in Loutraki, Greece
- FEBS sponsored grant to attend the 33rd FEBS Congress -Biochemistry of Cell Regulation -in Athens, Greece
- Awarded FENS sponsored grant to attend the 6th Forum of European Neuroscience, Geneva, Switzerland

VII – Laboratory Training:

- Cell culture (cell lines, primary cultures and neuronal stem cells, cell transfection of multiple cell types and methods)
- Protein biochemistry (SDS – Page, Western Blotting, ELISA, recombinant protein expression and purification, immunoprecipitation)
- PCR, qRT-PCR, cloning, site directed mutagenesis, luciferase reporter gene assay, southern blot, super array
- histological techniques (immunohistochemistry, immunofluorescence, perfusion, *in vitro* brain explants)
- Microscopy (confocal, fluorescence)
- Handling of laboratory animals (knockout and transgenic mouse lines and rats) including basic and applied knowledge of stereotaxic techniques

VIII – Academic activities

• 2005 -Member of the Austrian Association for Genetics and Genetic Engineering
• 2006 -Member of the Federation of European Neurosciences
• 2006 -Member of the Austrian Neuroscience Association
• 2006 -Representative of the PhD students of the Vienna Biocenter International PhD Program
• 2007 -Member of the Organizing Committee of the 6th Vienna Biocenter PhDSymposium 2008
• 2008 -Member of the Austrian Association for Biochemistry and Molecular Biology

IX -Teaching experience

- October 2004-July 2005: Tutor practical course. Course: COMOBIS I: „Computer Modellierung in den Biowissenschaften“ at the Paris Lodron University in Salzburg, Austria.
- March 2007-July 2007: Tutor practical course. Course: “Praktikum Genetik und Biochemie“ at the Medical University Vienna, Austria.
- March 2008-July 2008: Tutor practical course. Course: “Praktikum Genetik und Biochemie“ at the Medical University Vienna, Austria.
- *December 2008: Tutor practical course. Courses: “Chain Migration Assay from Rat Sub-Ventricular Zone Explants” and “Identification of Migratory Neurons by Doublecortin Staining” at the Fachhochschule FH – Campus Wien, Austria*

7 Acknowledgements

I want to thank my supervisor Johannes Nimpf for great scientific atmosphere and constant support. The amount of freedom I had during my PhD project gave me the opportunity to enjoy science outside bench work and I am thankful for scientifically open-minded discussions and his dedication.

I want to thank all past and present members of the Nimpf lab. Working together with Sarah, Nuno, “little” Johannes, Stephan, Viktoria, Mariella, Tarek, Ilse and Hary was awesome.

Thanks to my best friend Melanie for talks, talks, talks, lots of fun and constant support. Mel you’re the best! Also to Gerald for bringing me to Vienna -greetings to Munich -and all friends form the autumn 2006 VBC PhD selection! Thanks for the great time. I will miss you all very much.

Special thanks to Stefan for constant support, advice and encouragement. Looking forward to London!

Last, but not least I want to thank my parents for their love, support and belief in me. I wouldn’t have managed it without you.

This is for you, dad.